Hydrogen Production from Renewable Bio-Based Sources

by

Shyamsundar Ayalur Chattanathan

A dissertation submitted to the Graduate Faculty of
Auburn University
In partial fulfillment of the
Requirements for the Degree of
Doctor of Philosophy

Auburn, Alabama

May 3, 2014

Keywords: Hydrogen production, dry reforming, steam reforming, bio-oil, aqueous phase reforming, biogas

Approved by

Sushil Adhikari, Chair, Associate Professor of Biosystems Engineering
Xinyu Zhang, Associate Professor of Polymer and Fiber Engineering
Maobing Tu, Associate Professor of Forestry and Wildlife Sciences
Oladiran Fasina, Professor of Biosystems Engineering

Abstract

Efficient means of power generation is the key to coping with increasing energy demands due to population expansion. Non-renewable sources like fossil fuels, coal, and methane contribute to the carbon footprint, resulting in various unfavorable repercussions such as climatic changes, global warming, air pollution and numerous health effects. Consequently, there is a noticeable propensity towards utilizing renewable sources for the purpose of power generation. One such way is hydrogen production from various bio-based sources. Hydrogen produces only water during combustion, and is therefore seen as an alternative fuel for locomotive application. The crux of this dissertation lies in exploring different techniques to find ways for efficiently generating hydrogen from renewable bio-based resources particularly, bio-derived liquids or gases. An introduction to hydrogen production from conventional sources, along with motivations to pursue renewable bio-based sources has been discussed briefly in Chapter 1. Specific research goals and rationale have also been listed in this chapter. Chapter 2 summarizes a detailed literature review of the existing hydrogen production techniques. The important factors (temperature, steam to carbon ratio, catalyst size and weight) known to affect hydrogen yield were identified. Coke formation during reforming of bio-oil was found to be a major challenge.

Bio-oil, one of the substrates used for this study is a viable source for hydrogen production. Chapter 3 elaborates on H_2 production from an aqueous bio-oil by a process called "two-phase reforming" which is a modified version of steam reforming and aqueous phase reforming. Some background information about bio-oil and its properties have also been

discussed in this chapter. The effect of different factors such as time (1, 4 and 10 h), temperature (180, 230 and 280 ºC) and bio-oil concentration (5, 10 and 15 vol%) on H_2 yield has been studied. Statistical analysis was carried out in order to determine if the factors affected the exit gas composition significantly. The efficiency of Ru/Al_2O_3 catalyst on the reforming reaction was quantified in terms of H_2 selectivity and decrease in activation energy.

In Chapter 4, H_2 production from synthesis gas, which is a product of biomass gasification, has been discussed in detail. Methane (CH_4) and CO_2 present in syngas are known to cause greenhouse effect, and hence their conversion to H_2 and CO is vital. Simultaneous catalytic steam and dry reforming was investigated using Box-Behnken design of experiments to evaluate the interactive effect of process variables like temperature, CO_2:CH_4, and CH_4: H_2O ratios. Statistical analyses were also performed to determine optimum conditions for maximum CH_4 and CO_2 conversions and three dimensional response surface plots were plotted.

In Chapter 5, H_2 production by dry reforming of model biogas containing an impurity (H_2S) and its effect on CH_4 conversion has been explored. Steady state gas concentrations as a function of temperature were predicted using a simulation tool called ASPEN Plus, and were compared to the experimental results obtained. The poisoning effect of the impurity during biogas reforming has been demonstrated using three model biogas mixtures containing different H_2S concentrations (0.5-1.5 mol %). This chapter pinpoints the risk involved in ignoring H_2S present in biogas during H_2 production by dry reforming. A summary of findings and a few recommendations for continuing future work in each of the objectives have been discussed in the final Chapter (Chapter 6).

Acknowledgements

I would like to express my gratitude to my mentor Dr. Sushil Adhikari for his sincere efforts in not only reviewing this dissertation, but also for providing constant guidance during the doctorate program. Without his constant support and encouragement, this dissertation would not have taken form. Thanks to the committee members Dr. Xinyu Zhang, Dr. Maobing Tu, and Dr. Oladiran Fasina. I would like to express my appreciation to all my colleagues especially Nour, Avanti and Suchitra for making the work environment interesting, collaborative, and competitive. I am greatly indebted to my parents (Chattanathan and Banumathi) for providing me with a good education, and am grateful to my sister (Chithra) for her persistent motivation. Also special thanks to my wife (Shravanthi) for being supportive, encouraging and understanding during challenging times. Finally, thanks to Auburn University and the entire staff of the Biosystems Engineering Department for making my stay at Auburn University joyful.

Table of Contents

List of Tables

List of Figures

Chapter 1

Introduction

Increase in energy demand and growing environmental awareness has increased interest for alternative energy sources over the last few years. Hydrogen produces only water during combustion, and therefore, it is seen as an alternative fuel for locomotive application. Nonetheless, hydrogen is not an energy source; rather, it is an energy carrier. Different techniques are being explored to find an economical way of generating hydrogen from renewable resources. Hydrogen production from water using sunlight is still expensive. However, there are various reforming techniques that are being used on a commercial scale to produce hydrogen from a wide range of substrates. These techniques are discussed in detail in the next chapter.

Hydrogen is the most abundant element in the universe, and the third most abundant element on the earth's surface [1]. It is very light, highly flammable and burns with pure oxygen producing heat and water in contrast to fossil fuels which produce CO_2 on combustion [1]. It has a very high energy content of 140 MJ kg^{-1} compared to that of gasoline (44.4 MJ kg^{-1}). Hydrogen is considered as an energy carrier instead of an alternative fuel because it is not available freely [1-3]. It can be produced from both conventional sources (such as coal, natural gas) and alternate sources (like biomass, wind and solar). The primary methods for producing hydrogen are: thermochemical (gasification, reforming), electrochemical (electrolysis, photo-electrolysis), and biological (anaerobic digestion, fermentative microorganisms) [4]. Bartels *et al.* conducted an economic survey based on which they reported the cost of H_2 production from coal and natural

gas to be 0.36-1.83 $/kg and 2.48-3.17 $/kg, respectively [5], while that produced using photovoltaic cells has been reported as 3.5-38 $/kg [6]. The percentage of hydrogen produced currently from major sources worldwide is shown in Figure 1.1 [7]. It should be noted that a major portion comes from natural gas and fossil fuels because the technology is mature and cost effective. However, there are some disadvantages associated with these conventional sources. For instance, limited availability of fossil fuels and high energy intensiveness in the case of electrolysis are a few to list.

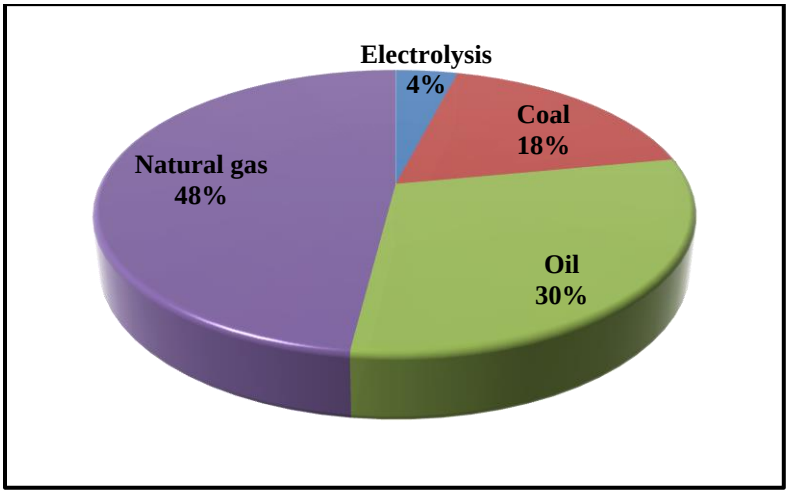

Figure 1.1: A pie chart representing the percentage of hydrogen produced worldwide from various sources

1.0 Research Plan

Although the conventional sources are a cheaper option, bio-based sources have drawn increased attention due to their renewable and sustainable nature. There are various bio-based sources such as biomass, bio-ethanol, bio-butanol, algae, bio-diesel, etc. that are currently being used for hydrogen production.

The focus of this research is on three main bio-based renewable sources to produce hydrogen:

1. Bio-oil obtained from fast-pyrolysis of biomass;
2. Synthesis gas obtained from gasification of woody biomass; and
3. Biogas or landfill gas produced during anaerobic digestion of plant and animal waste.

Different reforming techniques were employed based on the nature of the substrate, and the overall story is pictorially represented in Figure 1.2. Hydrogen production from bio-oil was studied using a process called - "two-phase reforming", while production from syngas obtained from biomass gasification was studied using a combination of steam and dry reforming. The biogas was subjected to dry reforming in the presence of H_2S as an impurity.

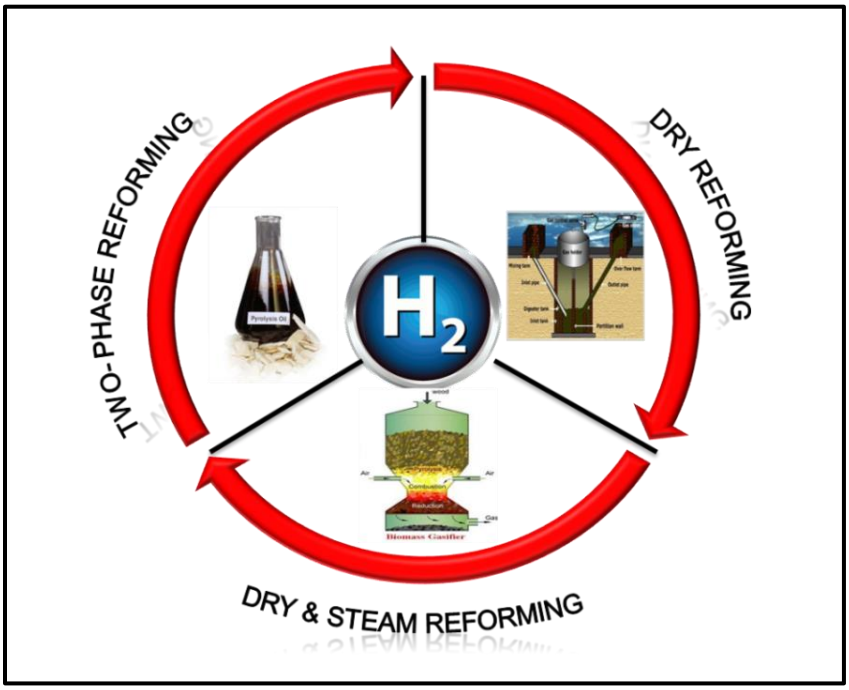

Figure 1.2: Pictorial representation of H_2 production from three different bio-based sources

This work is divided into three specific objectives which are outlined below:

1.0.1 Two-Phase Reforming of Aqueous fraction of Bio-oil using Ru supported on Al_2O_3

Rationale: Pyrolysis oil contains about 7% hydrogen by weight which could be utilized for H_2 production using reforming techniques. The study is proposed to explore the possibility of introducing modifications to already existing reforming techniques in order to make them more efficient. A batch reactor was chosen to examine the H_2 yield, coke deposition and kinetics in the presence of Ru/Al_2O_3 catalyst.

1.0.2 Conversion of CO_2 and CH_4 in Biomass Synthesis Gas for Hydrogen Production

Rationale: Syngas produced during gasification of biomass is rich in methane (CH_4) and carbon dioxide (CO_2). The premise of this research is to find whether CH_4 and CO_2 produced during biomass gasification could be converted to carbon monoxide (CO) and hydrogen (H_2). Simultaneous steam-and dry- reforming was conducted by selecting three process parameters (temperature, CO_2:CH_4, and CH_4:H_2O ratios) in the presence of a commercial methane reforming catalyst.

1.0.3 Hydrogen Production from Biogas Reforming and the Effect of H_2S on CH_4 Conversion

Rationale: Biogas produced during anaerobic decomposition of plant and animal wastes consists of high concentrations of methane (CH_4), carbon dioxide (CO_2) and traces of hydrogen sulfide (H_2S). The primary focus of this research was on investigating the effect of a major impurity hydrogen sulfide that is commonly found in biogas, on a commercial methane reforming catalyst during hydrogen production. A thermodynamic equilibrium model (with ASPEN Plus) was also used to compare the experimental results with the predicted conversions.

Chapter 2

Literature Review

2.0 Hydrogen Production Techniques

Although there are various hydrogen production methods, majority of the studies are focused on the steam reforming process since it is the most commonly used industrial technique. These techniques are discussed below in detail taking bio-oil as the common reacting substrate. Reactions with other substrates could be found elsewhere [8-10],[11].

2.0.1 Steam-reforming

Steam reforming is an efficient process for hydrogen production and has been in practice since 1930 [12]. Standard Oil Co., USA began the first steam reforming plant in 1930 with light alkanes as feed [13]. It is an endothermic process in which the substrate is treated with steam in the presence of catalyst to produce carbon monoxide (CO), CO_2 and hydrogen (H_2) [14]. The chemical reactions for steam reforming of bio oils are given below [15]:

$$C_nH_mO_k + (n\text{-}k)\, H_2O \longrightarrow n\, CO + \left(\frac{n+m}{2-k}\right) H_2 \qquad \text{(Eq.2-1)}$$

The CO can be further converted to CO_2 by the water-gas shift reaction (Eq. 2-2).

$$CO + H_2O \longrightarrow CO_2 + H_2 \qquad \text{(Eq.2-2)}$$

Overall reaction is given as presented in Equation 2-3.

$$C_nH_mO_k + (2n\text{-}k)\ H_2O \longrightarrow nCO_2 + \left(2n + \frac{m}{2} - k\right)\ H_2 \quad \text{(Eq.2-3)}$$

The amount of biological material that contains one gram atom of carbon is termed as one mole of the biological material [16]. Table 2.1 summarizes a comparison of the moles of H_2 produced per mole of the source in different methods which includes steam reforming, partial oxidation and supercritical water reforming of various substrates like ethanol, ethyl lactate, glycerol, and bio-oil and its aqueous fraction. On an average, it is found that one mole of bio-oil substrate produces 2 moles of H_2.

Table 2.1: Theoretical estimation of number of moles of H_2 produced per mole of the source

Substrate/Source	**Technique**	**Moles of H_2 produced /mole of source (Theoretical)**	**Reference**
Bio-oil / Poplar wood	Steam reforming	2.20	[17]
Bio-oil / Pine wood	Steam reforming	1.73	[17]
Bio-oil / Hardwood	Steam reforming	2.12	[17]
Aqueous fraction of bio oil	Steam reforming	1.92	[18]
Bio-oil / sawdust	Steam reforming	2.20	[19]
Bio-oil / rice husk	Steam reforming	2.15	[19]
Bio-oil / cotton stalk	Steam reforming	2.24	[19]
Bio-oil / Poplar wood (after cold storage for long time)	Steam reforming	2.19	[20]
Bio-oil / Poplar wood	Partial oxidation	1.66	[20]
Ethanol	Steam reforming	3.00	[21]
Ethyl lactate	Partial oxidation	1.00	[22]
Glycerol	Steam reforming	2.33	[14]
Glycerol	Super critical water reforming	2.33	[23]

2.0.1.1 Reforming Catalysts

Steam reforming is usually carried out in the presence of a catalyst which not only increases the reaction rate but also helps achieving equilibrium faster. Catalytic reforming of bio-oils has been studied by Chornet group [24-29]. Galdámez *et al.* [30] prepared Ni-Al catalysts by co-precipitation and studied the extent to which loading of La_2O_3 onto Ni-Al catalyst affected the hydrogen yield while, they also conducted non-catalytic steam reforming and confirmed that the H_2, CO_2 yields were low in the absence of catalyst. Galdámez *et al.* [30] also noticed that the total gas yield decreased with decrease in catalyst weight. Catalysts were usually reduced for an hour at high temperature with N_2/H_2 before their usage in experiments to increase activity. Galdámez *et al.* [30] reduced Ni-Al catalyst with a mixture of H_2 and N_2 gas for one hour at 650 $^{\circ}$C. Czernik *et al.* [28] and Kechagiopoulos *et al.* [31] used nickel-based naphtha reforming catalyst to produce hydrogen. Kechagiopoulos *et al.* [31] used C11-NK catalyst which has higher potassium content compared to other Ni catalysts. The higher potassium content plays a vital role in suppressing the coke formation and a 90% hydrogen yield was reported for the equimolar mixture of model compounds[31]. Pan *et al.* [32] employed C12A7-Mg catalyst and determined its lifetime to be about 210 min at 750 $^{\circ}$C. Steam reforming of bio-oil at 750^{o}C using this catalyst resulted in a hydrogen yield of 80%. Wang *et al.* [19] conducted reforming over three catalysts: C12A7 / 15% Mg, 12% Ni/gamma-Al_2O_3, and 1% Pt/gamma-Al_2O_3 at 650^{o}C and the observed hydrogen yields were 56.7%, 58.1%, and 66.8%, respectively. Yan *et al.* [33] reformed bio-oil with commercial Z417 catalyst along with CO_2 sequestration using calcined dolomite and reported a hydrogen yield of about 75%. Lin *et al.* [34] performed catalytic reforming of bio-oil over CoZnAl catalyst electrochemically by passing AC current in a Ni-Cr wire entwined around

the catalytic column. A detailed comparison of different studies in reforming of bio-oil has been made in Table 2.2.

Table 2.2: Comparison study of reforming techniques discussed in literature

Catalyst	Experimental Conditions	Key Findings	Fuel Type	Reference
Ni-Al promoted with La	Reactor: Fluidized bed T=450-700 ºC S/C: 5.58 Liquid feeding rate: 1.84-2.94 g/min	Use of catalyst showed an increase in total gas and H_2 yield. Promotion with La didn't affect H_2 yield with Ni-Al catalyst. H_2 yield: 0.029 g /g of acetic acid at 1.84 g/min feeding rate and 650 ºC	Model Compound: Acetic Acid	[30]
Commercial catalyst Z417	Reactor: Bench-scale Fixed bed Temperature:500-700 ºC	Optimum temperature with CO_2 capture: 550-650 ºC Water : Bio-oil ratio- 1:1 Use of Dolomite to capture CO_2 showed highest H_2 yield. H_2 yield : 75% at 600 ºC	Aqueous fraction of bio-oil	[33]
Ni based catalyst	Reactor: Fixed bed Temperature:600-900 ºC H_2O/C: 2-8.2 G_{C1} HSV : 300-1500 h^{-1}	The high potassium content in the catalyst suppressed coking. A H_2 yield of 60% was reported when aqueous phase of bio-oil was reformed, but 90% yield was reported for the model compounds at temperatures higher than 600 ºC.	Model compounds : acetic acid, acetone, and ethylene and aqueous phase of bio-oil	[31]

Ru/ Mgo/Al_2O_3	Reactor: Nozzle fed reactor T: 800 ºC P: 1 atm S/C:7.2	Role of MgO is vital in converting CO to CO_2 and enhancing steam adsorption capacity of the catalyst. The selectivity of H_2 in the form of pellets was the highest and was close to 100%	Model compound: Acetic acid and aqueous phase of bio-oil	[15]
C12A7 doped with 15%Mg, 12%Ni/γ-Al_2O_3 and 1% Pt/ γ-Al_2O_3	Reactor: Fixed-bed flow reactor T:750 ºC S/C: 6.0 GHSV: 26000 h^{-1}	C12A7/15% Mg exhibited high reforming activity, a H_2 yield of 71% and carbon conversion of 93%	Volatile organic components of crude bio-oil	[19]
Ni/CeO_2-ZrO_2	Reactor: Fixed bed Temperate: 450- 800 ºC Water/Bio-oil: 4.9 Ni-12% Ce-7.5%	Highest H_2 yield of 69.7% was achieved when T=800 ºC, W/B=4.9, Ni-12% and Ce-7.5%. Under same conditions H_2 yield was higher than commercial Z417 catalyst.	Aqueous fraction of bio-oil	[18]
Ni , Rh or Ir supported on calcium aluminates	Reactor: Fixed bed quartz reactor Temperature: 550-750 ºC S/C: 3 Space velocity: 30,000 h^{-1}	Coke deposition over Ni loaded catalyst was higher than that with the Rh or Ir. The Highest H_2 yield was obtained with 5% Ni/$CaO.2Al_2O_3$ catalyst and was about 70% at 750 ºC for acetone.	Model compounds: Acetic acid and Acetone	[35]
Ni-Al catalyst modified with Mg and	Reactor: Fluidized bed Temperature: 650 ºC	Coke formation was reduced by decreased space velocity and increased O_2. Mg modified catalyst performed better than	Aqueous fraction	[36]

Ca	G_{C1}HSV: 11,800 h^{-1}	Ca modified catalyst. A hydrogen yield of 0.1056 g/g of organics was reported for Magnesium modified catalyst.		
Commercial catalyst C11-NK and NREL#20	Reactor: Bench-scale Fluidized bed Temperature: 850 ºC S/C: 5.8 Space velocity: 920 h^{-1}	Steam reforming resulted in a H_2 yield of about 70-80%	Whole bio-oil	[37]
C12A7 doped with 18%Mg, C12A7 doped with 25%K, C12A7, C12A7 doped with 12%Ce, C12A7 doped with 12%Mg, Al_2O_3 doped with 12%Mg, Al_2O_3 doped with 18%Mg	Temperature: 200-750 ºC S/C: 1.5-9 Gas hourly space velocity(GSHV): 10,000 h^{-1} Reactor: Fixed bed micro-reactor Pressure: Atmospheric pressure	At 750 ºC, S/C>4, GHSV of 10,000 h^{-1} C12A718% Mg showed the highest hydrogen yield of 80% and carbon conversion of 96%	Whole bio-oil	[38]
Non-catalytic	Temperature: 625-850 ºC O:C(oxygen to carbon ratio): 1.4-1.6 Reactor:Tubular reactor	The partial oxidation resulted in a hydrogen yield of about 25%	Whole bio-oil	[20]

The reactors usually used are fluidized bed, bench-scale, and fixed bed reactors. From the table we can observe that model compounds are usually used – although a few of them have used aqueous fraction of bio-oil. This is attributed to the complex composition of bio-oils which form residual solids on heating. A common problem experienced in the above cases is coking.

2.0.1.2 Experimental Conditions

Since bio-oil is a complex mixture of many organic compounds, its steam reforming has been usually studied by either using its aqueous fraction or by using model compounds. Chornet and co-workers [25] conducted experiments with aqueous fraction of bio-oil. Many researchers have investigated H_2 production with acetic acid as a model compound [24-26]. Takanabe *et al.* [39] have studied steam reforming of acetic acid over Pt/ZrO_2. Kechagiopoulos *et al.* [31] used three model compounds for their investigation: acetic acid, acetone and ethylene glycol. Adhikari *et al.* [40] tested different noble metal based catalysts for steam reforming of glycerol.

2.0.1.3 Choice of Reactor

Type of reactor plays a vital role in steam reforming of bio-oil. Fixed reactors are not preferred for steam reforming of bio-oils, since the operating time is limited due to formation of carbonaceous deposits [30]. They were prescribed to be unfit for thermally unstable biomass liquids by Czernik *et al.* [28] who in turn used a fluidized bed reformer. Fluidized bed on the contrary, ensured continuous operation by gasification of carbonaceous deposits on catalyst particles [30]. Basagiannis *et al.* [15] established that using a nozzle-fed reactor, in which the liquid is fed into the reactor using high flow rate nozzles, decreased the carbon deposition to a great extent. Gongxuan *et al.* [41] performed a coupled steam reforming of bio-oil in a Y- type reactor design in which the catalyst bed was in the center and bio-oil and bio oil mixed with steam/water were sent through the other inlets. The important factors that affect H_2 production

are temperature, steam: carbon ratio, and space velocity. Figure 2.1 depicts the nozzle-fed and Y-type reactors used for bio-oil reforming.

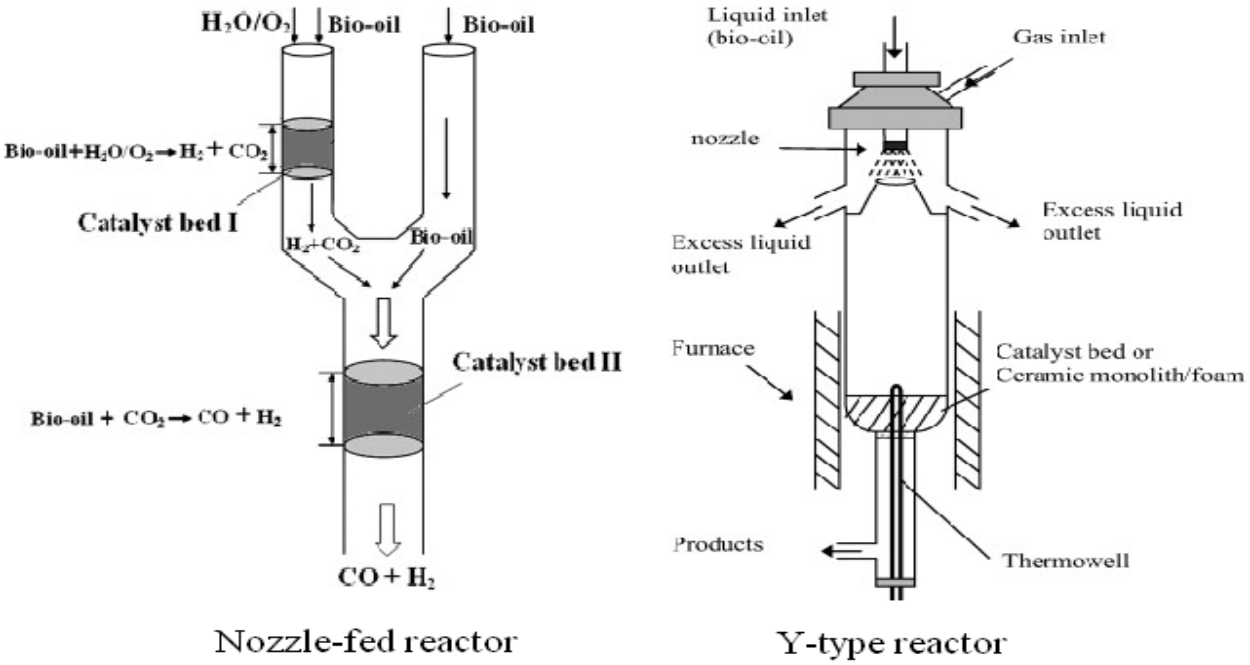

Figure 2.1: Schematic representation of unique reactors used

2.0.1.4 Temperature and S/C ratio

Since the steam reforming of bio-oils is accompanied by decrease in temperature, an increase in temperature shifts the equilibrium towards the right thereby leading to increase in H_2 yield. Similarly, the steam to carbon ration also affects H_2 yield to a great extent. Wang *et al.* [19] observed that H_2 production increased with increase in temperature and S/C ratio. This was accompanied with an increase in carbon conversion which was only 15% at 500 $^{\circ}$C but later on increased to 93% at 750 $^{\circ}$C. As S/C was increased from 1.5 to 6, both H_2 yield and carbon conversion increased. Galdámez *et al.* [30] conducted studies at 650 $^{\circ}$C and 13000 h^{-1} space

velocity using a fluidized bed reactor. Yan *et al.* [33] carried out steam reforming of bio-oil aqueous fraction in a fixed bed reactor with CO_2 capture (using CaO and dolomite). Interestingly, they found out that H_2 production decreased at high temperatures with the capture of CO_2. The optimal temperature as reported by them for H_2 production with CO_2 capture is between 550 $^{\circ}$C and 650 $^{\circ}$C. Kechagiopoulos *et al.* [31] observed an increase in H_2 yield with increase in H_2O/C ratios and decrease in pressure. They also found that the maximum yield for their experimental conditions was between 600 and 750 $^{\circ}$C. Czernik *et al.* [28] carried out steam reforming at temperatures 800-850 $^{\circ}$C, S/C range of 7-9 and space velocity of 700-1000 h^{-1}. Pan *et al.* [32] conducted steam reforming of bio-oils in a fixed bed micro-reactor where in the vaporized bio-oil was fed into the reactor at a space velocity of 10000 h^{-1}. They performed experiments in the temperature range 550-750 $^{\circ}$C at S/C 4.0.

The effect of liquid feed rate has been well addressed by Galdámez *et al.* [30] with respect to their experimental conditions. The residence time decreases as the liquid feed rate increases which should eventually result in lower H_2 yield. But, the result obtained indicated higher H_2 yield. This was due to the increase in partial pressure in the reaction bed with higher liquid feed rate. The typical residence time used was in the range 0.56 s to 0.44 s. Since the rate of the reaction was directly dependent on reactant concentration, higher partial pressure resulted in higher H_2 yield.

Kechagiopoulos *et al.* [31] reported a low hydrogen yield of about 60% by reforming the aqueous phase of bio-oil. Wang *et al.* [19] performed reforming over three different catalysts (C12A7/15%Mg, 12% Ni/γ-Al_2O_3, and 1%Pt/ γ-Al_2O_3), and found that at 700 $^{\circ}$C 1%Pt/ γ-Al_2O_3 showed the highest H_2 yield of 75%. Pan *et al.* [32] reported a maximum carbon conversion and

H_2 yield of about 95% and 80% at 750 ºC respectively which were higher than that obtained with naphtha and CH_4.

2.0.2 Partial oxidation

In this method, the substrate is oxidized with oxygen (in the presence or absence of catalyst), resulting in high temperature which in turn balances the energy required for the process. However, excess air leads to complete oxidation of the substrate resulting in the formation of CO_2 and water [14].

$$C_nH_mO_k + air \longrightarrow \text{carbon oxides} + H_2 + N_2 \quad \text{(Eq.2-4)}$$

Marda *et al.* [20] conducted non- catalytic partial oxidation of bio-oil, while Rennard *et al.* [22] performed autothermal catalytic partial oxidation of bio-oil using esters and acids as model compounds over platinum and rhodium based catalysts. Marda *et al.* [20] reported a low H_2 yield of about 25% while Rennard *et al.* [22] have concentrated on synthesis gas production.

2.0.3 Auto-thermal reforming

It is a combination of steam reforming and partial oxidation techniques in which the substrate is reformed in the presence of air and water to produce H_2.

$$C_nH_mO_k + Air + steam \longrightarrow CO + H_2 + N_2 \quad \text{(Eq.2-5)}$$

The advantage lies in the fact that the process does not require energy ideally because all heat produced during the oxidation step is consumed by steam reforming step. However, low H_2 yield compared to steam reforming process is a disadvantage of auto-thermal reforming.

Vagia *et al.* [42] performed thermodynamic analysis of autothermal reforming of selected components of aqueous bio oil fraction to determine the optimum amount of oxygen required to carry out an energy neutral process. They also studied the effect of temperature and pressure on H_2 production. They reported that at optimum operating conditions, 1 kmol of H_2 is produced from 0.245 kmol of bio-oil, which is 20% lower than the H_2 yield obtained by steam reforming method.

2.0.4 Aqueous-Phase reforming

This process which was developed by Dumesic and his co-workers is carried out at high pressure (at around 60 bar) and low temperature (at around 270 $^{\circ}$C) [43]. The advantages of this process are it produces low amount of CO and the process takes place in liquid phase (while the others take place in gas phase) so there is no need to vaporize the substrate used for producing hydrogen. The effect of catalyst size with pure and crude glycerol was studied by Claus and Lehnert [44] and the study revealed that H_2 selectivity was higher for larger particles. Iriondo *et al.* [45] used different promoters and found that Ni catalyst does not work very well for glycerol due to severe deactivation.

2.0.5 Supercritical water reforming

Water when heated and compressed to its critical temperature (374 ºC) and pressure 22.1 MPa becomes supercritical water. Supercritical water possesses characteristics of both liquid water and vapor which includes densities, viscosities, high diffusivity and good transporting properties [46, 47]. Penninger and Rep [48] conducted supercritical water reforming of aqueous wood pyrolysis condensate obtained from moist beech wood saw dust at 650 ºC and 28 MPa. They found that, there was no plugging at 28 MPa pressure and a small percentage of soda (0.1%) promoted hydrogen production. A hydrogen yield of 36.6 vol% was observed at a residence time

of 12.5s and a total feed flow of 690 g/h. Byrd *et al.* [49] studied hydrogen production from switchgrass biocrude by catalytic gasification in supercritical water. Ni, Co, Ru catalysts supported on TiO_2, ZrO_2 and $MgAl_2O_4$ were tested and among them Ni/ZrO_2 exhibited highest hydrogen yield of 0.98 mol H_2/ mol C at 600 ^oC and 250 bar. Yu *et al.* [50] and Antal *et al.* [51] reformed wet biomass to hydrogen, carbon dioxide and carbon monoxide using supercritical water at 600 ^oC and 35 MPa. Gupta and coworkers carried out supercritical water reforming of glycerol over Ru/Al_2O_3 catalyst which yielded 6.5 mol of H_2/mol of glycerol [23].

2.0.6 Sequential cracking

It is a two-step process in which the bio-oil is first catalytically cracked/reformed without addition of water followed by subsequent regeneration of the catalyst with oxygen [52]. Reactions to demonstrate the technique are given below taking methane as an example [53-58]:

Cracking: $CH_4 \longrightarrow C + 2H_2$ (Eq.2-6)

Regeneration: $C + O_2 \longrightarrow CO_2$ (Eq.2-7)

Davidian *et al.* [52] used two Ni based catalyst and found them to perform very well for producing hydrogen from bio-oil. Iojoiu *et al.* [59] used Pt and Rh catalysts supported in ceria-zirconia for H_2 production from bio oil obtained from beech wood residues. From the heat balance calculations, they also established that sequential cracking process could be operated auto-thermally. The possibility of removing large carbon deposits by catalyst regeneration is a great advantage of this method despite the reported sintering of ceria-zirconia support. The H_2 productivity was only 18 mmol H_2 g^{-1} as compared to 20 and 37 mmol H_2 g^{-1} (at 2.5 and 10 H_2O/C ratios) productivities in steam reforming method. The operating temperature was 700 ^oC and H_2 yield observed was 40%.

2.1 Thermodynamic Analysis

The composition of an exit gas stream and important process parameters affecting H_2 yield are usually predicted by the thermodynamic analysis. Vagia and Lemonidou [60] performed a detailed thermodynamic analysis of H_2 production via steam reforming with ASPEN 11.1 using acetic acid, ethylene glycol, and acetone as model compounds of bio-oil. Peng-Robinson property method and RGibbs reactor were selected with equilibrium compositions being computed by the minimization of Gibb's free energy. The important specifications fed into the software included reactant and product inlet composition, inlet temperature, pressure, reaction temperature, and steam to fuel (S/F) ratio. A study from Vagia and Lemonidou [60] showed that equilibrium concentrations of ethane, ethylene, acetylene and other oxygenated compounds in the product stream were negligible. It was established that H_2 yield was favored at increased temperatures and S/C (steam to carbon ratio) at atmospheric pressure. At optimum conditions of 627 $^{\circ}$C, atmospheric pressure and S/C =3 (steam to carbon ratio), 0.208 kmol/s of the mixture of the model compounds (acetic acid, ethylene glycol and acetone at 4:1:1 molar ratios) yielded about 1 kmol/s of hydrogen. No coke formation was reported at temperatures higher than 327 $^{\circ}$C. Vagia and Lemonidou [60] also established that bio-oil can be thermally decomposed to form a mixture of gases containing methane (CH_4), H_2, CO, CO_2 and water (H_2O).

Similar thermodynamic analysis was done by the same research group for H_2 production via autothermal reforming with the same model compounds[42]. They reported a maximum yield at 627 $^{\circ}$C but this was 20% lesser than the yield obtained by the steam reforming. Aktas *et al.* [61] conducted thermodynamic analysis of steam reforming using isopropyl alcohol, lactic acid and phenol as model compounds of bio-oil at temperatures from 327 $^{\circ}$C to 927 $^{\circ}$C, S/F ratio from 4 to

9 and total pressure of 30 bar. The fact that H_2 yield increased with increasing temperature and S/F ratio was confirmed.

2.2 Catalysts Characterization

Galdámez *et al.* [30] characterized Ni-Al catalyst using inductively coupled plasma (ICP), X-ray diffraction (XRD), nitrogen adsorption and temperature-programmed reduction (TPR) and found the surface area of the catalyst to be 150 m^2/g. When the catalyst was loaded with 8% and 12% La_2O_3 its surface area reduced to 141 and 131 m^2/g, respectively. Yan *et al.* [33] used differential thermogravimetric (DTG) and differential scanning calorimetric (DSC) curves to determine the decomposition mechanism of their sorbent dolomite. Pan *et al.* [32] used XPS to study their catalyst before and after steam reforming and found that there was an increase in carbon content on the surface of the catalyst after reforming. Lin *et al.* [34] used N_2 physisorption to determine Brunauer-Emmett-Teller (BET) and pore volume of the catalyst. Wang *et al.* [19] measured Mg, Ni and Pt contents in the catalyst using inductively coupled plasma (ICP) and atomic emission spectroscopy (AES). They also used XRD and N_2 physisorption at 196 $^{\circ}$C to determine the surface atomic composition, BET surface area and pore volume. A summary of analysis techniques used is given below. BET is used to determine the surface area of the catalyst. ICP is used to determine the metal and non-metal concentrations in the catalyst while XPS is used to determine the composition of the catalysts on the surface and different state of the metal used for catalyst. The temperature effects on the catalyst are determined using DTG and DSC curves. XRD is performed to get an idea about the crystallographic atomic structure of the catalyst.

2.3 Challenges and Conclusions

Coking is a major problem that is encountered in reforming processes. It results from thermal decomposition of organic compounds onto the catalyst resulting in its deactivation [31].

$$C_nH_mO_k \longrightarrow C_xH_yO_z + \text{Gas } (H_2, CO, CO_2, CH_4...) + \text{Coke} \quad \text{(Eq.2-8)}$$

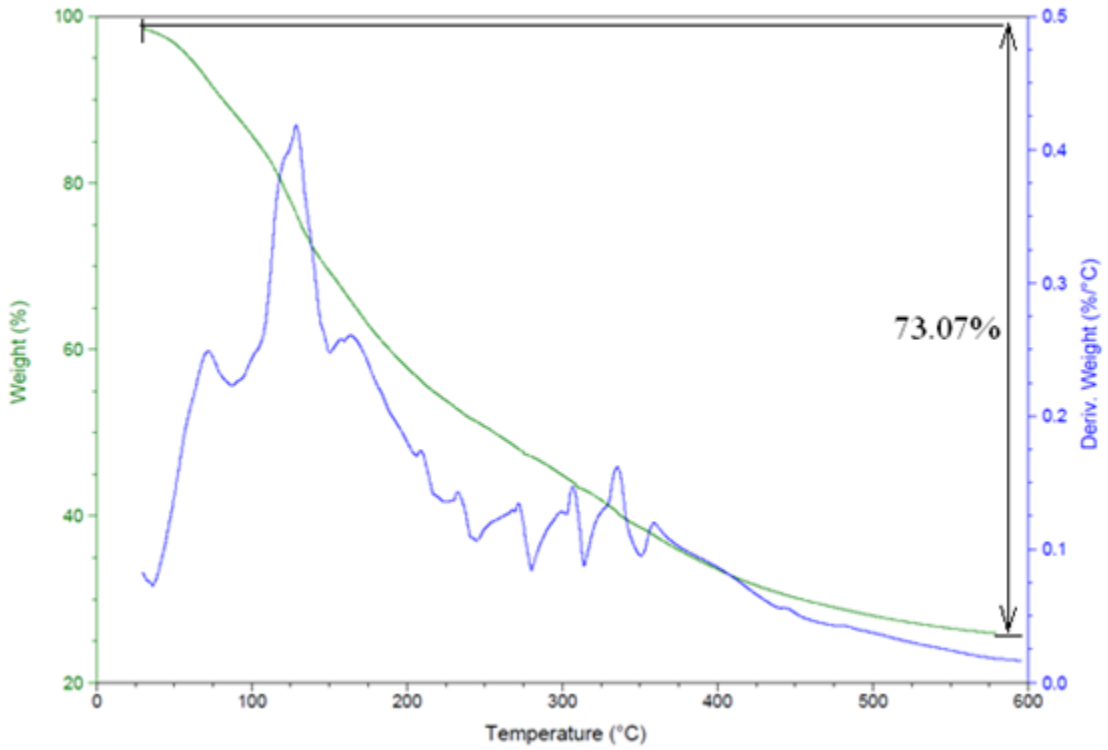

Figure 2.2: TGA results for bio-oil produced from pine wood

Thermogravimetric analysis (TGA) revealed that there is a maximum weight loss at 125 ºC, which could be mainly due to vaporization of water. At temperatures higher than 400 ºC, the weight loss decreased gradually and when the temperature reached 600 ºC there was no weight loss observed. From the TGA graph (Figure 2.2), it can be seen that there is a total weight loss of 73.07% at 600 ºC, which means that 26.93% of the bio oil fed into the reactor did not vaporize, and hence would result in clogging of the catalytic surface. Bio-oil cannot be completely

vaporized, and when heated, leads to the formation of residual solids. To overcome this operational difficulty while feeding, Basagiannis *et al.* [15] used a nozzle injection system to spray bio-oil into the reactor. This problem can also be avoided by increasing the temperature so that gasification of the carbonaceous deposits takes place thereby resulting in regeneration of the catalyst. Rennard *et al.* [17] established that high steam to carbon ratio helps reducing coke formation. However, the heat load increases, since more steam has to be supplied. Coke formation is also reduced by blending of bio-oil [17]. Oxidation of coke also helps in alleviating coking, although the presence of oxygen results in decreased experimental and theoretical H_2 yields [59, 62-65]. Medrano *et al.* [36] reported that the coke formation decreased from 149 mg C/g catalyst to 73 mg C/g catalyst with an addition of 4% oxygen. The use of $Ce_{1-x}Ni_xO_{2-y}$ as catalyst is also known to decrease the formation of carbonaceous deposits due to Ce ↔ O ↔ Ni interaction [66]. A catalyst ($Ce_{0.8}Ni_{0.2}O_{2-y}$) prepared using adapted micro emulsion method proved to be an excellent catalyst for ethanol steam reforming. It was not only less expensive than Rh/CeO_2 catalyst, but it also had a higher catalytic activity [67].

Estimating the world's current energy demands and foreseeing the demands in the upcoming years we realize the need for a pollution-free alternative source of energy. Hydrogen obtained from bio-oil would serve as a versatile energy carrier in this regard. The purpose of this review is to give a comprehensive update of various developments in the field of hydrogen production from bio-oil. Though we have specifically documented an overview of steam reforming of bio-oil, we have also discussed other methods like partial oxidation, auto-thermal, aqueous phase reforming and supercritical water reforming to show their differences. Quite a lot of work has been reported in the literature on steam reforming of bio oil but to the best of our knowledge, very few have been reported on aqueous phase reforming of bio oils. Experiments have been

conducted to check the change in H_2 yield with different catalysts and reactors at wide range of temperatures. Further emphasis must be given to the catalyst deactivation issue and ways to overcome the coking challenge during bio-oils reforming must be explored.

Chapter 3

Two-Phase Reforming of Aqueous fraction of Bio-oil using Ru supported on Al_2O_3

3.0 Abstract

Alternative energy from renewable sources has gained attention owing to higher energy demands resulting from population explosion. One option is to produce hydrogen from renewable resources such as bio-oil using reforming techniques. The primary objective of this study is to explore the possibility of introducing modifications to already existing reforming techniques in order to make them more efficient. Coking was the major disadvantage encountered during steam reforming of bio-oil, while high pressure in case of aqueous phase reforming negatively impacted the bio-oil to gas conversion according to Le Chatelier Braun principle. In an effort to overcome these drawbacks, experiments were carried out in the two-phase zone wherein liquid-vapor equilibrium exists. Aqueous bio-oil was used as substrate for this study and the effects of different factors (time, temperature and bio-oil concentration) on H_2 yield were investigated. Statistical analysis of time based study revealed that the H_2 concentration was not affected between 1 h and 10 h. Experiments carried out at three different temperatures (180, 230, and 280°C) under autogenous pressure indicated an increasing H_2 concentration with temperature. Bio-oil concentration in the range 5, 10 and 15 vol. % in water also played a major role on exit gas composition. Catalytic two-phase reforming of bio-oil was studied using Ru supported on Al_2O_3. The catalyst was found to have a positive effect on H_2 yield and selectivity. For instance,

catalytic two-phase reforming of 15 vol % bio-oil at 280°C resulted in a 13% increase in H_2 concentration and a 4% increase in H_2 selectivity compared to non- catalytic reforming. To further confirm the catalytic effect of Ru/Al_2O_3 a comparison of activation energies was done with the help of kinetic studies. The activation energy for the two-phase reforming reaction was found to reduce from 66 kJ/mol (without catalyst) to 56 kJ/mol in the presence of catalyst. The GC-MS analysis of the remaining reacted liquid after catalytic and non-catalytic reforming suggested the conversion of sugars, aldehydes and diols to simpler ketones during the two-phase reforming. The coke deposition trend was analyzed using catalyst characterization methods like TGA and BET surface area measurements. Coke deposition was found to reduce with increase in experimental temperature.

3.1 Introduction

Population explosion is a serious concern worldwide since it puts immense pressure on the energy sector. Environmental awareness has played a vital role in fueling the urge to search for cleaner renewable sources also called "green energy". Being rich in biomass, the United States of America has invested millions of dollars for research in bio-energy. The Union of Concerned Scientists (UCS) has estimated that by 2030, 680 million tons of biomass resources could be made available in a sustained manner which is equivalent to 732 billion kilowatt-hours of electricity[68]. In the year 2011, the United States of America produced 923 trillion BTU of renewable energy from biomass, which is one and half times that produced in the year 2000 [69]. Hence, an increasing trend in both biomass consumption and energy production has been observed over the decade explaining the vital contribution made by energy derived from biomass in the energy sector. The conversion of biomass to energy could be accomplished in three

different ways – direct combustion, gasification to produce synthesis gas and fast pyrolysis to produce bio-oil. The bio oil obtained could be reformed to produce hydrogen or upgraded to produce other hydrocarbons to be used as transportation fuel. The focus of this study lies in the production of H_2 through bio-oil reforming. Some of reforming techniques that have been used for H_2 production from bio-oil are steam reforming, aqueous phase reforming, autothermal reforming, partial oxidation, sequential cracking and supercritical reforming. An in-depth review on H_2 production by reforming of bio-oil can be found elsewhere [70]. Although there are different techniques for H_2 production majority of the studies are focused on steam reforming and aqueous phase reforming processes. A major drawback encountered during steam reforming is coking, and to overcome this, Dumesic and group pioneered aqueous phase reforming. The overall chemical reaction during aqueous phase reforming is given by Equation 3-1.

$$C_xH_yO_z + H_2O \xrightarrow[\Delta]{\text{Pressure}} H_2 + CO_2 \qquad \text{(Eq.3-1)}$$

Guo *et al.* (2012) investigated glycerol aqueous phase reforming using a Ni-B alloy catalyst. They reported that the Ni-B alloy catalyst resulted in 35-50% higher H_2 production rate and 17-31% higher H_2 selectivity compared to Raney Ni [71]. Manfro *et al.* (2011) used the same process for studying Ni on CeO_2 catalyst prepared using three different synthesis methods: wet impregnation, co-precipitation, and combustion. A maximum of 30% glycerol conversion was observed with the catalyst prepared by combustion method. They also reported that increasing the glycerol concentration decreased the H_2 formation and glycerol conversion [72]. Pan *et al.* (2012) studied H_2 production from aqueous phase reforming of ethylene glycol over Ni/Sn/Al hydrotalcite derived catalysts and reported that the catalyst showed 100% H_2 selectivity and a good stability for over 120 h [73]. Dumesic group has conducted extensive research on aqueous phase reforming of ethylene glycol using Ni, Pd, Pt, Ru, Rh and Ir supported over silica and

other bimetallic catalysts (PtNi, PtCo, PtFe and PdFe) [74],[75]. Xie *et al.* (2011) carried out thermodynamic analysis of aqueous phase reforming of model compounds such as methanol, acetic acid, and ethylene glycol for H_2 production and reported a maximum H_2 selectivity of 10% [76]. Pan *et al.* (2012) conducted aqueous phase reforming of low-boiling fraction of bio-oil derived from pyrolysis of rice-husk in the presence of Pt/Al_2O_3 catalyst in the temperature range 230 – 290ºC and reaction time from 1 – 4h. At 533 K H_2 yield of about 65% was observed [77]. However, there are a few disadvantages associated with aqueous phase reforming owing to the experimental conditions. The application of high pressure has a negative effect on liquid to gas conversion which could be explained by Le Chatelier Braun principle. Therefore, in this study, some process design modifications have been incorporated in an effort to overcome the shortcomings linked to steam and aqueous phase reforming techniques. The region in the PV diagram where liquid-vapor equilibrium exists is the two-phase reforming zone investigated in this research.

Assuming model compounds may not be accurate owing to the complexity of the reactions and therefore aqueous fraction of bio-oil has been used as substrate for this study. The specific objectives of this study are : a) Examine the factors (time, temperature and bio-oil concentration) affecting the two-phase reforming process; b) Investigate catalytic and non-catalytic two-phase reforming of aqueous bio-oil; and c) Compare the H_2 yield, selectivity and activation energies with and without Ru/Al_2O_3 catalyst.

3.2 Background Information on Bio-Oil:

Bio-oil is a dark to brown organic liquid containing degradation products of the three main components, namely cellulose, hemicelluloses and lignin. It is produced by a process called fast-pyrolysis of biomass. Fast pyrolysis is the degradation of biomass at around 500^{o}C in the absence of oxygen to yield a liquid fuel (hereafter, bio-oil), as well as solid (biochar) and noncondensable gases [78-80]. Bio-oil (also called pyrolysis oil or biocrude) has an energy density of around 20 MJ/m^3, which is about ten times that of biomass, making bio-oil an excellent alternative source of energy[25].

The composition of bio-oil varies depending on the biomass source as well as the process conditions. Nonetheless, it typically consists of water and a complex mixture of organic compounds such as hydroxyaldehydes, hyroxyketones, sugars, carboxylic acids and phenolics from the breakdown of biomass carbohydrates and lignin [81]. Its main elemental constituents are carbon (C), hydrogen (H), and oxygen (O), and hence its empirical chemical formula is given as $C_nH_mO_k.xH_2O$ [19]. Bio-oil can be separated into organic and aqueous phases by adding water to it and volatile compounds constitute about 60% of bio-oils [32].

Bio-oil has numerous applications which includes its usage in boilers for heat and electricity, in engines and turbines for electricity, in chemicals production such as phenols, organic acids, and oxygenates or in transportation fuel production [79]. However, bio-oil derived transportation fuels require expensive upgrading techniques, and this route is currently less attractive for motor fuels production. To alleviate this disadvantage, reforming of bio-oil has been proposed and employed to produce hydrogen, another viable fuel for the future.

3.3 Bio-Oil Feedstock and Characterization

Bio-oils have been produced from different biomass feedstock such as corn stover [82] rice husk [18, 83], saw dust [34, 84], wood [85] [31], barley straw [86], poultry litter [87] and many others. A detailed review on bio-oil production techniques and its properties can be found elsewhere [88]. Physical and chemical properties of bio-oil are highly influenced by the composition of biomass. For example, Wang *et al.* [19] reported that sawdust has 54.5% C, 6.7 % H and 38.7 %O, while rice husk has 41% C, 7.4% H and 51.2% O and cotton stalk has about 42.3% C, 7.9% H and 49.4% O. Hydrogen yield is also affected by the chemical composition of bio-oils and therefore, the feedstock used to generate bio-oil plays a vital role in hydrogen production. Estimating the bio-oil composition is important in calculating the stoichiometric hydrogen (H_2) yield, which is discussed in the next section. Typical properties of bio-oil are summarized in Table 3.1 [89]. It is interesting to note that bio-oils are acidic in nature and the pH value is also highly dependent on the biomass type. For example, the bio-oils generated from sawdust, rice husk and cotton stalk had pH of about 2.1, 3.2, and 3.3, respectively [19].

Table 3.1: Typical properties of bio-oil

Water content	15-30
pH	2.5
Specific gravity	1.2
HHV (MJ/kg)	16-19
Viscosity, at 500^{o}C (cP)	40-100

Elemental Analysis, wt%:

C	54-58
H	5.5-7.0
N	0-0.2
O	35-40
Ash	0-0.2

3.4 Experimental

3.4.1 Materials

Aqueous phase of bio-oil obtained from fast-pyrolysis of pine was used for conducting all the experiments in this reforming study. A stock solution containing 15% by volume of aqueous bio-oil was prepared initially, and all further experiments were done using this stock solution directly or by diluting from it. This was done to eliminate possible dilution errors that might arise during preparation of reaction mixture. The elemental composition of the aqueous bio-oil stock solution and the 15% diluted bio-oil solution (listed in Table 3.2) were obtained from CHNS-O Elemental Analyzer (Model # 2400) purchased from PerkinElmer (MA, USA). All reactions were carried out in a 400 mL stainless steel high pressure batch reactor (Parr Model 4567, Parr Instrument Co., Moline, IL, USA) equipped with a mechanical stirrer and temperature controller system. The catalyst used - 0.05% of Ru supported in Al_2O_3 was in the form of pellets of size 3.2 mm (purchased from VWR, USA). The exit gas produced after the reaction was sent to a gas chromatography instrument for analysis. The GC equipped with TCD (Multigas 2, SRI 8610C, Torrance, CA) consisted of two columns - molecular sieve and Haysep D and Argon gas was used as the carrier gas throughout the study. Hydrogen, CH_4, N_2, and CO peaks appeared in the molecular sieve column, while the CO_2 peak appeared in the second column. One-point calibration was carried out with a standard gas before every experiment. The volume of gas produced after each run was measured using a flow meter coupled with a totalizer (Cole Parmer IL, USA). The carbon content of the reaction mixture and the reacted liquid was analyzed using Total Organic Carbon Analyzer (Shimadzu, USA). The compounds present in bio-oil and reacted liquid were determined using GC-MS (Agilent, USA). The BET surface area measurements of

the catalysts were done using Autosorb (Quantachrome, FL). The thermogravimetric analysis was carried out to determine the coke deposition using TGA (Shimadzu, USA).

Table 3.2: The elemental composition of the aqueous bio-oil stock solution and the 15% diluted bio-oil

Substrate	**C**	**H**	**N**	**S**	**O**
Bio-oil stock	18.28	8.58	0.91	0.34	71.89
15% Bio-oil	2.66	5.71	0.05	0.27	91.31

3.4.2 Experiments

As mentioned earlier, reforming experiments were performed in an air-tight glass reactor of 400 mL volume secured and clamped in a stainless steel case. Initially, about 50 mL of aqueous bio-oil of known concentration was added into the reactor vessel. For catalytic study, 0.05% Ru/Al_2O_3 catalyst was calcined for 3 h, reduced with 5% H_2 gas for 2 h at 500ºC and stored in desiccator. About 0.2 g of this calcined and reduced catalyst was added every time to the substrate. In order to remove the atmospheric gases present in the void volume, the reactor was washed out five times with inert N_2 gas. The reaction mixture was then agitated with a mechanical stirrer at 400 rpm, heated to desired temperature and allowed to undergo chemical reactions under autogenous pressure. The time for each run includes the heating rate to attain the reaction temperature. After the run, the reaction mixture was allowed to cool down to room temperature, and the volume of gas was measured using a flow meter coupled with a totalizer. The gases were then allowed to flow to the GC-TCD for exit gas composition analysis. The volume of liquid left over in the reactor was measured and then vacuum filtered over Whatman

filter paper (#2) to find the weight of residue left over. This liquid was stored in an air-tight container for the measurement of the total organic carbon. All experiments were conducted in triplicates. Statistical analysis was performed on the experimental data using JMP version 11 to determine whether the factors: time (1, 4, and 10 h), temperature (180, 230, and 280˚C) and bio-oil concentration (5, 10, and 15 vol %) affected the exit gas composition significantly.

A one-way ANOVA was initially performed to determine the p-values. A p-value greater than 0.05 implied there was no significant effect. For cases, when the p-values are lesser than 0.05, Tukey's test was performed to analyze the effect of each factor at three different levels.

3.5 Results and Discussion

Batch experiments were conducted to study the effect of three parameters at three different levels: time, temperature, and bio-oil concentration. The triplicate data were statistically analyzed to identify the factors that significantly affect the exit concentrations.

3.5.1 Effect of time on exit gas composition

Experiments were carried at three time points: 1, 4 and 10 hours to determine the appropriate runtime for each experiment and the exit gas composition was plotted as a function of time (shown in Figure 3.1). The H_2 concentration was found to increase initially, reaching a maximum at 4 h and then decrease. To determine if the change in H_2 concentration is statistically significant, one-way ANOVA was performed and the results are given in Table 3.3. The CO concentration followed a decreasing trend and attained a minimum value at 10 h and therefore, a four hour time period was chosen as the run time for all experiments henceforth. From the p-

values of time-based triplicate data (shown in Table 3.3), it can be concluded that there was significant effect of time on all the gas compositions except H_2.

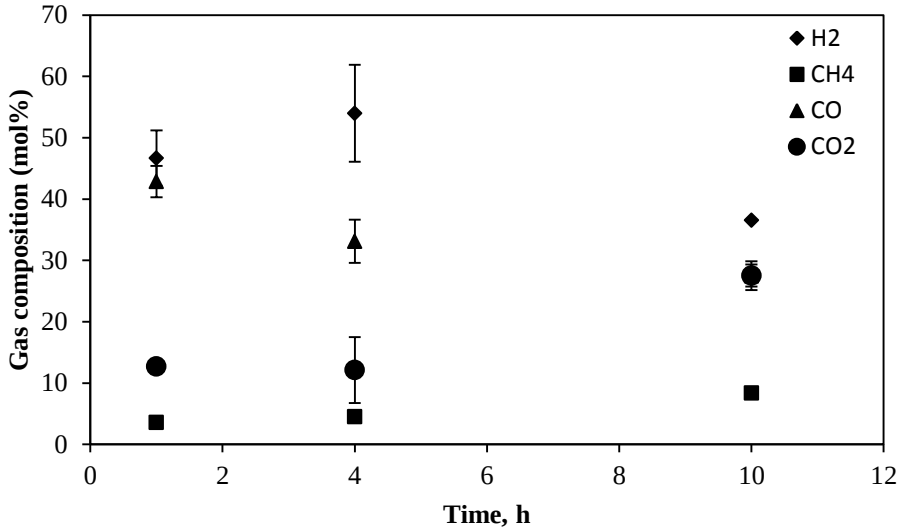

Figure 3.1: Exit gas composition as a function of time at 280 ºC for 15% bio oil solution

3.5.2 Effect of temperature on exit gas composition

Experiments were conducted to study the effect of temperature on two phase reforming of bio oil (Figure 3.2). It was found that an increase in temperature resulted in increased H_2 concentration, while the CO concentration was found to decrease with temperature. This can be explained by a two-step process: the first step being the decomposition of bio-oil and the second step being the water gas shift (WGS). Increase in temperature results in breaking down of the substrate to produce CO. The CO produced takes part in water gas shift reaction (WGS) [90] to produce more H_2 and CO_2 (Equation 3-2) which is evident from the Figure 3.2. The more CO is produced, the more WGS takes place and hence more H_2 is produced. This is also supported by the increasing trend in CO_2 concentration with temperature. However, no noticeable variation was observed in the CH_4 concentration. Since, the exit gas H_2 concentration was maximum at

280 ºC, this temperature was chosen for the concentration study. From the p-values it was found that the CH_4 composition was not significantly affected by the temperature (Table 3.4).

$$CO + H_2O \rightarrow H_2 + CO_2 \quad \Delta H^0_{298\,K} = -41\ kJmol^{-1} \qquad \text{(Eq.3-2)}$$

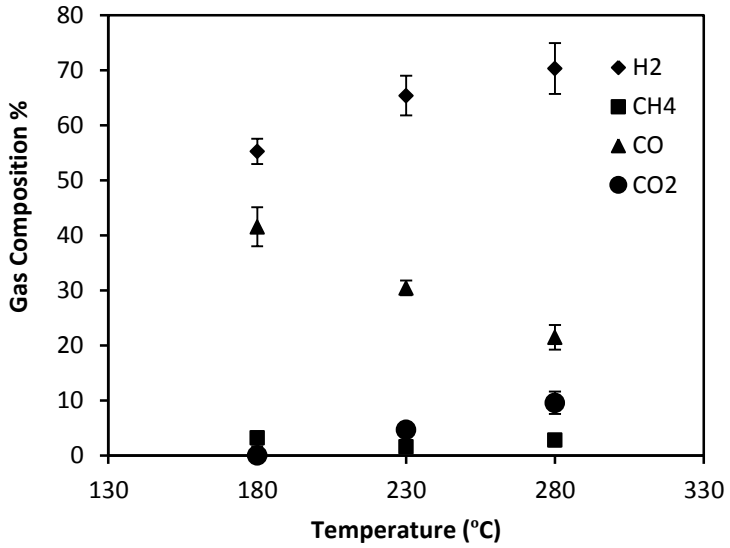

Figure 3.2: Exit gas composition as a function of temperature for 5% bio oil solution

3.5.3 Effect of concentration on exit gas composition

In order to study the effect of bio-oil concentration on the exit gas composition, three concentrations – 5%, 10% and 15% by volume in water were used. At 5% bio-oil concentration maximum H_2 yield and minimum CO yield were observed. The H_2 concentration was found to decrease with increase in concentration and the CO concentration was found to increase with concentration (Figure 3.3). The decomposition of bio-oil results in CO formation. However, as the substrate concentration increases, the amount of water available to take part in WGS reactions decreases. Hence, we see a decreasing trend in H_2 concentration and an increasing

trend in CO concentration. From the p-values, it can be concluded that the CO_2 composition was not significantly affected by the bio-oil concentration (Table 3.5).

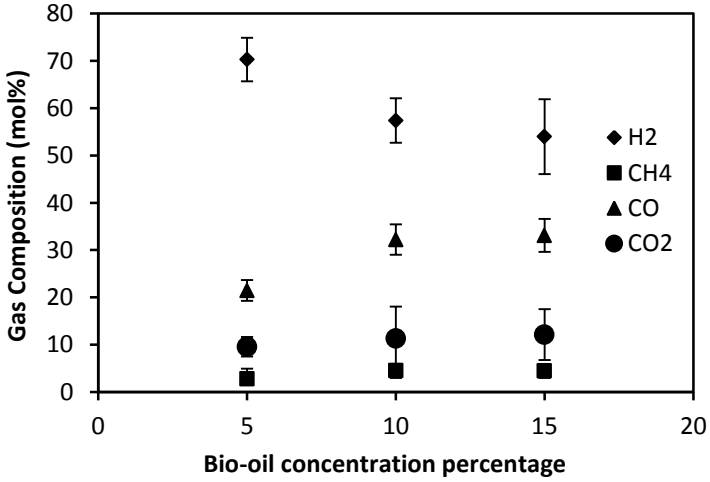

Figure 3.3: Exit gas composition as a function of bio-oil concentration at 280 ºC

Table 3.3: The least mean square values of exit gases listed as a function of time.

	H_2	CH_4	CO	CO_2
p-Value	0.0549	0.0003	0.0053	0.0091
Significance	Insignificant	Significant	Significant	Significant
1 h	-	$3.6B_1$	$42.9C_1$	$12.7D_1$
4 h	-	$4.5B_1$	$33.1C_2$	$12.1D_1$
10 h	-	$8.4B_2$	$27.5C_2$	$27.5D_2$

Note: Levels not connected by same subscript numbers are significantly different at the 0.05 level.

Table 3.4: The least mean square values of exit gases listed as a function of temperature.

	H_2	CH_4	CO	CO_2
p-Value	0.0061	0.8102	0.0002	0.0002
Significance	Significant	Insignificant	Significant	Significant
180 ˚C	$55.2A_1$	-	$41.5C_1$	$8.8E\text{-}16D_1$
230 ˚C	$65.4A_2$	-	$30.4C_2$	$4.7D_2$
280 ˚C	$70.3A_2$	-	$21.5C_3$	$9.6D_3$

Note: Levels not connected by same subscript numbers are significantly different at the 0.05 level.

Table 3.5: The least mean square values of exit gases listed as a function of bio-oil concentration

	H_2	CH_4	CO	CO_2
p-Value	0.0338	0.0062	0.0058	0.8254
Significance	Significant	Significant	Significant	Insignificant
5%	$70.3A_1$	$2.8B_1$	$21.5C_1$	-
10%	$57.4A_{12}$	$4.5B_2$	$32.2C_2$	-
15%	$54.0A_{23}$	$4.5B_2$	$33.1C_2$	-

Note: Levels not connected by same subscript numbers are significantly different at the 0.05 level.

3.5.4 Carbon distribution across different phases

Determining the carbon present in solid, liquid and gaseous phase helps in understanding the overall carbon conversion during the two-phase reforming process. For experiments performed at 280 ºC with 15% bio-oil solution, a maximum of about 25% gas phase carbon conversion was

achieved. The liquid phase carbon was about 45% at all bio-oil concentrations. The solid phase carbon was determined as the difference between the total carbon loaded into the system and the carbon in liquid and gas phases. The solid phase carbon was found to exhibit a decreasing trend with increasing bio-oil concentration. Figure 3.4 shows the carbon distribution across the three different phases as a function of bio-oil concentration.

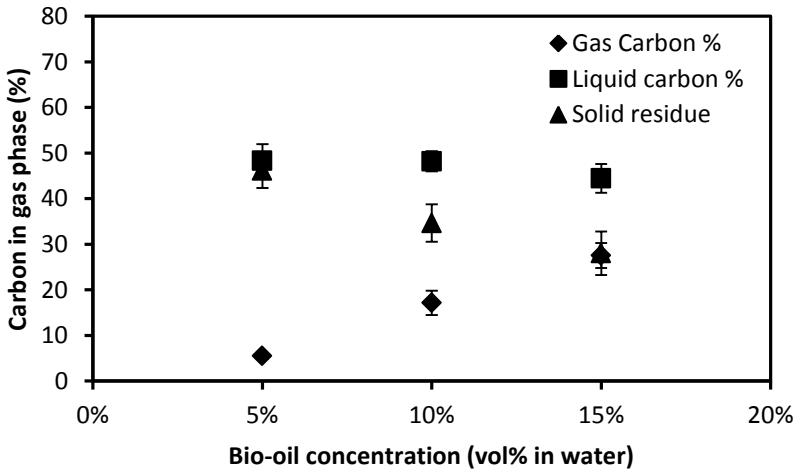

Figure 3.4: Carbon distribution across the three different phases as a function of bio-oil concentration at 280 ºC

3.5.5 Catalytic two-phase reforming

In order to improve the H_2 concentration in the exit gas, Ru supported on Al_2O_3 was used as catalyst to study bio-oil two-phase reforming. About 0.2 g of catalyst was calcined and reduced at 800 ºC for 4 h before adding it to the reactor and the positive effect of catalyst on H_2 yield is shown in Figures 3.5 and 3.6. Figure 3.5 shows a comparative study of catalytic and non-catalytic exit gas compositions for 4 h runs carried out at 280 ˚C with 15% bio-oil. It is evident that there is an increase in H_2 concentration and decrease in CO concentration with the use of catalyst.

Figure 3.6 shows a comparison of H_2 and CO concentration trends with increasing temperature in the presence and absence of catalyst. In the absence of catalyst, H_2 and CO concentrations were found to increase and decrease respectively with temperature. The introduction of catalyst brought about a noticeable increase in H_2 concentration at all the three temperatures. However, the catalyst was found to be most effective at the lowest temperature (180 ˚C).

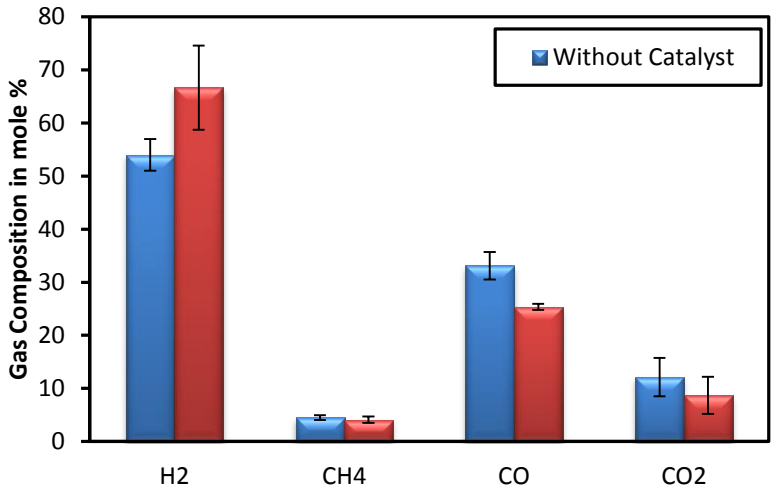

Figure 3.5: A comparison of exit gas compositions from catalytic and non-catalytic experiments run for 4 h at 280 ˚C with 15% bio-oil.

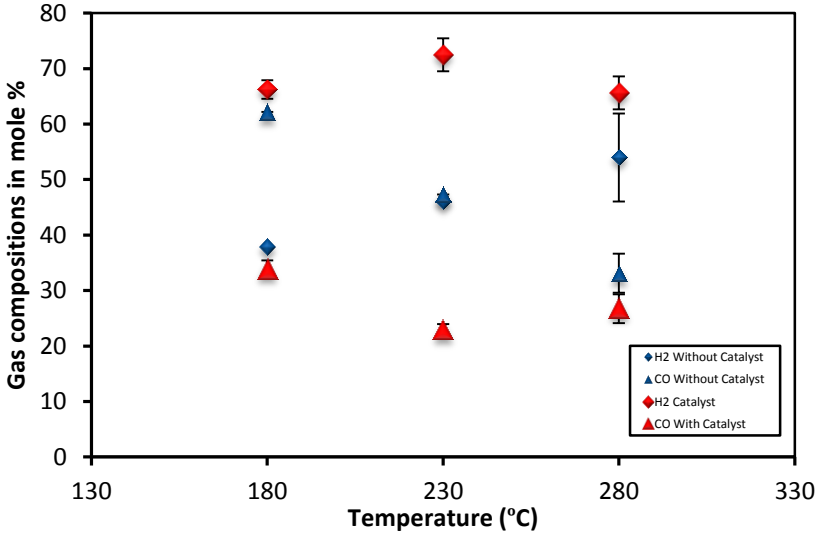

Figure 3.6: A comparison of H_2 and CO concentrations during catalytic and non-catalytic reforming as a function of temperature.

3.5.6 GC-MS analysis

In order to understand the reaction mechanism, the organic compounds in the substrate (aqueous bio-oil) and reacted liquid were analyzed using a GC-MS. The results confirmed the conversion of sugars, aldehydes and diols to simpler ketones during two-phase reforming. Five carbon ketone: 2-cyclopenten 1-one was formed during the absence of catalyst. Further simplified four carbon ketones such as butyrolactones were formed in the presence of Ru/Al_2O_3 catalyst. The list of compounds from GC-MS analysis of raw bio-oil and reacted bio-oil (from catalytic and non-catalytic experiments) is listed in Appendix I.

3.5.7 Activation Energy Determination

In order to investigate the catalytic effect of Ru/Al_2O_3 on carbon conversion from liquid phase, a kinetic study was carried out. The activation energy for the reforming reactions was determined using the rate law and the Arrhenius equation. The general rate equation for any n^{th} order chemical reaction is given by Equation 3-3.

$$\frac{dC}{dt} = - KC^n \qquad \text{(Eq.3-3)}$$

The rate constant *K* can be obtained from the intercept of the graph of *ln (dc/dt)* versus *ln C*. The change in concentration over time was determined from the difference in carbon content of the bio-oil fed and the liquid present after the reaction has taken place. This carbon concentration data was obtained from TOC.

The relationship between activation energy (E_a) and reaction rate for any chemical reaction is given by the Arrhenius equation:

$$K = K_o e^{-Ea/RT} \qquad \text{(Eq.3-4)}$$

where R is the gas constant, T is the reaction temperature, K_o is the frequency factor and K is the rate constant.

The activation energy was determined from a plot between *ln K* and *1/T*, the slope of which gives $-E_a/R$ (Figure 3.7). Dave and Pant (2011) determined the activation energy during steam reforming of glycerol over Ni / Ceria promoted with Zr to be 43.4 kJ/mol [91]. Praharso *et al.* (2004) reported an activation energy of 44 kJ mol^{-1} for iso-octane steam reforming over Ni-based catalyst [92]. The activation energy for non-catalytic two-phase reforming of bio-oil was found to be 65.57 kJ/mol, which was later reduced to 56.05 kJ/mol with the use of Ru/Al_2O_3 catalyst. This result is comparably lower than the apparent activation energies reported for APR of ethylene glycol (100 kJ/mol) and methanol (140 kJ/mol) using Pt/Al_2O_3 catalyst [93].

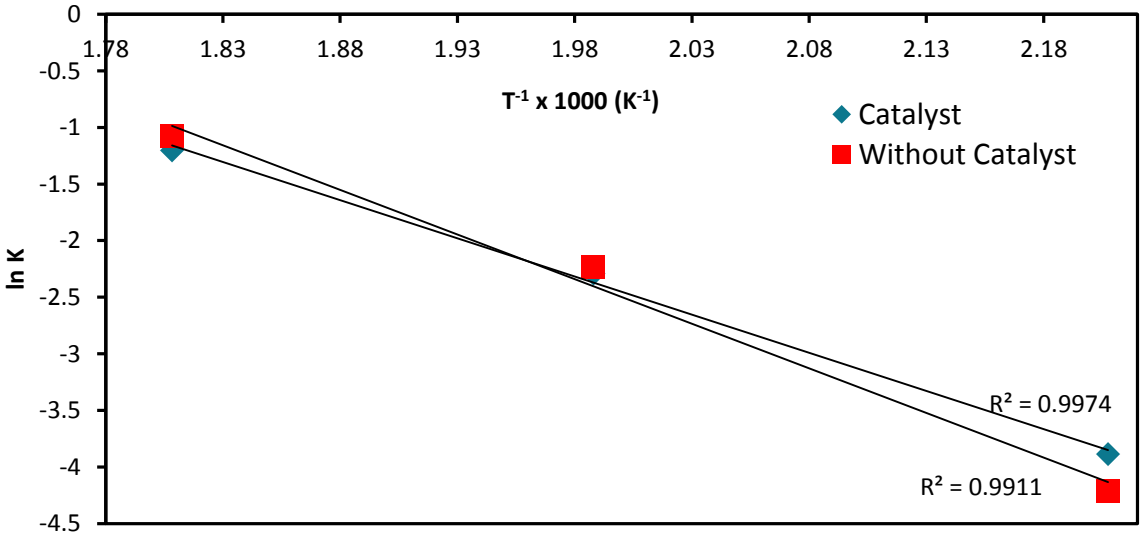

Figure 3.7: A plot of *ln K* against *1/T* for experiments done with and without catalyst

3.5.8 Hydrogen selectivity

The selectivity of a product is an effective way to measure the efficiency of a chemical reaction. The quality of the gas produced by the two-phase reforming process was given in terms of H_2 selectivity. The H_2 selectivity for a chemical reaction is given by Equation 3-5

$$S_{H_2} = \frac{M_{H_2}}{\Sigma M_T} \times 100 \qquad \text{(Eq.3-5)}$$

where, S_{H_2} is selectivity of H_2, M_{H2} is the number of moles of H in H_2 and M_T is the total number of moles of H in the product (H_2 and CH_4).

Figure 3.8 depicts a plot of H_2 selectivity versus temperature. The selectivity was found to exhibit a decreasing trend when the temperature was increased from 180 ºC to 280 ºC for both catalytic and non-catalytic two-phase reforming. However, in the presence of Ru/Al_2O_3 catalyst, the H_2 selectivity was found to be higher than that of non-catalytic reforming at 230 and 280 ºC. At 180 ºC, the H_2 selectivities were found to be 100% due of the absence of CH_4 at that temperature. The catalyst was found to effectively increase the H_2 selectivity at higher temperatures.

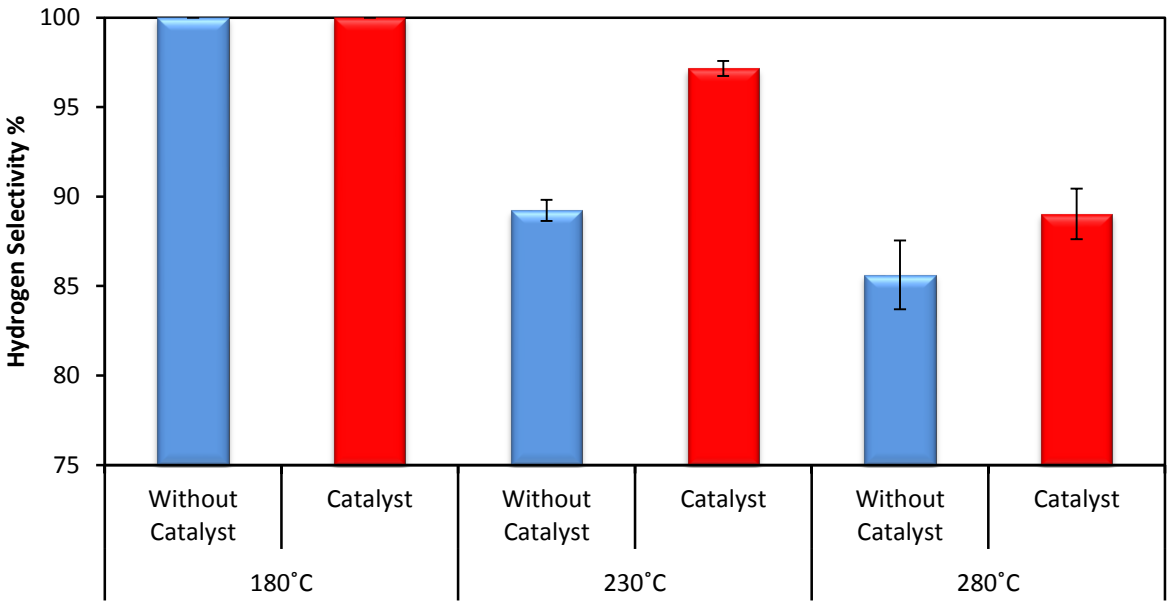

Figure 3.8: Comparison of Hydrogen selectivity for non-catalytic and catalytic bio-oil reforming as a function of temperature for 15% bio-oil solution.

The carbon percentage in the gas phases was calculated from the CH_4, CO_2 and CO concentrations in the exit gas and that present in the liquid phase was determined directly from the total organic carbon analyzer. The solid phase carbon was obtained from the difference between total carbon fed into the system and the carbon present in the liquid and gas phases. A comparison of the carbon distribution across different phases during catalytic and non-catalytic reforming is shown in Figure 3.9. It can be observed that there is more coke formation in the presence of Ru/Al_2O_3 catalyst compared to non-catalyst reforming. Also, the carbon conversion to gas phase is lesser in the presence of catalyst. This implies that the catalyst is not very effective in gas phase carbon conversion although it improves H_2 yield.

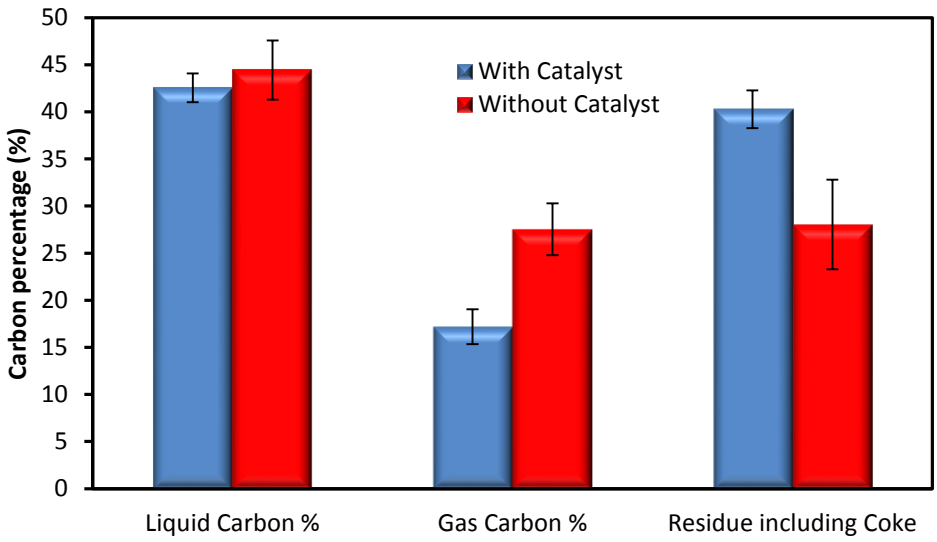

Figure 3.9: The carbon distribution in the three different phases during non-catalytic and catalytic runs performed at 280 ºC on 15% bio-oil solution

3.5.9 Coke deposition analysis

In order to determine the coke formation on the surface of the catalyst a thermogravimetric analysis (TGA) of the fresh and spent catalysts was carried out and the TGA graph is illustrated in Figure 3.10. About 10 mg of the catalyst was heated at 30 ºC /min to 800 ºC in an airflow rate of 20 mL/min. The change in weight with temperature was recorded and the percentage of total weight lost was calculated. The total weight loss during the analysis is equivalent to the coke deposited on the catalytic surface. As expected, the fresh catalyst did not show any measurable weight loss. The percentage of coke deposited on catalyst recovered from experiments performed at 280 ºC was the least while maximum deposition was observed at 180 ºC. Coke deposition on catalyst recovered at three different temperatures using 15% bio-oil solution has been reported in Table 3.6.

Table 3.6: The coke deposition on catalytic surface as a function of experimental temperature

Experimental Temperature (ºC)	Coke Percentage (%)
180	15.65
230	12.23
280	7.89

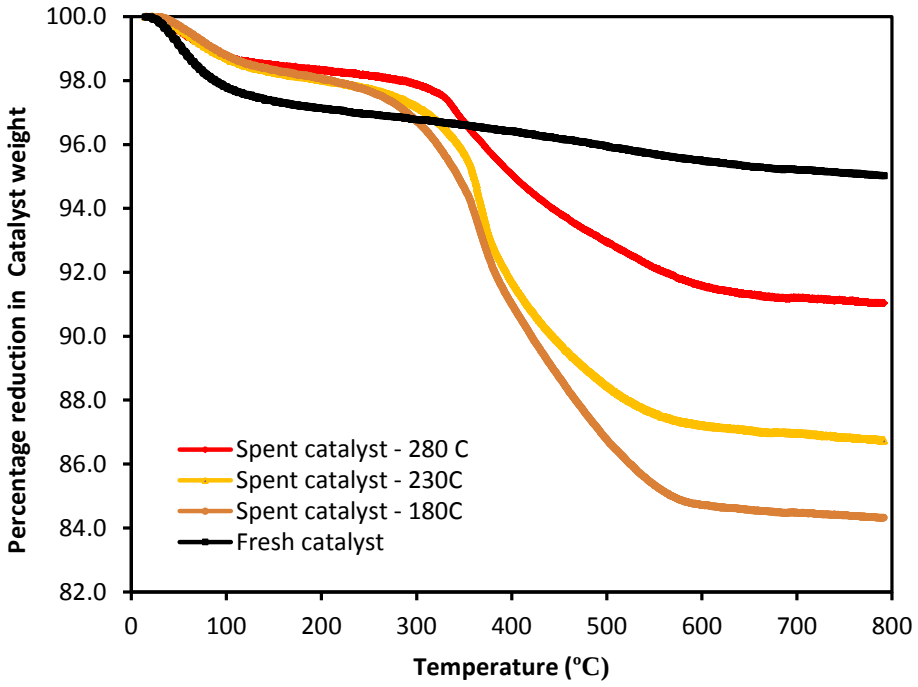

Figure 3.10: TGA plot for fresh and spent Ru/Al_2O_3 catalyst obtained at three experimental temperatures

3.5.10 Surface area measurement

Brunauer-Emmett-Teller (BET) surface area measurements were determined using Autosorb (Quantachrome, FL) to confirm the coking trend established by TGA. The surface area of the fresh catalyst was found to be much higher than that of spent catalyst at three different experimental temperatures (shown in Table 3.7), which is expected due to the absence of carbon

deposition on the fresh catalyst. It was observed that the spent catalyst obtained at higher experimental temperature (280 ºC) exhibited higher surface area compared to the ones obtained from lower experimental temperatures (180 and 230 ºC). An increasing trend in the BET surface area was observed with increase in experimental temperature implying that the coke formation decreases with temperature. This reconfirms the coking trend established by TGA.

Table 3.7: The BET surface area comparison between fresh catalyst and spent catalyst obtained at three experimental temperatures.

Catalyst type	**BET surface area (m^2/g)**
Fresh catalyst	45.233
Spent catalyst obtained at 180 ºC	3.273
Spent catalyst obtained at 230 ºC	3.539
Spent catalyst obtained at 280 ºC	4.071

3.6 Conclusion

Non-catalytic and catalytic two-phase reforming of aqueous bio-oil was carried out at three different temperatures, the reaction kinetics and H_2 selectivities were investigated. During non-catalytic reforming, the average molar concentration of H_2 was found to increase with temperature and reached a maximum of 70% at 280 ºC for 15% bio-oil concentration. The addition of Ru/Al_2O_3 catalyst improved H_2 concentration and selectivity. The H_2 selectivity decreased with temperature for both non-catalytic and catalytic two-phase reforming of aqueous bio-oil. However, in the presence of catalyst, the selectivity was found to be higher at elevated temperatures (230 ºC and 280 ºC). Further, kinetic studies revealed a decrease in activation

energy as compared to non-catalytic reforming. The activation energies during catalytic and non-catalytic bio-oil two-phase reforming were: 56 kJ/mol and 66 kJ/mol, respectively. The GC-MS results revealed the complete conversion of sugars, aldehydes and diols to simpler ketones during the reforming process. Although the catalyst enhanced the H_2 yield during bio-oil two-phase reforming, it did not improve the gas carbon conversion. The TGA and BET surface area measurements concluded that the coke deposition on the catalyst reduced with increase in temperature.

Chapter 4

Conversion of CO and CH_4 in Biomass Synthesis Gas for Hydrogen Production

4.0 Abstract

The premise of this research is to find whether methane (CH_4) and carbon dioxide (CO_2) produced during biomass gasification can be converted to carbon monoxide (CO) and hydrogen (H_2). Simultaneous steam-and dry- reforming was conducted by selecting three process parameters (temperature, CO_2:CH_4, and CH_4:H_2O ratios). Experiments were carried out at three levels of temperature (800^0C, 825^0C and 850^0C), CO_2:CH_4 ratio (2:1, 1:1 and 1:2), and CH_4:H_2O ratio (1:1, 1:2 and 1:3) at a residence time of 3.5×10^{-3} g_{cat}min/cc using a custom mixed gas that resembles biomass synthesis gas, over a commercial catalyst. Experiments were conducted using a Box-Behnken approach to evaluate the effect of the process variables. The average CO and CO_2 selectivities were 68% and 18%, respectively, while the CH_4 and CO_2 conversions were about 65% and 48%, respectively. The results showed optimum conditions for maximum CH_4 conversion was at 800^0C, CO_2:CH_4 ratio and CH_4:H_2O ratios of 1:1.

4.1 Introduction

The conversion of biomass to synthesis gas and subsequent conversion to gasoline or diesel range compounds have a significant potential in reducing the United States' dependence on current petroleum imports. Nonetheless, synthesis gas produced from biomass gasification

contains methane (CH_4) and carbon dioxide (CO_2), which are often undesirable compounds for liquid fuel production process such as Fischer-Tropsch synthesis. Methane and CO_2 are considered as greenhouse gases (GHG), and the carbon that is produced from photosynthesis process is being lost as undesirable compounds. The primary GHGs in the earth's atmosphere are CO_2, CH_4, water vapor and ozone. Amongst them CO_2 and CH_4 contributes to 9-26% and 4-9% of the total greenhouse effect, respectively and hence, mitigation of both of these gases is of a major concern [94]. Combustion of fossil fuels also results in CO_2 emissions affecting environment. Dry reforming of methane (DRM) not only utilizes the GHGs (CH_4 and CO_2) but also produces valuable synthesis gas. Synthesis gas or syngas (H_2 and CO) finds its use in Fischer-Tropsch synthesis to produce liquid hydrocarbons and the hydrogen produced in DRM can also be used in fuel cells [95]. The dry reforming of CH_4 is given in the Equation 4-1:

$$CH_4 + CO_2 \longrightarrow 2\,H_2 + 2\,CO \qquad \Delta H^o_{298K} = 247 \text{ kJ-mol}^{-1} \qquad \text{(Eq.4-1)}$$

As it is observed, each mole of CH_4 reacts with a mole of CO_2 to form two moles of H_2 and two moles of CO. This process is accompanied by several side reactions such as reverse water-gas shift (Equation 4-2), methane cracking (Equation 4-3) and Boudouard reaction (Equation 4-4) [96].

$$CO_2 + H_2 \longrightarrow CO + H_2O \qquad \Delta H^o_{298K} = 41 \text{ kJ-mol}^{-1} \qquad \text{(Eq.4-2)}$$

$$CH_4 \longrightarrow C + 2\,H_2 \qquad \Delta H^o_{298K} = 75 \text{ kJ-mol}^{-1} \qquad \text{(Eq.4-3)}$$

$$2\,CO \longrightarrow C + CO_2 \qquad \Delta H^o_{298K} = -171 \text{ kJ-mol}^{-1} \qquad \text{(Eq.4-4)}$$

Steam reforming of CH_4 is given by the following equation (Eqn. 4-5) [97],

$$CH_4 + H_2O \longrightarrow 3\,H_2 + CO \qquad \Delta H^o_{298K} = 206 \text{ kJ-mol}^{-1} \qquad \text{(Eq.4-5)}$$

Dry and steam reforming processes are highly endothermic but the gasification temperatures are favorable for this type of reaction. In addition, catalyst plays an important role in CH_4 reforming by absorbing CH_4 on to the metal sites and producing hydrogen and CH_x (x=0-4). Commonly used catalysts consists of metals like Ni, Ru, Rh, Pt, Pd, Co, and Ir supported on oxide supports such as Al_2O_3, MgO, SiO_2, TiO_2, La_2O_3 and ZrO_2 [94]. Other factors that affect CH_4 include reaction temperature, gas hourly velocity, and residence time.

Brungs *et al.* [98] demonstrated dry reforming of CH_4 with Mo_2C catalyst on various supports at 947^0C, 8 bar and a gas hourly space velocity of 0.43×10^2 min^{-1} and found that Al_2O_3 was the most stable support among them. Ruthenium catalyst supported over silica and γ- alumina were used by Ferreira-Aparicio *et al.* [99] to carry out CH_4 dry reforming who also proposed reaction kinetics. Maestri *et al.* [100] did a thermodynamic study using microkinetic model for steam and dry reforming of CH_4 on Rh. Laosiripojana *et al.* [101] conducted experiments with Ni/Al_2O_3 doped with 0 -14% Ce catalyst (size 100-200 μm) at a residence time of 5×10^{-4} g min/cc in the temperature range of 825^0C and 900^0C. Their study found out that the high surface area Ce synthesized had a better reforming ability and coke resistance compared to Ni/Al_2O_3. Similar experiments were conducted by Courson *et al.* [102] using Ni supported on olivine from 600 ^{0}C to 850 ^{0}C at a feed flow rate of 50 cc/min. Guo *et al.* [103] carried out experiments at 750 ^{0}C using Ni supported on magnesium aluminate spinels at residence time of 0.67×10^{-3}g min/cc. Among the three supports used (γ-Al_2O_3, MgO-γ-Al_2O_3, and $MgAl_2O_4$) $MgAl_2O_4$ exhibited stable activity without deactivation. Sahli *et al.* [104] used Ni/Al_2O_4 to study dry reforming of CH_4 from 700 ^{0}C to 800 ^{0}C at 4×10^{-3}g min/cc. They proposed that reduction of Ni at low temperatures is facilitated at Ni/Al ratios higher than 0.5. Martinez *et al.* [105] studied the effect of La_2O_3 loading on Ni/Al_2O_3 in a similar study. Tomishige *et al.* [106] studied the effect of

contact time on the process using Pt and Ni on Al_2O_3 support as catalyst at 850 ^{0}C. They found that catalyst fluidization coupled with high pressure alleviated carbon formation. The effect of MgO weight percent on Co/SiO_2 catalyst at was 800 ^{0}C investigated by Bouarab *et al.* [107]. They proposed an improved catalytic activity by addition of magnesia. Liu and Au [108] studied catalytic stability using $La_2NiO_4/\gamma\text{-}Al_2O_3$ for CO_2 reforming of CH_4 at a residence time of 1.25×10^{-3} g min/ cc and found that the H_2 and CO yields obtained using catalyst calcined at 800 ^{0}C were higher than that calcined at 500 ^{0}C. Tsyganok *et al.* [109] reported a novel method of catalyst preparation for mixed oxide catalyst and carried out dry reforming of CH_4 over Ni containing Mg–Al layered double hydroxides (LDH). Although there is plethora of studies available on dry reforming of CH_4 using different metal supported catalyst, the interest of this study was to test commercial catalysts for reforming CH_4 and CO_2, produced during biomass gasification.

The overall goal of this study is to minimize CO_2 and CH_4 formation while maximizing CO and H_2 production that can be used for liquid synthesis using process like Fisher-Tropsch. The reason for using the commercial catalyst reformax 250 for this research is that it is a Ni based CH_4 reforming catalyst. In addition, although a number of studies have been carried out on dry reforming of CH_4, most of the work was focused on using "one-factor at a time approach" to analyze the influence of process parameters. The one-factor approach, unlike this study, will not reveal interaction effects of those variables and process optimization is often difficult. Although a lot of research has been carried out on the use of different metal supported catalyst for CH_4 reforming, no work is available in the open literature on the effect of simultaneous steam and dry CO_2 reforming of CH_4 using Ni based CH_4 reforming commercial catalyst-reformax 250. The catalyst (reformax 250) was chosen due to its methane reforming ability. The objective of this

study was to examine the collective effect of temperature, CO_2:CH_4 ratio (dry reforming) and CH_4: steam ratio (steam reforming) on CH_4 reforming using a commercial catalyst. The objective of this work includes reduction of CH_4 and CO_2 concentrations, production of H_2 and CO (syngas) and find out whether the H_2:CO ratio can be increased by varying the selected process parameters.

4.2 Materials and Methods

Simultaneous dry and steam reforming of CH_4 was carried out in a fixed-bed reactor of 0.5 inch diameter and 18 inches long at temperatures from 800^0C to 850^0C and atmospheric pressure in the presence of a commercial CH_4 reforming catalyst (reformax 250). The reactor was packed with quartz wool on both sides with the catalysts in-between. An alloy (Inconel 620) was selected as the reactor material because of its stability at high temperatures. The inlet gas consisted of a mixture of 20% H_2, 10% CH_4, 25% N_2, 20% CO_2, and 25% CO, (all in mole percentage) and the flow rate of synthesis gas was maintained at 100 cc/min using a mass flow controller(Omega, Stamford, CT). The basis for selecting this mixture is to have an inlet stream with concentrations similar to that of syngas produced during biomass gasification. Experiments were conducted at three levels of temperature (800^0C, 825^0C and 850^0C), CO_2:CH_4 ratios (2:1, 1:1, and 1:2), and CH_4: steam ratios (1:1, 1:2, and 1:3). The CO_2:CH_4 ratios were adjusted by having an additional CH_4 stream and CH_4: steam ratios were adjusted by varying the water pumping rate. A syringe pump (Chemyx, Nexus 3000 series, Stafford, TX) was used to pump in water through a tubular furnace, which was maintained at 200^0C, in order to produce steam. The size of the commercial catalyst used was between 0.595mm and 2.38 mm, however its composition is proprietary.

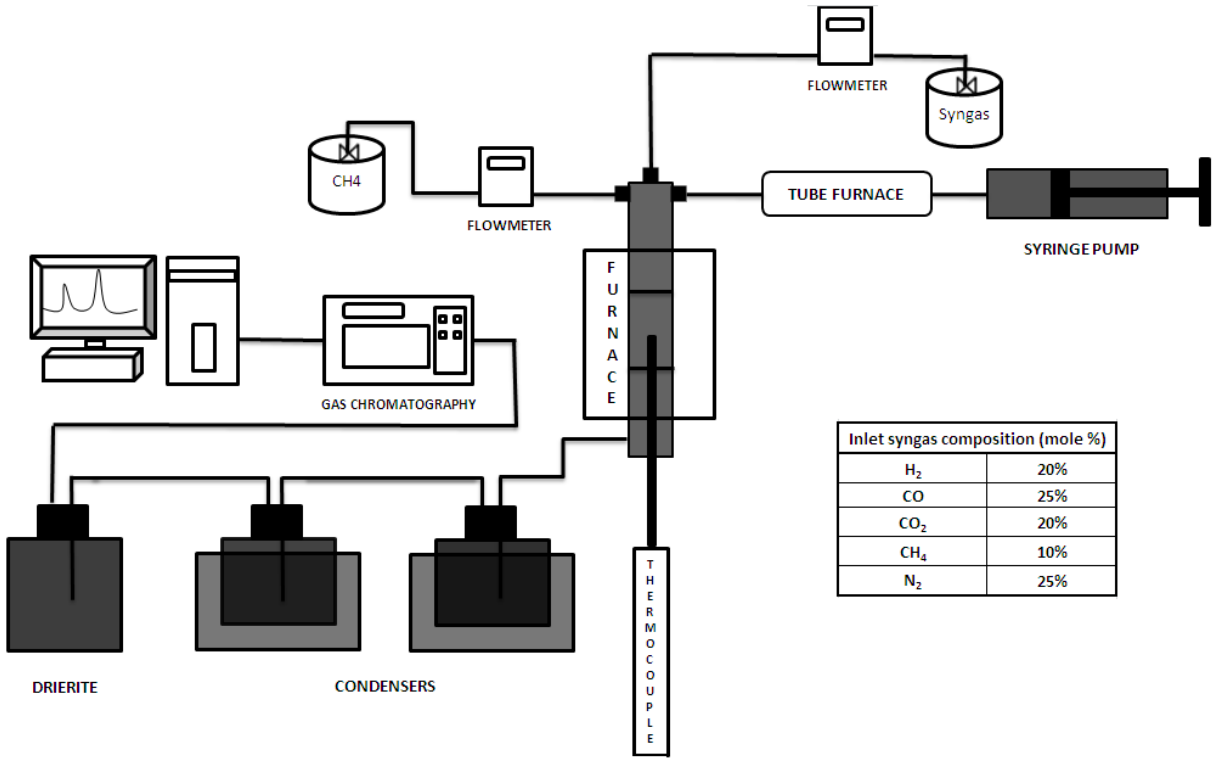

Figure 4.1: An experimental setup used for methane reforming

An experimental setup used for this study is illustrated in Figure 4.1. A known weight of the catalyst (0.35g) was loaded into the reactor, heated to 800^0C and reduced *in-situ* with 35 cc/min of 5% H_2 in helium for two hours each time before an experiment was conducted. The residence time (defined as the ratio of weight of catalyst (0.35 g) to the flowrate (100 cc/min) of inlet gas) used for the experiments was $3.5\times10^{-3}g_{cat}$ min/cc. Experiments were carried out for 20 h to test the stability of a catalyst under different experimental conditions. Temperature inside the reactor, at the catalyst-bed, was measured using a K-type thermocouple (Stamford, CT) and recorded continuously using a data logger. The exit gas, produced after the reaction, was cooled using two ice-bath condensers and then passed through a moisture trap to remove water vapor before sending it to a gas chromatography (GC) for gas analysis. The GC (Multigas 2, SRI 8610C, Torrance, CA) consisted of two columns –molecular sieve and Haysep D. Hydrogen, CH_4, N_2,

and CO peaks appeared in the molecular sieve column while CO_2 peak appeared in the second column. One-point calibration was carried out with a standard gas before conducting an experiment. Argon gas was used as the carrier gas throughout the study, and the gas compositions were recorded every 10 minutes for 20 h.

Initially, the superficial inlet gas velocity was varied from 4.6×10^{-3} m/s to 1.3×10^{-2} m/s to check if there is a mass-transfer limitation. At both the superficial gas velocities, CH_4 reforming rate were found to be same indicating the mass transfer effect was negligible. A similar test runs were conducted based on catalyst size to find out if there were any intra-particle diffusion limitations. The commercial catalyst was obtained in pellet form and was crushed to reduce the size so that it can be inserted inside the reactor. Different particle sizes were obtained by sieving, and the size of the catalyst used to check intra-particle diffusion ranged from 2.38 mm to 0.595 mm. The performance of the commercial catalyst was presented in the form of CO and CO_2 selectivities (Eqn. 4-6) and CH_4 and CO_2 conversions (Eqns. 4-7 and 4-8). The equations for the parameters are given below.

$$\text{Selectivity of species I} = \frac{\text{Moles of C in species i}}{\text{Total moles of C in product}} \times 100 \qquad \text{(Eq. 4-6)}$$

where species i = CO, CO_2, and CH_4 [110].

$$\text{Methane conversion} = \frac{\text{(Methane in – Methane out)}}{\text{Methane in}} \times 100 \qquad \text{(Eq. 4-7)}$$

$$\text{Carbon dioxide conversion} = \frac{CO_2 \text{ in} - CO_2 \text{ out}}{CO_2 \text{ in}} \times 100 \qquad \text{(Eq. 4-8)}$$

The analysis of variance (ANOVA) for the experimental results was performed using Minitab 15 software at 95% confidence level. The significant and insignificant terms were identified after

carrying out the analysis of variance (ANOVA) for the exit gas concentrations for the three factors.

4.3 Response Surface Methodology

Response surface methodology is a statistical optimization tool that aids in establishing a relationship between different experimental factors and the results of interest. This powerful technique helps in finding the optimum response in relation to the experimental factors which are designated as A (temperature), B (CO_2:CH_4 ratio) and C (CH_4:H_2O ratio). Performing the statistically designed experiments, estimating the coefficients in the quadratic polynomial equation and predicting the response are the three major steps involved in surface response methodology [111]. The response for a system involving three independent variables can be given by a quadratic polynomial equation of second order as shown in Equation (4-9):

$$Y = X_0 + X_1 A + X_2 B + X_3 C + X_{12} A B + X_{13} A C + X_{23} B C + X_{11} A^2 + X_{22} B^2 + X_{33} C^2 \quad \text{(Eq. 4-9)}$$

where,

Y = predicted result,

X_0 = constant,

X_1, X_2, X_3 = linear coefficients,

X_{11}, X_{22}, X_{33} = quadratic coefficients,

X_{12}, X_{13}, X_{23}= cross product coefficients.

A Box-Behnken design was implemented because it involves fewer runs (15 runs) than a full factorial design. However, this design allows three runs around the center point for a uniform

estimate of the prediction variance over the design space. The high, middle and low levels of each variable were designated 1, 0 and -1 as shown Table 4.1. Temperatures were chosen with a difference of 25 ^{0}C from the middle value (825 ^{0}C), one 25 ^{0}C higher and the other one 25 ^{0}C lesser while the ratios were chosen with increasing and decreasing moles from the middle value. For example, in case of CO_2:CH_4 ratio, the CH_4 moles increased from levels 0 to 1 and decreased from levels 0 to -1 by the same factor. Similar systematic trend was chosen for CH_4:H_2O ratio.

Table 4.1: High, middle and low levels of the variables

Factor levels	**Temperature (°C)**	**CO_2: CH_4**	**CH_4: H_2O**
-1	800 (-1)	2:1 (-1)	1:1 (-1)
0	825 (0)	1:1 (0)	1:2 0)
1	850 (1)	1:2 (1)	1:3 (1)

4.4 Results and Discussion

Figure 4.2 compares the inlet synthesis gas with the exit gas steady-state concentrations for the 20 h run with and without catalyst under same experimental conditions. Figure 3.3 shows the exit gas concentrations at 800^{0}C for a 12 h run with and without catalyst under identical experimental conditions. As can be seen in Figure 4.3, the catalyst activity is fairly stable. From Figures 4.2 and 4.3, it can be observed that there is an appreciable increase in H_2 and CO concentrations along with a simultaneous decrease in CO_2 and CH_4 concentrations. The H_2 and CO concentrations increased by 29% and 48% respectively, while the CO_2 and CH_4 concentrations decreased by 65% and 94% respectively with the use of catalyst. The stable exit gas concentration even after 12 h implies that the catalytic capacity did not reach saturation and reuse of the catalyst without reactivation was possible.

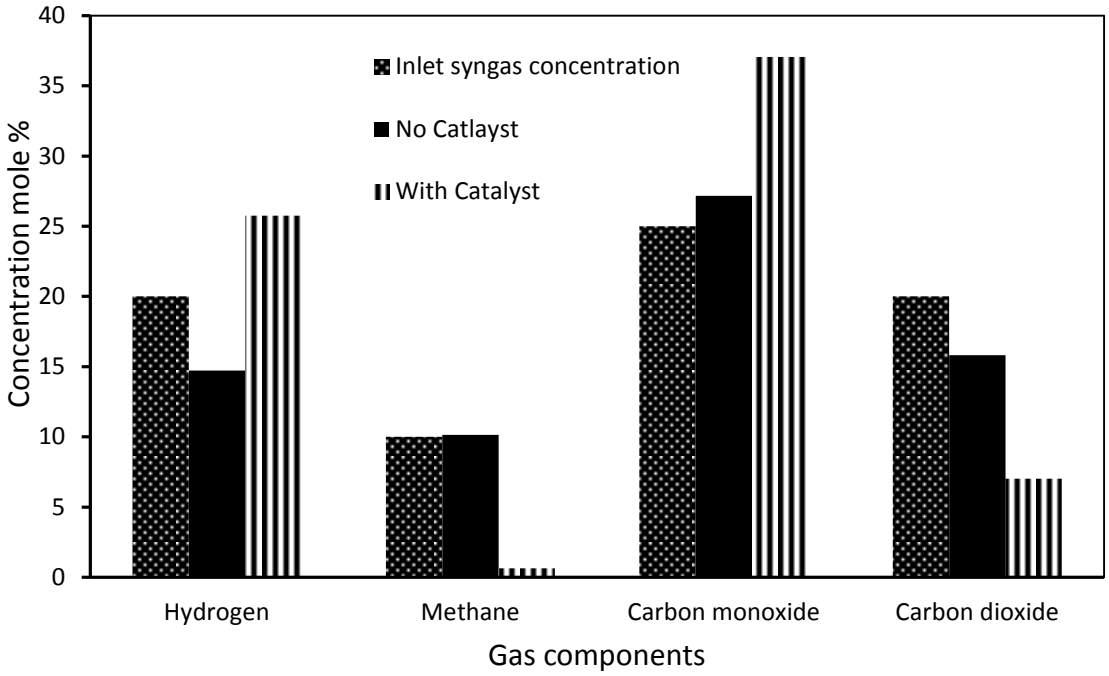

Figure 4.2: Comparison of inlet synthesis gas and the steady-state exit gas with and without catalyst (Experimental conditions: inlet syngas concentration at room temperature; "with catalyst" and "no catalyst": steady state exit gas concentration data at 800^0C, and CO_2:CH_4 ratio of 2:1at 20^{th}hr, residence time: 3.5×10^{-3}g min/cc)

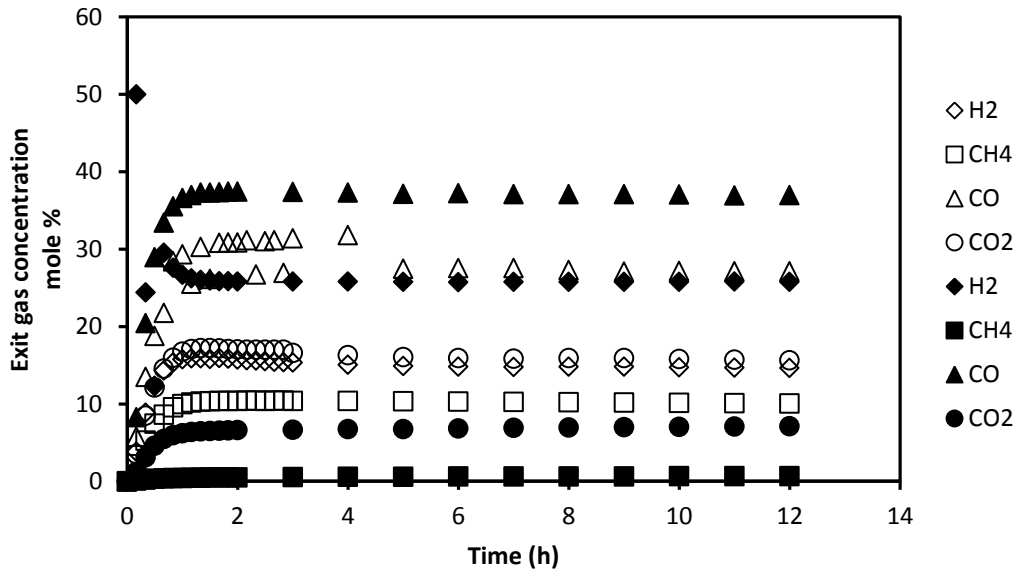

Figure 4.3: Comparison of exit gas concentrations with and without catalyst at 800^{0}C, CO_2:CH_4 ratio 2:1[with catalyst (filled symbols); without catalyst (open symbol)]

Table 4.2 summarizes the design of experiments along with the exit gas concentrations, H_2:CO ratios, CO and CO_2 selectivities and CH_4 and CO_2 conversions. For the simultaneous reforming process using commercial catalyst (reformax 250), the average CO and CO_2 selectivities were found to be 68% and 18% respectively, while CH_4 and CO_2 conversions were about 65% and 49% respectively. The goal here is to decrease the selectivity of CO_2 while increasing CO's selectivity. Based on the experimental conditions, the ratio of H_2:CO did not increase although high conversions of CH_4 and CO_2 were achieved. Bouarab *et al.* [107] reported CH_4 and CO_2 conversions of 42.7% and 55.6% at 600^{0}C under thermodynamic equilibrium which is comparable to the average CH_4 and CO_2 conversions (65% and 49%) obtained in this study. Castro Luna *et al.* [96] achieved maximum CH_4 and CO_2 conversions of 85% and 91% respectively at 750 ºC using Ni/Al_2O_3 catalyst. The maximum CH_4 and CO_2 conversions obtained in our experiments are 89% and 61% respectively. Courson *et al.* [102] established that

95% and 88% CH_4 conversion took place at 750^{0}C for dry and steam reforming, respectively which is also similar to the results obtained in this study.

Table 4.2: Design of experiments along with responses

DOE	H_2:CO	CH_4	CO	CO_2	H_2	Selectivity		Conversion	
						CO	CO_2	CH_4	CO_2
0 -1 -1	0.67	1.53	40.13	6.6	26.84	83.15	13.68	81.86	61.20
0 0 0	0.69	3.98	35.08	9.77	24.23	71.84	20.01	78.00	46.24
0 1 1	0.84	15.24	30.07	7.22	25.18	57.24	13.74	47.05	49.72
-1 0 1	0.73	5.7	30.78	12.01	22.33	63.48	24.77	69.46	35.81
0 0 0	0.69	3.81	35.06	9.78	24.26	72.07	20.1	78.45	44.83
-1 0 -1	0.72	1.83	39.38	7.51	28.43	80.83	15.41	89.32	56.17
1 1 0	0.83	12.69	31.28	5.89	25.99	62.74	11.81	56.37	59.44
1 0 -1	0.72	3.35	34.75	8.58	25.19	74.44	18.38	81.34	52.26
-1 -1 0	0.66	2.54	38.33	8.04	25.44	78.37	16.44	70.32	53.43
-1 1 0	0.78	17.39	26.54	8.66	20.69	50.47	16.47	42.91	43.04
1 0 1	0.71	3.23	35.57	9.37	25.32	73.84	19.45	81.68	46.85
1 -1 0	0.76	4.45	27.97	11.36	21.24	63.89	25.96	53.61	41.38
0 1 -1	0.69	17.79	31.07	8.31	21.42	54.35	14.54	43.24	46.84
0 -1 1	0.58	5.7	36.42	10.34	21.19	69.42	19.71	38.43	44.65
0 0 0	0.62	6.52	33.5	12.06	20.76	64.32	23.16	65.44	36.2

4.5 Analysis of Variance (ANOVA)

The analysis of variance was performed at 95% confidence level to fit H_2, CH_4, CO, CO_2 concentrations and CH_4 and CO_2 conversions with a quadratic second order equation. The terms with p-values > 0.05 were considered insignificant and were omitted. Table 3 presents the list of Box-Behnken design coefficients for the terms that affect the exit gas concentrations significantly along with the adjusted R-square values. Quadratic equations can be formulated to predict H_2, CH_4, CO, CO_2 concentrations and CH_4 conversion from the constants and coefficients listed in Table 4.3. For example, CH_4 conversion can be written as shown in Equation 10.

Table 4.3: Significant terms along with the coefficients for exit gas concentrations

Coefficients	**H_2**	**CH_4**	**CO**	**CO_2**	**CH_4 Conversion**	**CO_2 Conversion**	**Coke %**
A							0.48
B		6.11	-2.99		-6.83		
C			-1.56		-7.39	-4.93	
A*A							
B*B		5.52	-3.97	-1.65	-22.98		
C*C							
A*B	2.38	-1.65	3.78	-1.52	7.54	7.11	
A*C			2.36				
B*C	2.35	-1.68			11.81		
X_o(Constant)	23.08	4.77	34.55	10.54	73.96	42.42	1.22
R-Sq(adj)	64.74%	96%	84.13%	63.93%	88.13%	60.26%	73.70%

$$Y_{\text{Methane conversion}} = 73.96 - 6.83\,B - 7.39\,C - 22.98\,B^2 + 7.54\,AB + 11.81\,BC \qquad \text{(Eq.10)}$$

From the R- square values (Table 4.3), it can be clearly observed that a very good fit was achieved for CH_4 and CO concentrations and CH_4 conversion which are further validated by the comparison between predicted and actual values tabulated below (Table 4.4a,b,c,d). The normal probability plots for the residuals were also plotted (Figures 4.4a, 4.5a, and 4.6a).The residuals falling on or around the straight line on the plot substantiates the validity of assumed distribution. Similarly, the nonexistence of biases was confirmed from the absence of obvious patterns in the residuals versus fitted values plot (Figures 4.4b, 4.5b, and 4.6b).

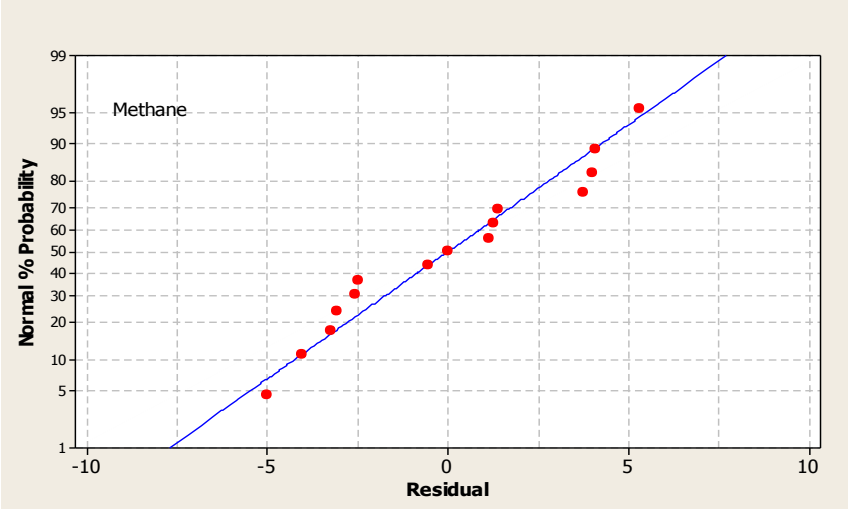

Figure 4.4a: Normal probability plot for CH_4

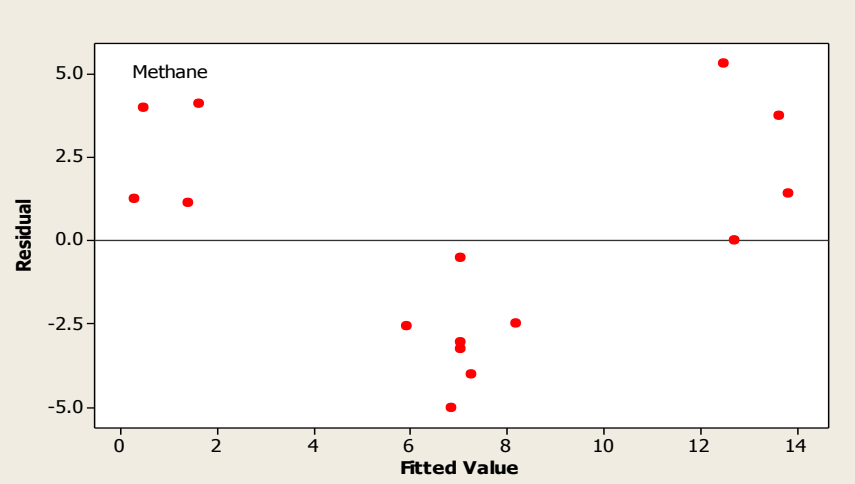

Figure 4.4b: Residual Vs fitted value plot for CH_4

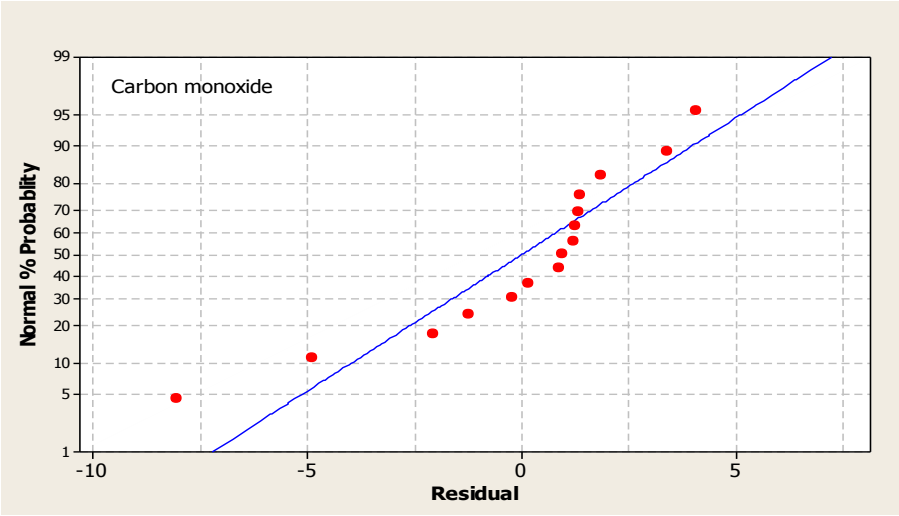

Figure 4.5a: Normal probability plot for CO

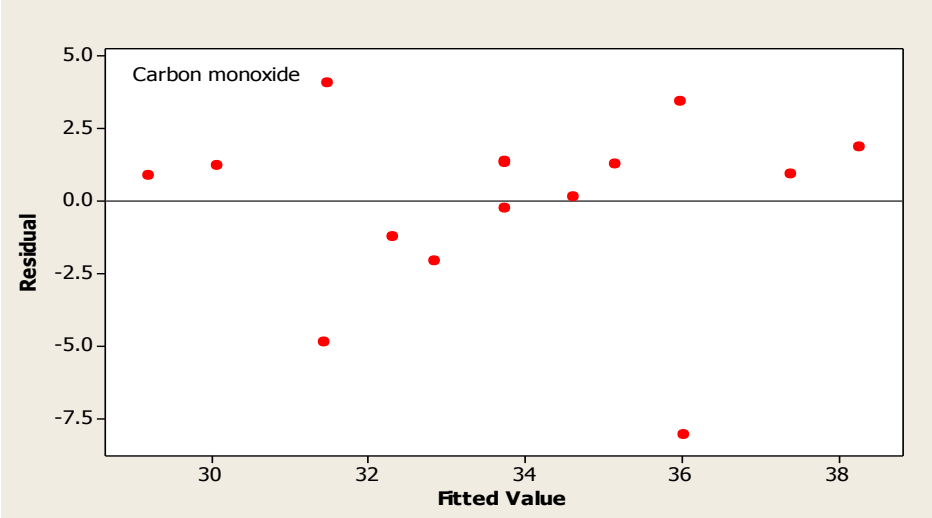

Figure 4.5b: Residual Vs fitted value plot for CO

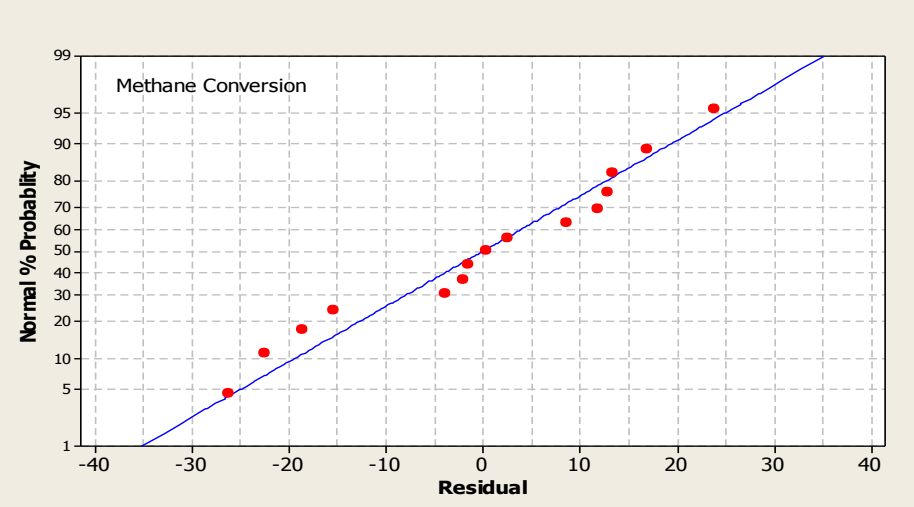

Figure 4.6a: Normal probability plot for CH_4 conversion

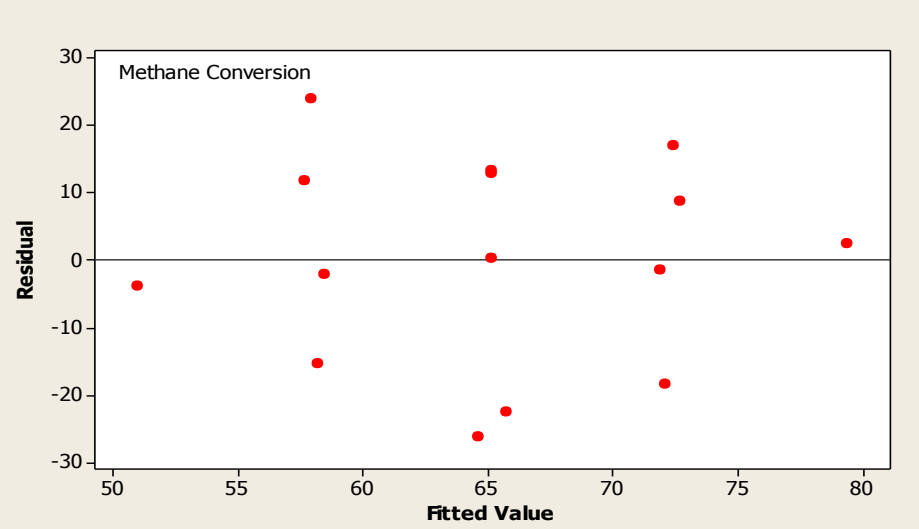

Figure 4.6b: Residual Vs fitted value plot for CH_4 conversion

4.6 Response Surface Plots

From careful observation of the surface response plots, the optimum conditions for maximum CH_4 conversion were established. From Figure 4.7a, it can be seen that the CH_4 conversion increased with the increase in CO_2:CH_4 ratio and attained a maximum value of 89% at a CO_2:CH_4 ratio of 1:1 and then started to drop down. Figure 4.7b re-emphasizes the same conclusion. While at high temperature, an increase in CH_4: steam ratio from (1:1 to 1:3) increases the conversion, which goes to a maximum at 1:3 ratio, the opposite trend is followed at low temperatures which is evident from Figure 4.7c. On the contrary from surface response plots, it can be said that temperature does not play a major role in the given range for CH_4 conversion. This can be reconfirmed from Table 4.3 where linear coefficients for all the components in the exit gas are insignificant.

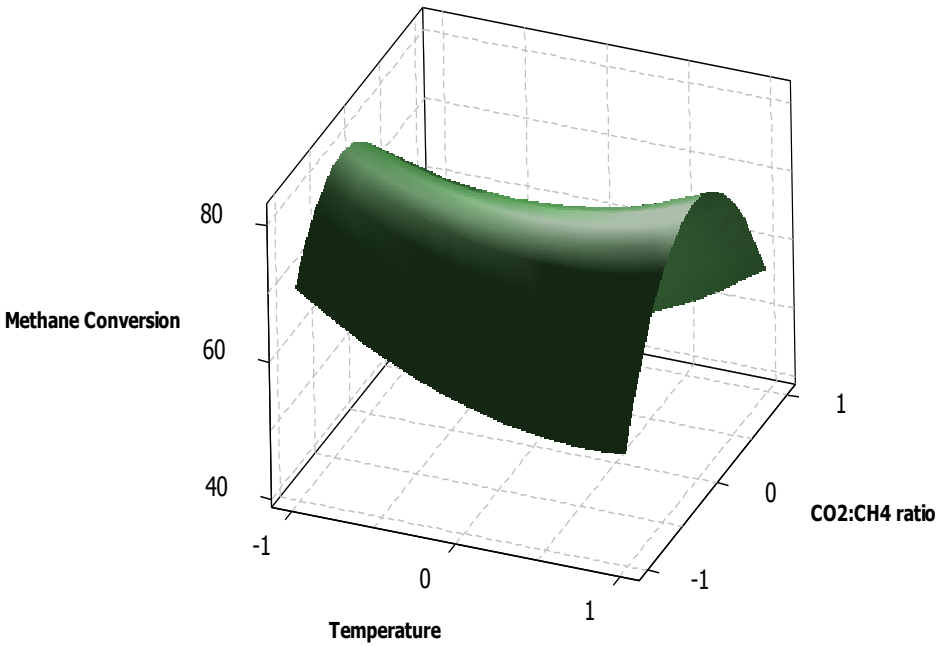

Figure 4.7a: Surface plot of CH_4 conversion versus CO_2: CH_4 ratio and temperature (CH_4: Steam ratio - held at mid value zero)

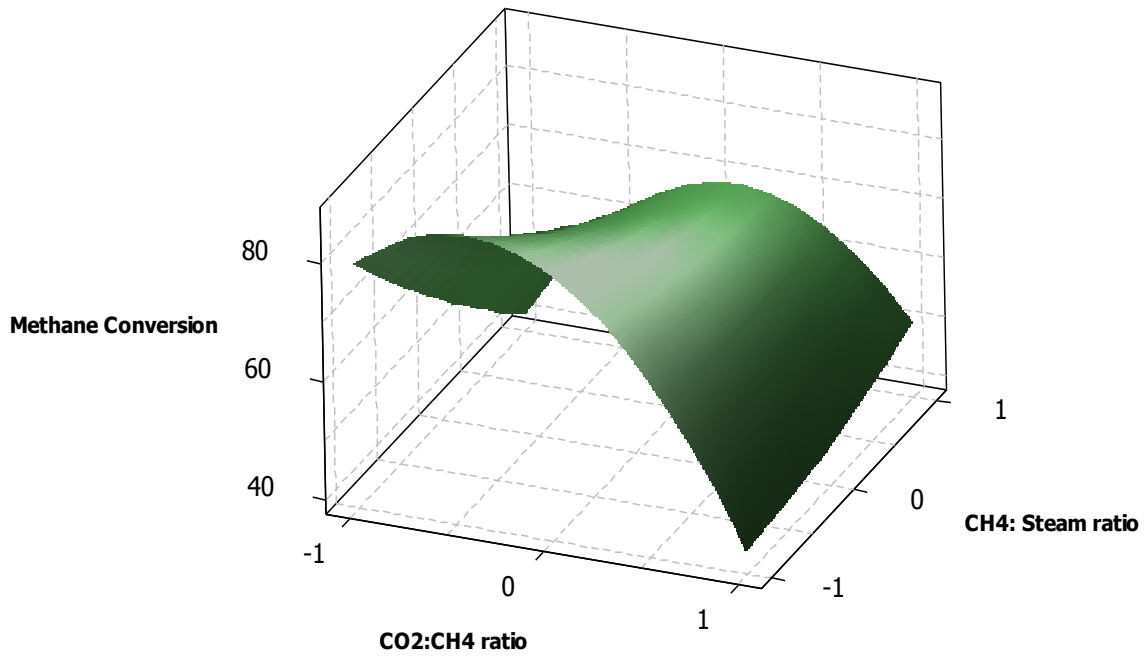

Figure 4.7b: Surface plot of CH_4 conversion versus CO_2:CH_4 and CH_4: Steam ratios (temperature - held at mid value zero)

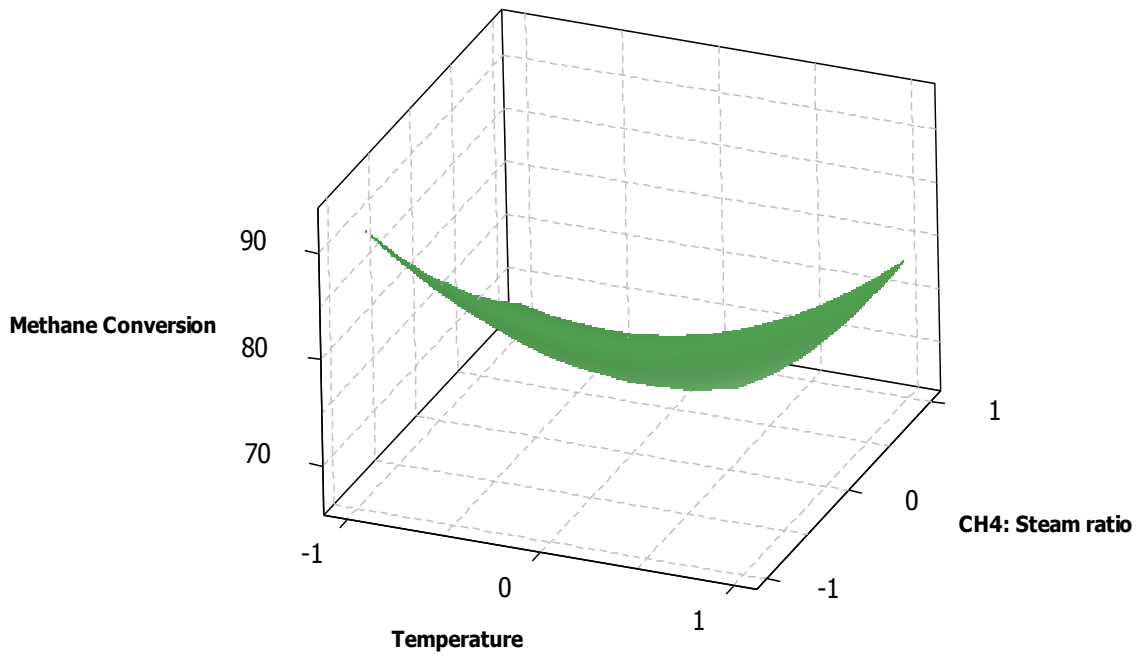

Figure 4.7c: Surface plot of CH_4conversion Vs CH_4: steam ratio and temperature (CO_2:CH_4 ratio - held at mid value zero)

4.7 Coke Analysis

To determine the coke percentage on the catalyst surface, a thermogravimetric analysis (TGA) of the fresh and spent catalyst was carried out and TGA graphs are illustrated in Figure 4.8. About 9 mg of the catalyst sample was heated at 20^0C/min to 550^0C and then held at this temperature for 30 min in a 15 mL/min of air flow rate. As the temperature went beyond 350^0C, an increase in the sample weight was observed in case of reduced catalyst, both spent (Figure 4.8) and unspent (not shown here). This could be due to the activation of metal ions present in the reduced catalyst

which possibly underwent oxidation (by air) to form metal oxides resulting in a weight increase. On the other hand, there was no weight increase observed in non-reduced catalyst (Figure 4.8), in turn emphasizing on the importance of catalyst reduction with hydrogen prior to usage for increasing the catalytic activity. The coke percentage on catalyst was calculated by keeping the reduced catalyst as the basis. The difference in mass loss between the fresh (reduced) catalyst and the spent catalyst gave the percentage of coke deposited on the catalyst after the 20 h run. The percentage of carbon deposited on the catalytic surface for different set of experiments is depicted in Table 4.4. In addition, a carbon balance was also done on the exit gas concentration and an average of 88% closure was achieved. This suggests that the remaining carbon could have converted in other compounds that were not analyzed in this study.

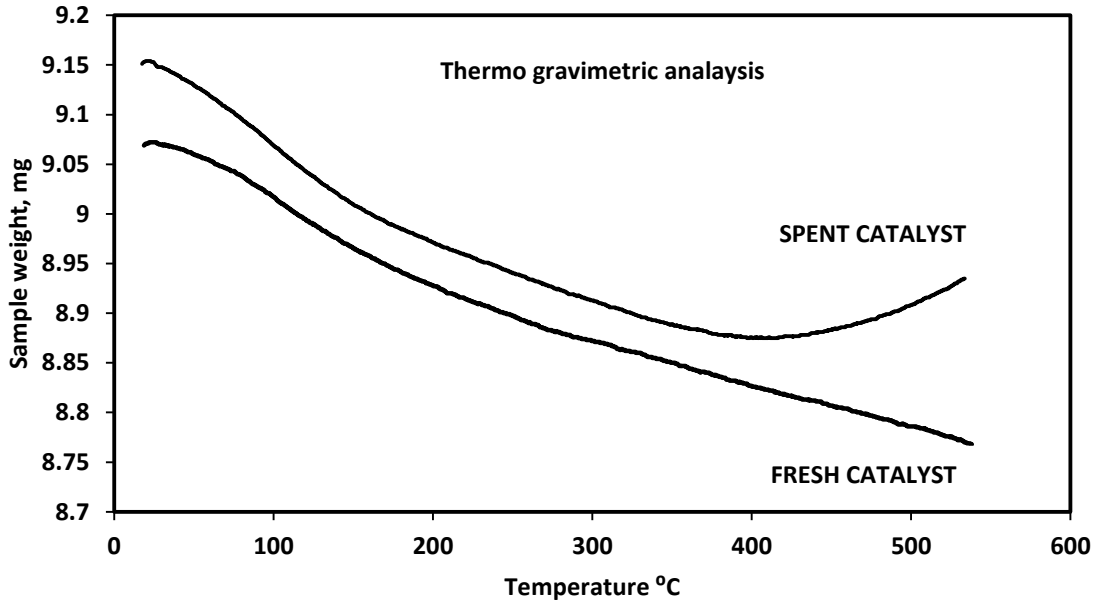

Figure 4.8: TGA plot for the spent catalyst and fresh catalyst (non-reduced)

Table 4.4: Percentage of carbon deposited on the catalytic surface for different set of experiments

Experiment	Coke Percentage	Carbon Balance %
0 -1 -1	0.12	103.82
0 0 0	1.27	84.17
0 1 1	1.11	87.21
-1 0 1	1.12	81.12
0 0 0	1.17	85.87
-1 0 -1	0	87.80
1 1 0	1.43	82.33
1 0 -1	1.32	81.52
-1 -1 0	0	103.50
-1 1 0	0.07	81.57
1 0 1	1.12	85.42
1 -1 0	1.17	83.77
0 1 -1	1.33	87.43
0 -1 1	0.80	103.40
0 0 0	1.21	86.32

4.8 Conclusions

The outcome of the simultaneous steam and dry reforming of CH_4 research using reformax 250 catalyst helped to identify the optimum conditions for maximum CH_4 conversion. An average of 65% and 48% CH_4 and CO_2 conversions along with 68% and 18% average CO and CO_2 selectivities were determined, respectively. A Box-Behnken design was used to find the interaction effects of three factors and quadratic second order equations were postulated to predict the responses at different conditions. The maximum CH_4 conversion and minimum coke formation were achieved at a temperature of 800^0C, CO_2:CH_4 ratio of 1:1 and CH_4: H_2O ratio of 1:1.

Chapter 5

Hydrogen Production from Biogas Reforming and the Effect of H_2S on CH_4 Conversion

5.0 Abstract

Biogas produced during anaerobic decomposition of plant and animal wastes consists of high concentrations of methane (CH_4), carbon dioxide (CO_2) and traces of hydrogen sulfide (H_2S). The primary focus of this research was on investigating the effect of a major impurity (H_2S) on a commercial methane reforming catalyst during hydrogen production. The effect of temperature on catalytic biogas reforming was studied at three different levels (650, 750 and 850 ºC) to determine the optimum conditions for maximum conversions. The experimental CH_4 and CO_2 conversions thus calculated were found to follow a trend similar to the simulated conversions obtained using ASPEN plus. The gas compositions at thermodynamic equilibrium were estimated as a function of temperature to understand the intermediate reactions taking place during biogas dry reforming. The exit gas concentrations as a function of temperature during catalytic reforming also followed a trend similar to that predicted by the model. Finally, catalytic reforming experiments were carried out using three different H_2S concentrations (0.5, 1.0 and 1.5 mole %). It was observed that even with the introduction of small amounts of H_2S (0.5 vol%), the CH_4 and CO_2 conversions dropped to about 20% each as compared to 65% and 85%, respectively in the absence of hydrogen sulfide. The results also established that it

would be inaccurate to assume the effect of H_2S to be negligible while studying H_2 production by biogas dry reforming.

5.1 Introduction

Growing energy demand due to population expansion has heightened the need for alternate energy sources. An ideal source of energy would be cheap, clean, renewable and sustainable in nature. One such energy source is biogas produced by anaerobic decomposition of plant and animal wastes typically consisting of 55-75% methane (CH_4), 25-44% carbon dioxide (CO_2) and 0.5-2% of hydrogen sulfide (H_2S) [112]. It is usually produced in landfills, sewage sludge and bio-waste digesters [113]. Methane and CO_2 are two main greenhouse gases which upon release into earth's atmosphere, yield unfavorable results such as global warming. Methane and CO_2 contribute to 4-9% and 9-26% of the total greenhouse effect, respectively, and hence their emission needs to be checked [114]. The steady increase in the atmospheric CH_4 concentration (0.6-0.8% annually) has been a major concern [115]. Landfills are an important source for the emission of methane into the atmosphere and contribute to about 10% of total anthropogenic methane emitted [116]. About 2.6 million tons of CH_4 are captured annually from landfills across US, 70% of which is converted to heat and electricity [117]. Dry reforming, steam reforming, and partial oxidation (Equations 5-1, 5-2 and 5-3, respectively) are three major techniques for conversion of CH_4 in biogas to useful H_2 and CO.

Steam reforming [90]: $CH_4 + H_2O \longrightarrow 3\,H_2 + CO\ \Delta H^{\circ}_{298\,K} = 206\ kJ\ mol^{-1}$ (Eq. 5-1)

Partial oxidation reforming[118]: $CH_4 + \frac{1}{2}\,O_2 \longleftrightarrow 2\,H_2 + CO\ \Delta H^{\circ}_{298\,K} = -35.7\ kJ\ mol^{-1}$

(Eq. 5-2)

Hydrogen has a very high energy content of 144 MJ kg^{-1} and burns clean without leaving ashes [70]. Braga *et al.* conducted an economic and ecological analysis of H_2 production by steam reforming of biogas and reported the process was economically feasible and free from causing environmental impacts. The cost for H_2 production was estimated to be 0.27 US$/kWh with a payback period of 8 years and the ecological efficiency was 94.95% [119].

Although there are various reforming techniques, the focus of this work is on dry reforming of biogas for the conversion of both CH_4 and CO_2 to more useful syngas: H_2 and CO. Syngas can be converted to liquid hydrocarbons in the presence of Fe and Co catalyst by Fischer-Tropsch reaction [120]. Dry reforming reaction is an endothermic reaction usually dominant at 750 ºC to 850 ºC [90]. The reaction is given by Equation 5-3:

$$CH_4 + CO_2 \longrightarrow 2\,H_2 + 2\,CO \quad \Delta H^{\circ}_{298\,K} = 247\ kJ\ mol^{-1} \qquad \text{(Eq. 5-3)}$$

Many researchers have studied dry reforming of biogas. Lau *et al.* studied the conversion of biogas to syngas using dry and oxidative reforming. They reported that oxidative reforming is dominant at low temperatures while, dry reforming is dominant at higher (> 600 ºC) temperatures [121]. Asencios *et al.* tested the performance of NiO-MgO-ZrO_2 catalyst on reforming model biogas at 750ºC and demonstrated that the addition of MgO to Ni/ZrO_2 improved CH_4 and CO_2 conversions [122]. A comparative study of fixed bed reactor and micro-reactor for H_2 production by biogas reforming using Ni, Rh-Ni promoted on alumina catalyst was done by Izquierdo *et al*. Furthermore, the importance of catalytic surface properties and morphology in driving the reforming reaction was emphasized by performing physicochemical catalyst characterizations like TPR, SEM, XPS, XRD, H_2 chemisorption, N_2 physisorption and ICP-AES [123]. Xu *et al.* investigated biogas reforming over Ni and Co/ Al_2O_3-La_2O_3 catalyst in

a fixed bed reactor using an inlet gas consisting of CH_4 and CO_2 having a molar ratio of one. They found that the addition of Co improved the performance of the Ni/Al La catalyst in terms of CH_4 and CO_2 conversions [124]. Lucredio *et al.* investigated the effect of adding La on Ni-Rh / Al_2O_3 catalyst during reforming of model sulfur-free biogas. They observed that La reduced the carbon deposition by favoring gasification of carbon species [125]. Kohn *et al.* studied dry reforming of biogas in the presence of CH_3Cl using 4% Rh/Al_2O_3 catalyst in the temperature range 350 - 700 ºC. They observed an increase in acidity of the catalyst due to the adsorption of chloride on its surface. They also reported that thermodynamically, the chloride adsorption is less favored at higher temperatures. However, the CH_4 concentration did not change and the only factor that was affected by CH_3Cl was H_2:CO ratio [126].

Although various studies have been conducted on biogas reforming, most of them have assumed a model gas mixture that does not contain H_2S. The work done by Appari et. al 2013 is an exception who proposed a detailed kinetic model capable of simulating the reforming of biogas even in the presence of H_2S over Ni based catalyst. They reported that operating at high temperatures (1173 K) mitigates sulfur adsorption, while lower temperature (973 K) operation results in complete catalyst deactivation[127].

The goal of this study is to investigate the acceptability of neglecting H_2S while conducting biogas reforming studies. The poisoning effect on the commercial catalyst was evaluated in terms of reduction in CH_4 and CO_2 conversions with the introduction of H_2S at three different concentrations.

5.2 Materials and Methods

5.2.1 Materials

Dry reforming of biogas was carried out in a fixed-bed reactor (0.5 inch in diameter and 18 inches long) at temperatures from 650 ºC to 850 ºC and atmospheric pressure in the presence of a commercial CH_4 reforming catalyst (reformax 250). The reactor was packed with quartz wool on both sides with the catalysts in-between. An alloy (Inconel 620) purchased from Microgroup (USA) was selected as the reactor material because of its stability at high temperatures. Experiments were conducted both in the presence and absence of H_2S. For runs done in the absence of H_2S, the inlet gas consisted of a mixture of 59% CH_4, 2% N_2, and 39% CO_2, (all in mole percentage). For runs conducted in the presence of H_2S, the inlet gas composition had CH_4 and CO_2 in the molar ratio 1.5, H_2S concentrations were 0.5, 1.0 and 1.5% and the balance being N_2. The basis for selecting this mixture is to have an inlet stream with concentrations similar to the typical concentrations in biogas [128]. The flow rate of the model biogas was maintained at 60 cc/min using a rotameter (Omega, Stamford, CT). Experiments were conducted at three levels of temperature (650, 750 and 850 ºC). The size of the commercial catalyst (reformax 250 – purchased from Sud Chemie, USA) used was between 707 µm and 420 µm, however, its composition is proprietary. Initially, TPR analysis (Temperature Programmed Reduction) was carried out using Autosorb (Quantachrome, FL) to measure the optimum temperature for catalyst reduction.

5.2.2 Experiments

An experimental setup used for this study is illustrated in Figure 5.1. A known weight of the catalyst (0.20 g or 0.35 g) was loaded into the reactor, calcined and reduced in-situ at 800 ºC with 60 cc/ min of 5% H_2 in He for 2 h each time before an experiment was conducted. The

residence time (defined as the ratio of weight of catalyst (0.20 g) to the flow rate (60 cc/min) of inlet gas) used for the experiments was 3.3×10^{-3} g_{cat} min/cc. Experiments were carried out for 5 h to test the stability of the catalyst under different experimental conditions. Temperature at the catalyst-bed was measured using a K-type thermocouple (Stamford, CT) and recorded continuously using a data logger. The exit gas, produced after the reaction, was cooled using two ice-bath condensers and then passed through a moisture trap to remove water vapor before being sent to a gas chromatography (GC) for gas analysis. The GC (Multigas 2, SRI 8610C, Torrance, CA) consisted of two columns: molecular sieve and Haysep D. Hydrogen, CH_4, N_2, and CO peaks appeared in the molecular sieve column while CO_2 peak appeared in the second column. One-point calibration was carried out with a standard gas before conducting each experiment. Argon was used as the carrier gas throughout the study, and the gas compositions were recorded every 10 min. Initially, the catalyst weight was varied from 0.20 g to 0.35 g while maintaining a constant gas flow rate to check for mass transfer limitation. Similar test runs were conducted based on catalyst size to determine if there were any intra-particle diffusion limitations. The commercial catalyst was obtained in pellet form and was crushed to reduce the size so that it could be inserted into the reactor. Different particle sizes were obtained by sieving, and the size of the catalyst used to check intra- particle diffusion ranged from 0.707 mm to 0.420 mm. The performance of the commercial catalyst was presented in terms of CH_4 and CO_2 conversions (which were calculated using Equation 5-4) and H_2 concentration in the exit gas.

$$\text{Conversions of species i} = \frac{C_i - C_e}{C_i} \times 100 \qquad \text{(Eq. 5-4)}$$

where C_i – Inlet gas concentration in mole percentage
C_e – Exit gas concentration in mole percentage,
i- CH_4 and CO_2

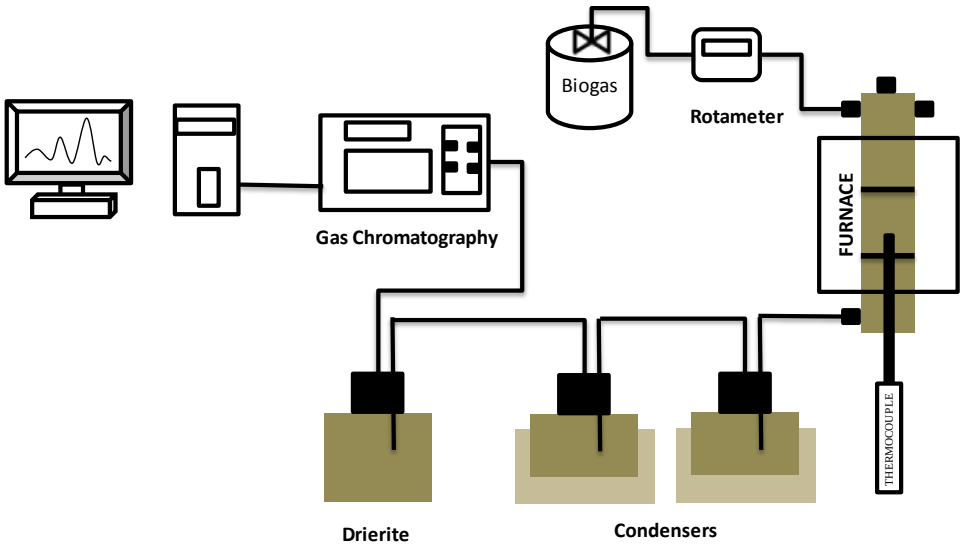

Figure 5.1: An experimental setup used for biogas reforming

5.3 Process simulations using ASPEN Plus

In order to understand the temperature effect on the conversions preliminary simulations were carried using ASPEN Plus (Version 7.1). ASPEN Plus is commonly used software for process simulation. A Gibbs reactor model was used to represent the dry reforming reaction at specified temperatures. The Gibbs reactor performs minimization of Gibbs free energy in order to determine the product gas composition at thermodynamic equilibrium. The inlet gas concentrations along with temperature data were input into the model to simulate steady state gas composition. The process diagram has been given below in Figure 5.2.

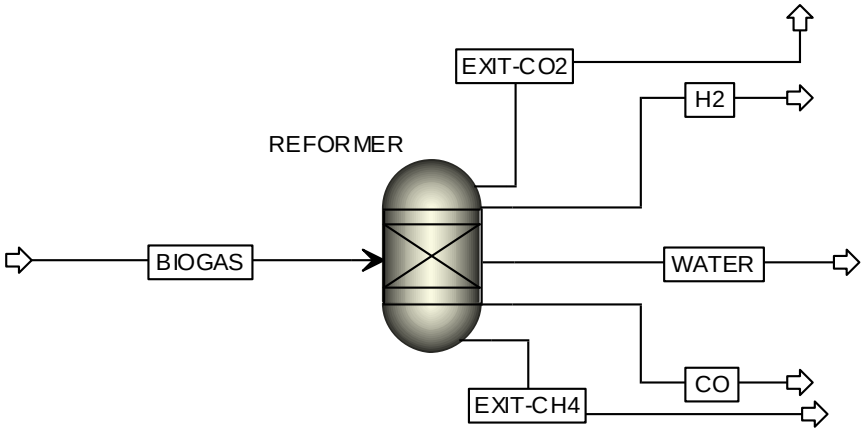

Figure 5.2: The process diagram for carrying out ASPEN plus simulations

5.4 Results and Discussion

5.4.1 Temperature Programmed Reduction

A TPR analysis of the catalyst was carried out in order to determine the precise reduction temperature. A ten point moving average of the signal generated corresponding to H_2 consumed was plotted as a function of temperature (Figure 5.3). It is evident from the plot that maximum H_2 consumption (implying best reduction) takes place at 800 ºC and hence that temperature was selected to be the reduction temperature for the catalyst.

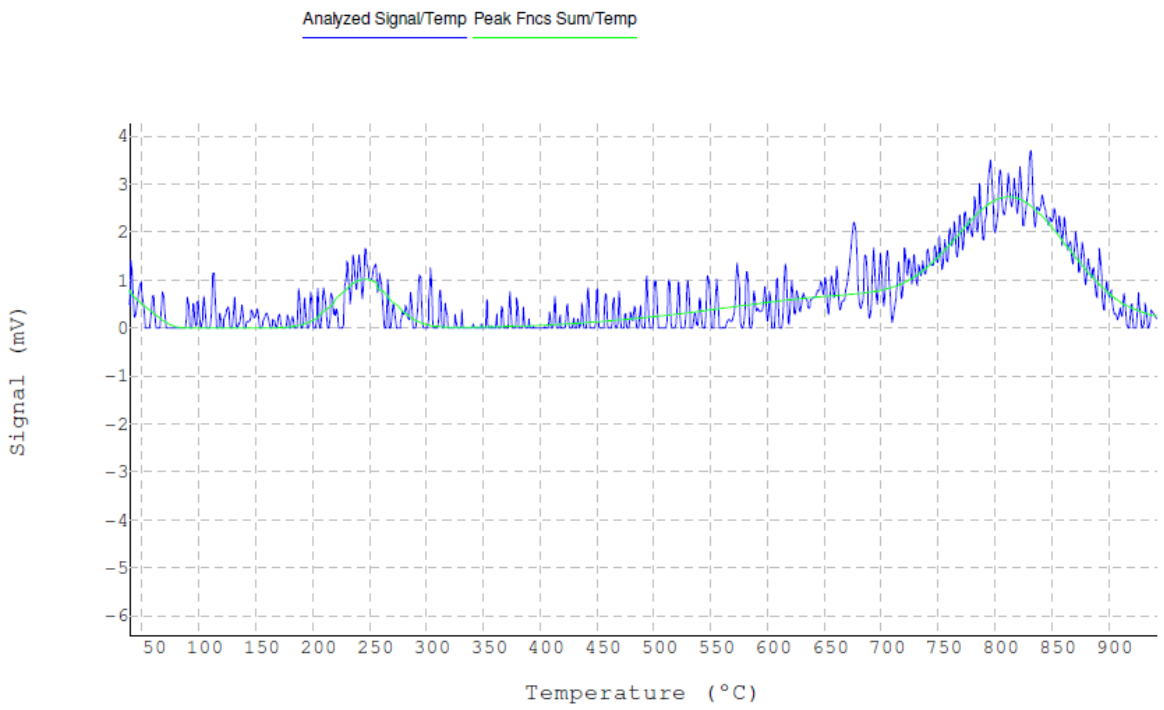

Figure 5.3: Temperature programmed reduction analysis for the catalyst

5.4.2 Test for mass transfer limitation

For a given catalyst weight and size, a minimum flow rate of inlet gas is necessary to overcome the mass transfer limitation due to the stagnant film around the catalyst surface. In order to check for mass transfer limitation, the catalyst weight was varied from 0.2 g to 0.35 g (at constant inlet gas flow rate: 60 cc/min). The CH_4 and CO_2 conversions at both catalyst weights were found to be similar indicating that the mass transfer effect was negligible. The exit gas compositions and conversions for the two cases have been presented in Figure 5.4.

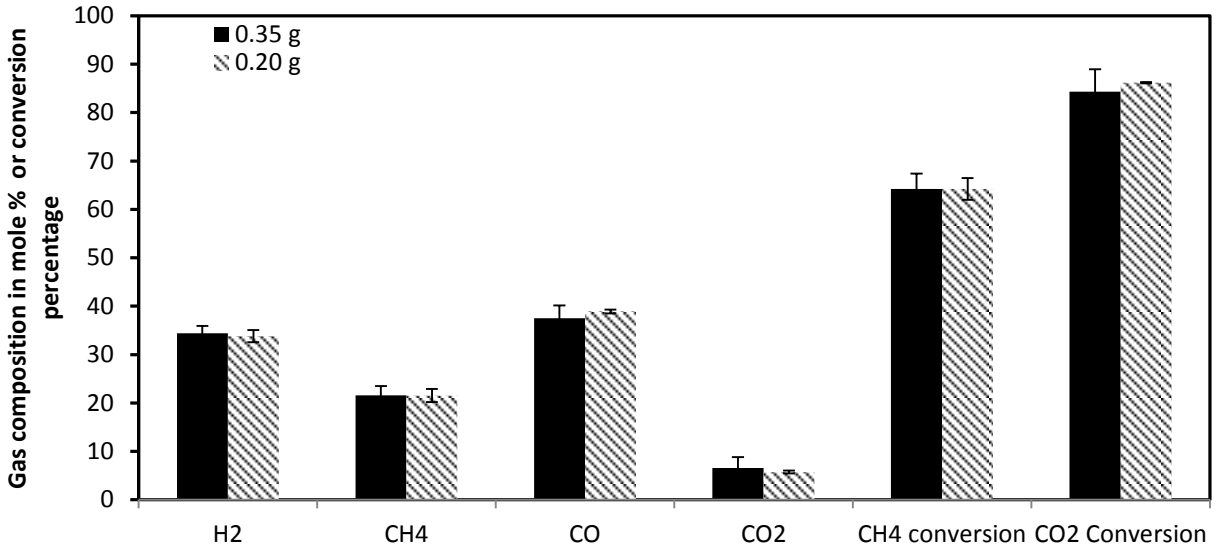

Figure 5.4: Experiments to confirm the absence of mass transfer limitation

5.4.3 Experimental versus ASPEN plus conversion comparison

The simulated CH_4 and CO_2 conversions were compared with the experimental conversions observed during catalytic dry reforming process and plotted as a function of temperature (shown in Figure 5.5). The conversions for both experimental and simulated results were observed to increase when temperature was increased from 650 to 750 ºC, reaching a maximum and remaining constant thereafter even with further increase in temperature. Although the experimental conversions and simulated conversions followed a similar trend in the temperature range, the difference between them (for both CH_4 and CO_2) at lower temperature (650 ºC) is much greater compared to that at higher temperatures (750 ºC and 850 ºC). This is because, dry reforming reaction is more pronounced at higher temperatures (750-850 ºC). At lower temperatures, the experimental results are kinetically limited while ASPEN plus simulations are obtained by assuming infinite residence time.

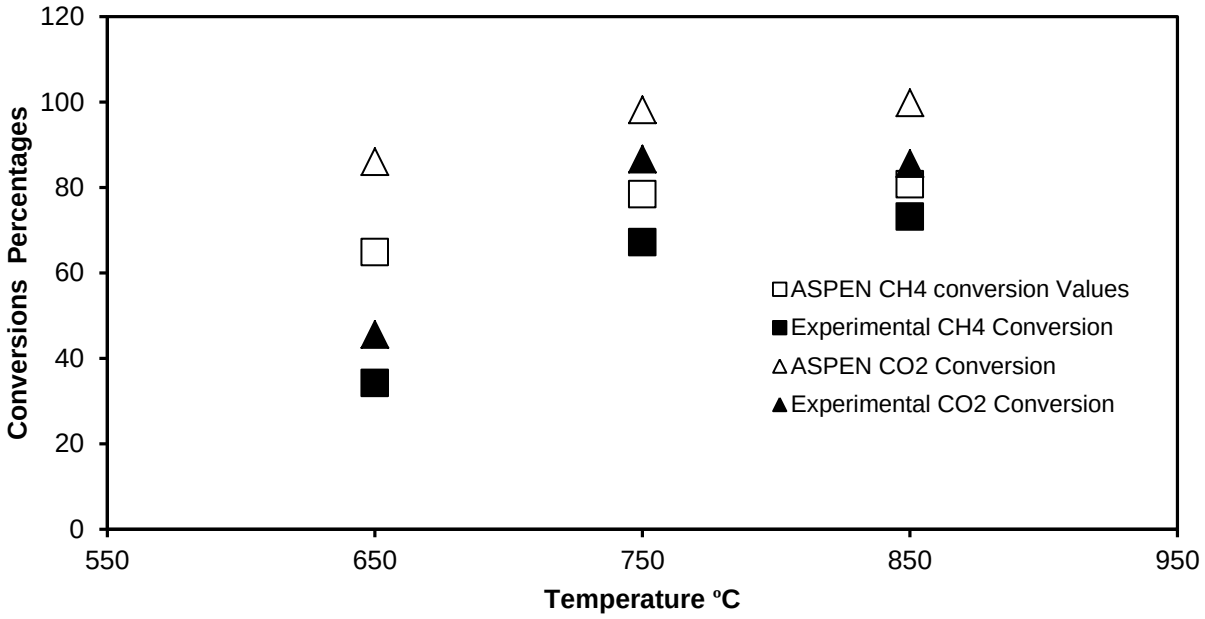

Figure 5.5: Comparison of experimental conversions versus ASPEN plus simulated conversions

In order to understand the reaction mechanism of the dry reforming process, a thermodynamic analysis was performed to determine the steady state gas composition at different temperatures. Figure 5.6 illustrates the inlet and exit gas composition at the different experimental temperatures. According to the dry reforming reaction mentioned in Equation 3, equal moles of H_2 and CO have to be produced. However, it can be observed that the exit H_2 and CO concentrations at 650 ºC are not equal; in fact the H_2:CO ratio is 0.86, while at 750 and 850 ºC the H_2:CO ratio is about 0.98. This could be attributed to the methanation reaction that occurred (given by the Equation 5-5). The reaction is dominant at lower temperatures (350-600 ºC) and hence the decrease in H_2O with increase in temperature supports this argument. The gas composition at thermodynamic equilibrium at different temperatures is shown in Figure 5.6.

$$CO + 3H_2 \longrightarrow CH_4 + H_2O \quad \text{(Eq. 5-5)}$$

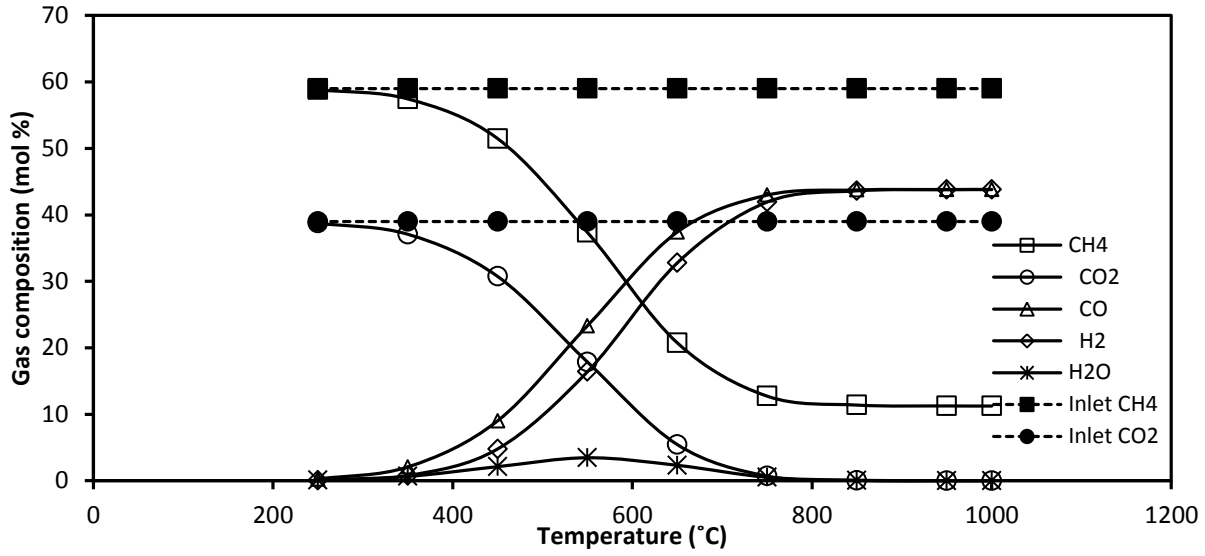

Figure 5.6: Gas composition at thermodynamic equilibrium as a function of temperature

A comparison of steady state exit gas composition during catalytic and non-catalytic dry reforming of biogas is shown in Figure 5.7. Negligible amount of H_2 and CO are produced during non-catalytic reaction at all the experimental temperatures while, about 40 % (mole %) of H_2 and CO are produced at 850 ºC in the presence of catalyst. It can also be noted that the concentration trend followed by the exit gases during catalytic reforming is similar to the ones simulated by ASPEN Plus shown in Figure 5.6.

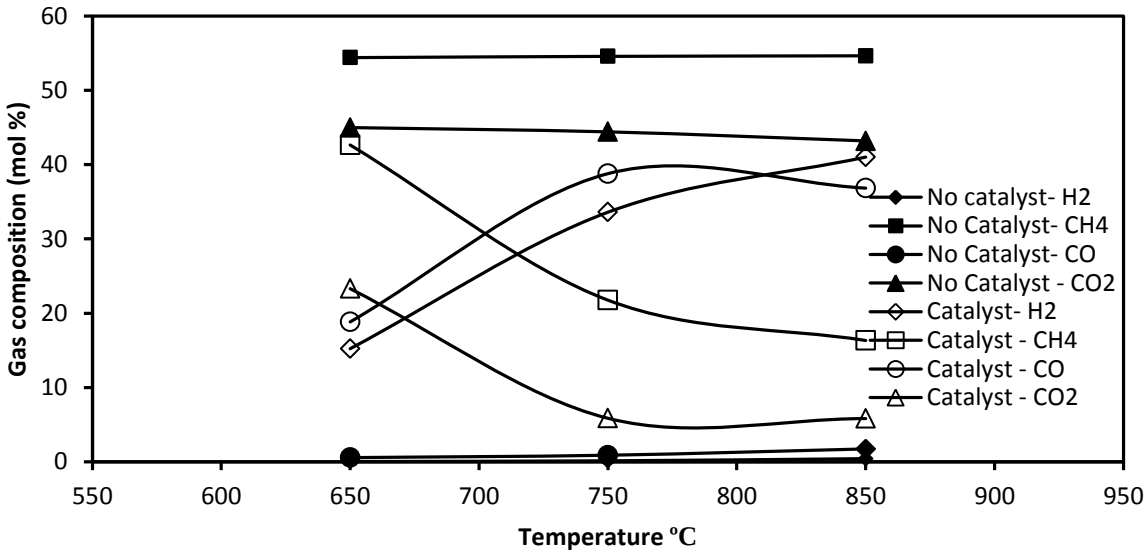

Figure 5.7: Comparison of steady state exit gas composition for catalytic and non-catalytic reforming reactions plotted as a function of experimental temperature

5.4.4 Catalytic dry reforming

The steady state exit gas compositions and CH_4, CO_2 conversions for catalytic (0.20 g catalyst) and non-catalytic reforming experiments performed at 750 ºC are shown in Figure 5.8. While no H_2 and CO were observed during non-catalytic reforming, about 33 mole % of H_2 and 39 mole % of CO were observed in the presence of catalyst. The CH_4 and CO_2 conversions during catalytic reforming were about 64% and 86%, respectively which were much higher compared to non-catalytic experiments: 30% and 14%, respectively. This confirms that the catalyst helps in promoting dry reforming reaction. The catalyst was also found to be stable for over a 5 h run shown in Figure 5.9.

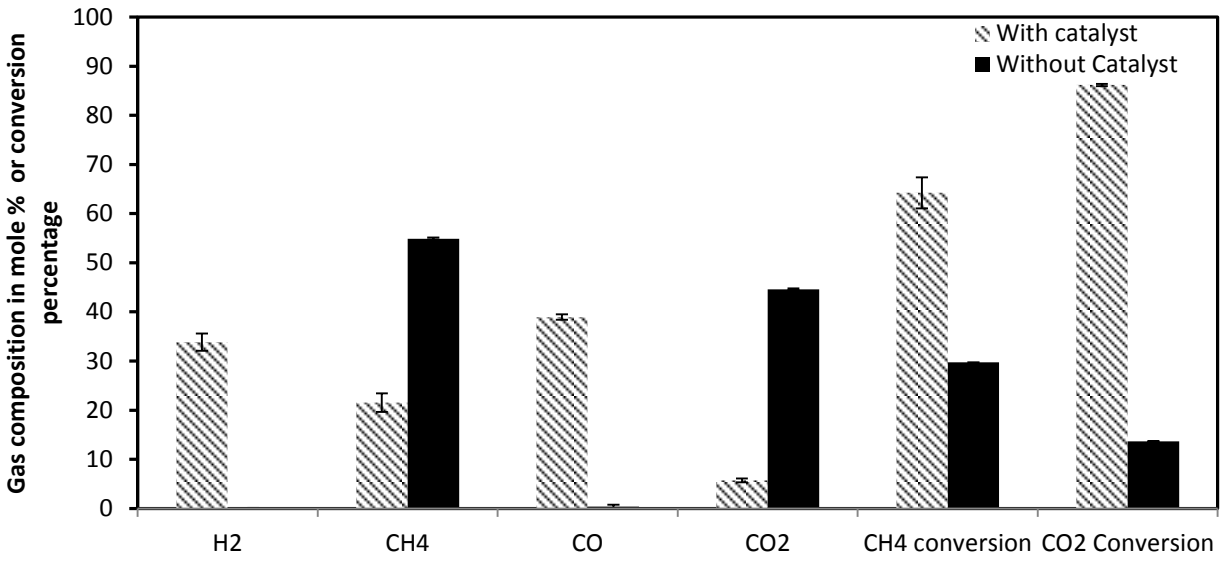

Figure 5.8: Steady state exit gas composition and conversions for catalytic and non-catalytic reforming experiments done at similar experimental conditions (750 ºC)

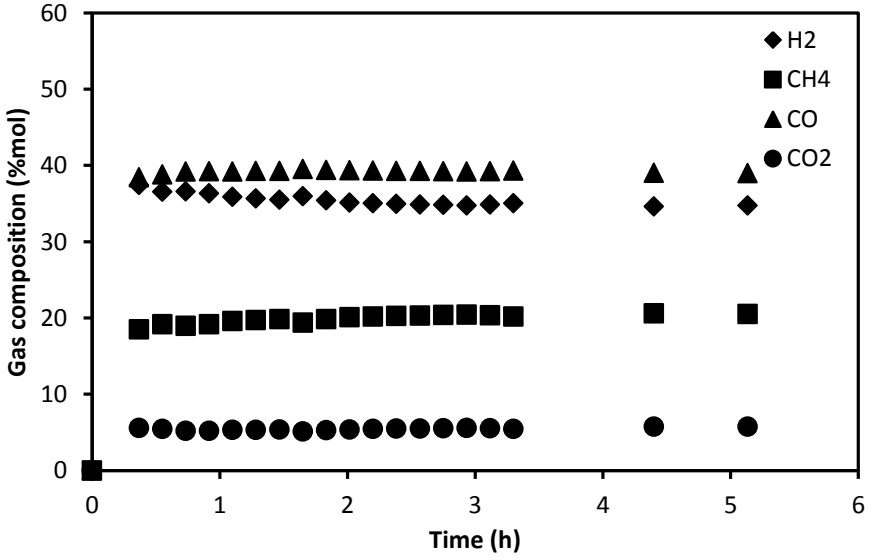

Figure 5.9: Exit gas composition for catalytic experiments done at 750 ºC and 0.2 g of catalyst for over 5 h

5.4.5 Introduction of H_2S

After conducting dry reforming experiments with a model gas that was free from H_2S, similar experiments were conducted in the presence of H_2S. In order to test the effect of H_2S on catalytic biogas reforming, gases with three different H_2S concentrations (0.5, 1.0 and 1.5 mole %) were chosen. A comparison of conversions at different H_2S concentrations is shown in Figure 5.10. From the graph it can be observed that the CH_4 and CO_2 conversions decreased drastically with the introduction of H_2S even at the lowest concentrations (0.5 mole %). The CH_4 conversion dropped from 67% to 16% while the CO_2 conversion decreased from 86% to about 16%. The exit gas concentration for a time period of about 5 h during dry reforming of biogas containing 1.5% (mole %) H_2S at 750 ºC is shown in Figure 5.11. From the graph it is evident that the poisoning effect on the catalyst is almost immediate and happens within the first 10 minutes.

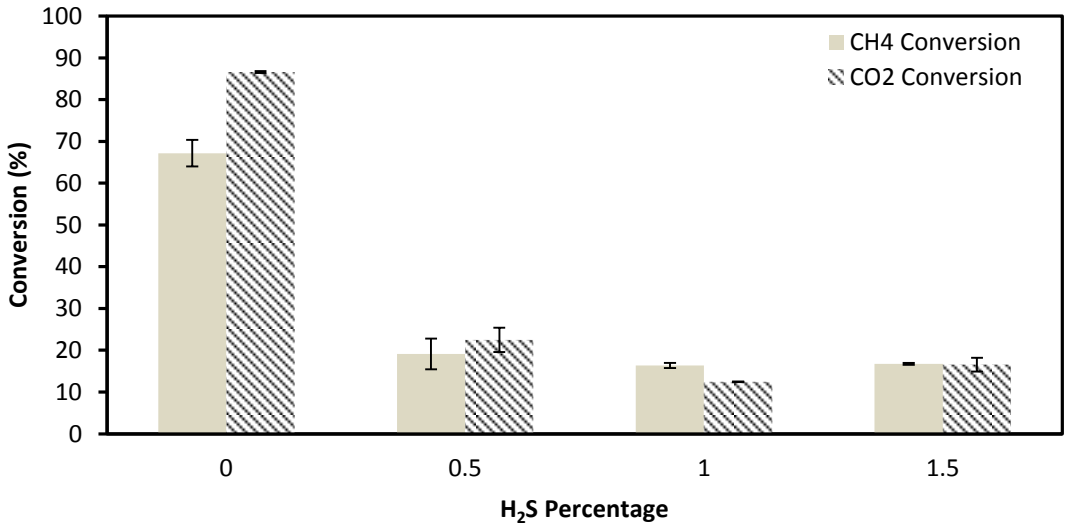

Figure 5.10: Comparison of conversions at different H_2S concentrations

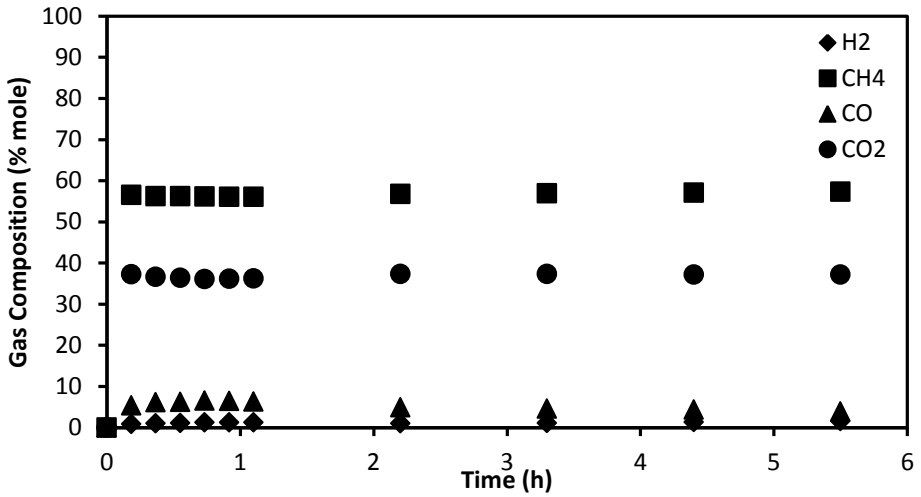

Figure 5.11: Exit gas concentration during catalytic biogas reforming in the presence of 1.5% H_2S at 750 ºC

5.4.6 Catalyst characterization

In order to understand the coke and sulfur deposition mechanism, scanning electron microscopic images (SEM) of the fresh catalyst and spent catalyst (before and after the introduction of H_2S) were obtained to compare the visible difference in the catalytic surface (Figure 5.12).

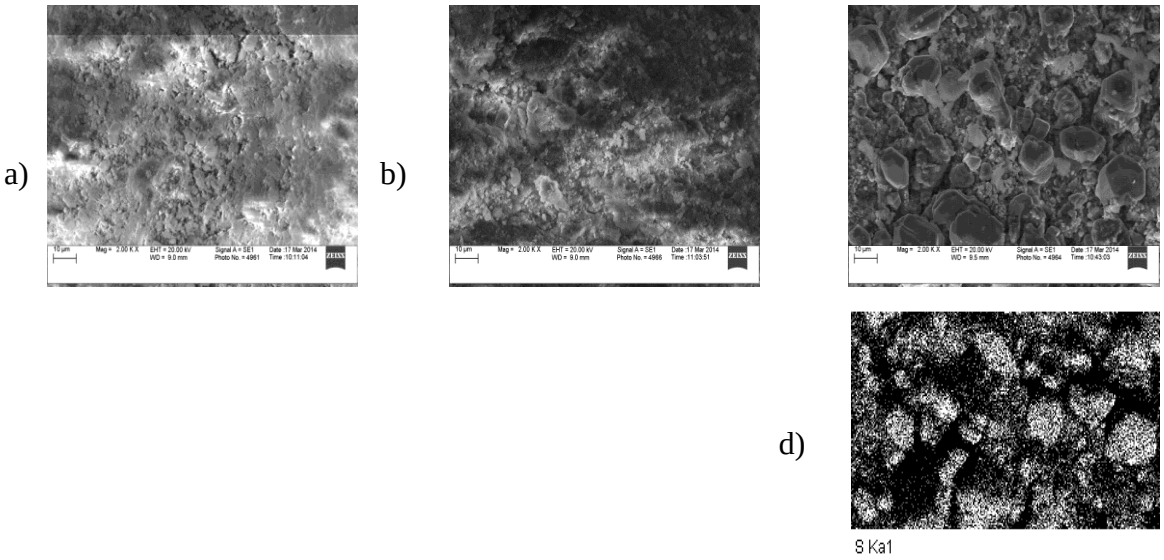

Figure 5.12: SEM images of a) the fresh catalyst b) spent catalyst before H_2S introduction c) spent catalyst with the introduction of 1% H_2S d) sulfur mapping

From the images, no visible difference could be spotted between the fresh catalyst and spent catalyst (before H_2S introduction). However, the SEM image of spent catalyst with 1% H_2S in the inlet gas stream showed localized agglomerations of sulfur crystals on the surface. This was also confirmed by the sulfur mapping shown in Figure 5.12 d. Energy dispersive X-ray spectroscopy (EDS) was performed to analyze the elements present in the fresh and spent catalyst (Table 5.1).

Table 5.1: EDS comparison of fresh and spent catalysts

Catalyst type	Carbon (wt%)	Sulfur (wt%)
Fresh Catalyst	1.36	0
Spent catalyst (No H_2S)	15.21	0
Spent catalyst (0.5% H_2S)	3.13	1.58
Spent catalyst (1.0% H_2S)	1.69	1.40
Spent catalyst (1.5% H_2S)	1.88	1.25

The EDS data revealed that in the absence of H_2S coking was found to be the dominant reaction (explained by the increase in carbon wt %), and no sulfur was observed as expected. While, in the presence of H_2S (0.5% - 1.5%) an increase in sulfur wt % along with no significant change in the carbon wt % can be observed indicating that catalyst poisoning due to sulfur dominates coke formation.

5.5 Conclusion

Catalytic conversion of biogas to syngas was studied using a commercial catalyst. Initially, temperature programmed reduction of the catalyst was carried out to determine the appropriate reduction temperature. Then, a comparison of experimental and ASPEN simulated conversions as a function of temperature was done to confirm that they exhibited similar trends. Preliminary experiments were performed to eliminate mass transfer limitations and further runs were conducted at optimum temperature (750 ºC) and catalyst weight (0.20 g). The effect of H_2S on the CH_4 and CO_2 conversions was studied by using gases with three different H_2S concentrations. It was noticed that even with the introduction of 0.5 mole % H_2S drastically reduced the CH_4 and CO_2 conversions from 67% and 87 % to 19% and 22% respectively. From the catalyst characterization it was observed that the coking reaction which was mainly dominant in the absence of H_2S became less pronounced with the introduction of H_2S while sulfur deposition reaction was more favored. Thus, based on the results of this study it can be stated that neglecting the presence of H_2S while investigating biogas reforming is not an accurate assumption.

Chapter 6

Summary and Future Work

Hydrogen production from three different bio-based renewable sources using three different reforming techniques was explored successfully in this dissertation. The three bio-based sources chosen for this study were – bio-oil, biomass syngas, and biogas and the respective techniques used were: two-phase reforming, combined dry and steam reforming and dry reforming.

In the first objective, the two-phase reforming in the presence of Ru / Al_2O_3 catalyst was established as a feasible method for hydrogen production from aqueous bio-oil. The H_2 selectivity was found to increase in the presence of catalyst. Kinetic studies showed a decrease in activation energy during catalytic reforming as compared to non-catalytic reforming. The activation energies during catalytic and non-catalytic bio-oil two-phase reforming were: 56 kJ/mol and 66 kJ/mol, respectively. The GC-MS results revealed the complete conversion of sugars, aldehydes and diols to simpler ketones during the reforming process. Catalyst characterization using TGA and BET surface area measurements concluded that the coke deposition on the catalyst reduced with increase in temperature.

The simultaneous steam and dry reforming of biomass syngas using reformax 250 catalyst helped to identify the optimum conditions for maximum CH_4 conversion. An average of 65% and 48% CH_4 and CO_2 conversions along with 68% and 18% average CO and CO_2 selectivities

were determined, respectively. A Box-Behnken design was used to find the interaction effects of three factors and quadratic second order equations were postulated to predict the responses at different conditions. The maximum CH_4 conversion, H_2 yield and minimum coke formation were achieved at a temperature of 800 ºC, CO_2:CH_4 ratio of 1:1 and CH_4: H_2O ratio of 1:1.

In the final objective, initial thermodynamic analysis revealed the optimum temperature for carrying out catalytic biogas dry reforming to be 750 ºC. The effect of H_2S on the CH_4 and CO_2 conversions was studied by using gases with three different H_2S concentrations. It was noticed that even with the introduction of 0.5 mole % H_2S drastically reduced the CH_4 and CO_2 conversions from 67% and 87 % to 19% and 22% respectively. From the SEM-EDS analysis of the fresh and spent catalyst it was observed that coking which was a dominant reaction in the absence of H_2S became less pronounced with the introduction of H_2S while sulfur deposition reaction was favored more. Thus, based on the results of this study it could be stated that neglecting the presence of H_2S while investigating biogas reforming is not an accurate assumption.

Regardless of the intensity of work being done in any research there is always scope for further improvements. Although H_2 production from different bio-based substrates has been investigated in a detailed manner, further focus in the prescribed areas is highly recommended. In the first objective, while studying two-phase reforming of bio-oil for H_2 production, establishing the effect of pressure on the H_2 yield and carbon deposition would add further value to the study. In order to achieve different pressures at constant temperatures, different sized batch reactors could be used. Also comparing the activation energies for a broad range of metal supported catalysts is recommended. The oxygen content of the bio-oil has been known to be the

cause for various problems like - acidity, aging, lack of stability, etc. In order to reduce the aforementioned drawbacks, pyrolysis-oil could be upgraded initially by catalytic hydrodeoxygenation (HDO) process before subjecting it to two-phase reforming process for H_2 production. Proposing a common catalyst that would work well during both feed pretreatment (HDO) and reforming would make the process cost-effective and easy to operate. The feasibility of the combined feed pretreatment and reforming technique on a continuous scale could be checked later on using a fixed bed reactor. A comparison study of the H_2 yield obtained from bio-oil two-phase reforming and APR process would give vital information about the efficiency of the technique. Also, a detailed study of the bio-oil conversion mechanism is highly required in order to further improve the efficiency of the process.

While examining the conversion of biomass synthesis gas to H_2 in the second objective, the efficiency of commercial catalyst could be compared to various other metal supported catalysts. Also, a fully composite experimental design of experiments could be implemented instead of a Box-Benhken design and the results could be compared.

In the third objective, a two-step pretreatment – dry reforming process for a more efficient conversion of biogas to energy has been recommended below.

Past studies in biogas dry reforming have been conducted assuming that a negligible amount of H_2S has little or no effect on the process. However, from the results reported in chapter 5, we have observed tremendous poisoning on a commercial reforming catalyst due to the presence of impurity. Hence, a pretreatment of biogas to get rid of H_2S is very much essential. The existing H_2S removal techniques involve the use of metal oxides (TiO_2, ZnO) which form metal sulfides and water upon reaction with the gas. However in this technique, the hydrogen in H_2S is lost in

the form of water. Clark *et al.* established that during catalytic partial oxidation of hydrogen sulfide, SO_2 formation by oxidation could be kept minimal by reducing the residence time thereby leading to the formation of H_2 [129]. Hence, a combination of H_2S conversion prior to dry reforming of biogas would have a dual advantage in solving both the energy and air pollution crises. Therefore, we propose a two-stage setup in which H_2S conversion to H_2 and S takes place in the first stage and dry reforming of H_2S free biogas takes place in the second stage. The partial oxidation reaction could be carried out at lower temperature (400˚C) in the presence of γ-Al_2O_3 catalyst while the dry reforming of biogas takes place at an elevated temperature (800˚C) in the second stage in the presence of a CH_4 reforming catalyst.

The intellectual merit of the proposed project lies in the idea of combining the H_2S removal for harnessing H_2 and biogas dry reforming to increase the overall H_2 yield. As it is evident from the chemical reaction given below, there is one mole of H_2 produced for two moles of H_2S oxidized.

$$2\ H_2S + ½\ O_2 \longrightarrow H_2 + H_2O + S_2\ \Delta H = -72.1\ kJ\ mol^{-1} \qquad \text{(Eq. 6-1)}$$

In addition, the effect of other metal oxide catalysts on the partial oxidation of H_2S to H_2 could be understood and the best catalyst for the reaction could be identified. More understanding will be obtained on the activity and regeneration of the metal oxide catalyst. A detailed understanding of H_2 generation from H_2S and various factors impacting the overall H_2 yield like residence time, catalyst, and temperature will be a definite outcome of this study. The successful completion of this study would result in a more efficient usage of biogas generated from landfills which are otherwise not made the best use of. The broader impacts not only include the production of cleaner fuel but also provide a healthy way of disposing bio-wastes. The leftover slurry is enriched organic manure that could be used as a substitute for fertilizers.

Appendix I

GC-MS analysis of raw bio-oil (Pg 52):

Library/ID	Qual	Area
Butyrolactone	78	122475
2(5H)-Furanone	83	410889
2(5H)-Furanone, 5-methyl-	64	36126
1,2-Cyclopentanedione, 3-methyl-	90	645048
Phenol	91	621049
Phenol, 2-methoxy-	95	614112
Phenol, 3-methyl-	90	220130
3-Hexene, 3-methyl-, (Z)-	64	71893
Phenol, 2-methoxy-4-methyl-	94	390828
Phenol, 4-ethyl-2-methoxy-	83	81711
2-Furancarboxaldehyde, 5-(hydroxymethyl)-	64	334917
1,2-Benzenediol	87	691496
Benzaldehyde, 3-hydroxy-4-methoxy-	97	425464
Ethanone, 1-(4-hydroxy-3-methoxyphenyl)-	90	260842
1,6-Anhydro-.beta.-D-glucopyranose (levoglucosan)	72	11490360

GC-MS analysis of solution obtained from non-catalytic two-phase reforming of 15% bio-oil carried out at 280 ºC for 4 hours.

Library/ID	Qual	Area
Propanoic acid	83	526046
2-Cyclopenten-1-one	86	424964
2-Cyclopenten-1-one, 2-methyl-	91	1510819
Ethanone, 1-(2-furanyl)-	83	55389
5H-1,4-Dioxepin, 2,3-dihydro-5-methyl-	78	110959
2-Cyclopenten-1-one, 2,3-dimethyl-	80	159518
2-Cyclopenten-1-one, 3-methyl-	91	187256
2-Cyclopenten-1-one, 3-methyl-	90	271068
Butyrolactone	64	261310
5,5-Dimethyl-1,3-hexadiene	80	163625
2-Cyclopenten-1-one, 2,3-dimethyl-	78	402145
Phenol	91	812493
Phenol, 2-methoxy-	95	844866
2-Cyclopenten-1-one, 3-ethyl-	90	90125
Phenol, 4-methyl-	93	278756
Phenol, 4-methyl-	91	209656
Phenol, 4-methyl-	91	186466
4-Octene, (E)-	72	61379
Phenol, 3,5-dimethyl-	72	119068
2-Acetonylcyclopentanone	64	151472
1,2-Benzenediol	90	144484
Hydroquinone	70	581190
Phenol, 4-[[2-(3,4-dimethoxyphenyl)ethylamino]methyl]-2-methoxy-	72	76579

GC-MS analysis of solution obtained from catalytic two-phase reforming of 15% bio-oil carried out at 280 ºC for 4 hours.

Library/ID	Qual	Area
Propanoic acid	74	296125
2-Cyclopenten-1-one, 2-methyl-	87	889637
2-Cyclopenten-1-one, 2,3-dimethyl-	80	53009
2-Cyclopenten-1-one, 2-methyl-	91	370616
Butyrolactone	72	227227
Cyclobutene, 1,2,3,4-tetramethyl-	83	87259
Phenol	91	703982
Phenol, 2-methoxy-	91	629724
Phenol, 4-methyl-	93	202538
Octane, 4-chloro-	64	51810
2-Methyl-3-ethyl-2-heptene	64	136701

Calculation of methane conversion Pg 71:

For example, assume 100% CH_4 is input into a system and 80% CH_4 appears in the exit. The conversion is given by,

CH_4 conversion $= \frac{CH4\ in - CH4\ out}{CH4\ in} \times 100 = \frac{100-80}{100} \times 100 = 20\ \%$

Calculation of selectivity determination for the exit gas concentration tabulated below:

Components	Concentration (mol%)
CO	40.13
CO_2	6.6
CH_4	1.53

$$\text{Selectivity of species i} = \frac{\text{Moles of C in species i}}{\text{Total moles of C in product}} \times 100$$

$$\text{Selectivity of CO} = \frac{40.13}{(40.13+6.6+1.53)} \times 100 = 83.15\%$$

$$\text{Selectivity of } CO_2 = \frac{6.6}{(40.13+6.6+1.53)} \times 100 = 13.68\%$$

Appendix II

Data set for figure 3.1

Time, h	H_2	CH_4	CO	CO_2
1	45.54	3.23	44.08	12.89
1	51.69	3.64	44.67	11.94
1	42.87	3.88	39.94	13.31
4	50.86	3.82	37.02	13.19
4	62.99	4.91	32.10	6.31
4	48.11	4.78	30.23	16.88
10	36.56	8.78	25.85	28.80
10	36.54	8.02	29.16	26.27

Data set for figure 3.2

Temperature, (ºC)	H_2	CH_4	CO	CO_2
180	57.32	0	42.67	0
180	55.62	0	44.37	0
180	52.75	9.69	37.55	0
230	64.08	1.57	30.95	4.92
230	69.44	1.64	28.91	4.53
230	62.58	1.44	31.42	4.55
280	65.24	3.14	22.73	11.47
280	74.23	3.02	22.74	9.82
280	71.41	2.29	18.89	7.39

Data set for figure 3.3

	5% Bio-Oil			10% Bio-Oil			15% Bio-Oil		
H_2	65.25	74.23	71.40	58.92	61.15	52.09	50.85	62.98	48.10
CH_4	3.14	3.02	2.29	4.76	4.63	4.20	3.82	4.90	4.78
CO	22.73	22.74	18.89	33.92	34.21	28.50	37.01	32.10	30.23
CO_2	11.47	9.82	7.39	3.60	15.22	15.19	13.18	6.30	16.87
Vol. of gas (cc)	140.00	121.40	150.00	162.6	167.20	161.5	266.0	348.8	220.0
Vol. of liq (ml)	44.60	44.40	47.00	44.40	46.00	46.8	41.00	47.60	44.0
Filtrate wt (g)	0.1556	0.20	0.20	0.26	0.36	0.33	0.51	0.40	0.45

Data set for figure 3.4

Concentration	Liquid Carbon %	Gas Carbon %	Residue including Coke
5%	49.32	6.23	44.45
5%	44.37	5.14	50.49
5%	51.41	5.1	43.49
10%	46.84	14.11	39.05
10%	47.04	18.98	33.98
10%	50.72	18.36	30.92
15%	41.26	28.14	30.6
15%	47.53	29.93	22.54
15%	44.54	24.51	30.95

Data set for figure 3.5

	Without Catalyst	With Catalyst
H_2	53.98	66.63
CH_4	4.50	4.09
CO	33.11	25.36
CO_2	12.12	8.67
Vol of gas (cc)	278.27	206.57
vol of liq (ml)	44.20	43.70
Filtrate wt (g)	0.46	0.59

Data set for figure 3.6

	Without Catalyst				With Catalyst			
T (ºC)	H_2	CH_4	CO	CO_2	H_2	CH_4	CO	CO_2
180	37.81	0	62.18	0	66.23	0	33.76	0
230	46.06	2.81	47.32	0	72.47	1.126	22.90	3.74
280	53.98	4.50	33.11	12.12	65.61	4.32	26.73	9.75

Data set for figure 3.7

t (h)	C_{in} mole/L	C_{out} moles/L	dC	dt	dc/dt	ln(dc/dt)	ln C
0	2.21	2.21	0	0	-	-	-
1	2.21	1.12	1.09	1	1.09	0.09	0.11
4	2.21	0.99	1.22	4	0.31	-1.19	-0.01

$\frac{dC}{dt} = -K_{280} C^n \Longrightarrow \ln(\frac{dC}{dt}) = \ln(-K_{280}) + n \ln C$

Intercept = ln ($-K_{280}$)

Intercept	-1.0807
K_{280}	0.339358

	Catalyst	Without Catalyst
1/T	ln K	ln K
2.21	-3.89	-4.21
1.99	-2.29	-2.23
1.81	-1.20	-1.08

Slope = $-E_a/R \Longrightarrow -7.886 = -E_a / 8.314 \Longrightarrow E_a = 65.57$ kJ/mol

Data set for figure 3.8:

	H_2 selectivity	
T(ºC)	Without Catalyst	Catalyst
180	100	100
180	100	100
180	100	100
230	89.86	97.28
230	88.7	97.48
230	89.13	96.67
280	86.93	90.44
280	86.51	89.05
280	83.41	87.6

Data set for figure 3.9

Catalyst	Liquid Carbon %	Gas Carbon %	Residue including Coke
Yes	40.84	17.33	41.83
Yes	43.77	15.26	40.97
Yes	43.03	18.98	37.99
No	41.26	28.14	30.6
No	47.53	29.93	22.54
No	44.54	24.51	30.95

Data set for figure 5.4

Catalyst mass (g)	H_2	CH_4	CO	CO_2	CH_4 conversion	CO_2 Conversion
0.35	35.49	20.18	39.40	4.93	66.48	87.60
	33.33	22.91	35.61	8.15	61.95	81.00
0.20	32.57	22.89	38.53	6.01	61.98	86.30
	35.05	20.18	39.31	5.45	66.47	86.02

Data set for figure 5.5

T (ºC)	CH_4 conversion	CO_2 conversion	CH_4 conversion-Experimental	CO_2 conversion-Experimental
650	64.84	86.05	34.15	45.58
750	78.42	98.20	67.15	86.62
850	80.71	99.85	73.19	85.621

Data set for figure 5.6

T (ºC)	CH_4	CO_2	CO	H_2	H_2O	N_2	CH_4 Conversion	CO_2 Conversion	Inlet CH_4	Inlet CO_2
250	58.83	38.76	0.25	0.06	0.10	2.00	0.29	0.61	59.00	39.00
350	57.45	37.08	2.08	0.77	0.65	1.97	2.63	4.92	59.00	39.00
450	51.48	30.74	9.02	4.78	2.12	1.86	12.74	21.17	59.00	39.00
550	37.35	17.87	23.32	16.40	3.46	1.60	36.69	54.19	59.00	39.00
650	20.74	5.44	37.42	32.78	2.32	1.30	64.84	86.05	59.00	39.00
750	12.73	0.70	42.97	41.93	0.52	1.15	78.42	98.21	59.00	39.00
850	11.38	0.06	43.75	43.62	0.06	1.13	80.71	99.85	59.00	39.00
950	11.25	0.01	43.81	43.79	0.01	1.12	80.92	99.98	59.00	39.00
1000	11.24	0.00	43.82	43.82	0.00	1.12	80.95	100.00	59.00	39.00

Data set for figure 5.8

	H_2	CH_4	CO	CO_2	CH_4 conversion	CO_2 Conversion
Catalyst	32.57	22.89	38.53	6.01	61.98	86.30
	35.05	20.18	39.31	5.45	66.47	86.02
No Catalyst	0.13	55.12	0.00	44.75	29.71	13.73
	0.13	54.57	0.94	44.35	29.74	13.67
	0.13	54.98	0.15	44.74	29.77	13.61

Data set for figure 5.10

H_2S concentration	CH_4 Conversion	CO_2 Conversion
0.5	16.53	20.42
0.5	21.72	24.57
1	16.78	12.48
1	15.90	12.36
1.5	16.90	15.41
1.5	16.60	17.70

References

[1] Armaroli N, Balzani V. The Hydrogen Issue. ChemSusChem. 2011;4:21-36.

[2] Rand D, Dell R, Dell R. Hydrogen energy: challenges and prospects: Royal Society of Chemistry; 2008.

[3] Hydrogen as a Future Energy Carrier. In: Zuttel A BA, Schlapbach L, editor. Weinheim: Wiley-VCH; 2008.

[4] Chaubey R, Sahu S, James OO, Maity S. A review on development of industrial processes and emerging techniques for production of hydrogen from renewable and sustainable sources. Renewable and Sustainable Energy Reviews. 2013;23:443-62.

[5] Bartels JR, Pate MB, Olson NK. An economic survey of hydrogen production from conventional and alternative energy sources. International Journal of Hydrogen Energy. 2010;35:8371-84.

[6] Bilgen E. Domestic hydrogen production using renewable energy. Solar Energy. 2004;77:47-55.

[7] IPHE. Renewable Hydrogen Report. International Partnership for Hydrogen and Fuel Cells in the Economy. March 2011 edMarch 2011.

[8] Borowiecki T, Denis A, Rawski M, Gołębiowski A, Stołecki K, Dmytrzyk J, et al. Studies of potassium-promoted nickel catalysts for methane steam reforming: Effect of surface potassium location. Applied Surface Science.

[9] Avraam DG, Halkides TI, Liguras DK, Bereketidou OA, Goula MA. An experimental and theoretical approach for the biogas steam reforming reaction. International Journal of Hydrogen Energy. 2010;35:9818-27.

[10] Pairojpiriyakul T, Kiatkittipong W, Assabumrungrat S, Croiset E. Hydrogen production from supercritical water reforming of glycerol in an empty Inconel 625 reactor. International Journal of Hydrogen Energy. 2014;39:159-70.

[11] Nichele V, Signoretto M, Menegazzo F, Rossetti I, Cruciani G. Hydrogen production by ethanol steam reforming: Effect of the synthesis parameters on the activity of Ni/TiO2 catalysts. International Journal of Hydrogen Energy. 2014;39:4252-8.

[12] Navarro R, Pena M, Fierro J. Hydrogen production reactions from carbon feedstocks: fossil fuels and biomass. Chem Rev. 2007;107:3952-91.

[13] Rostrup-Nielson J. Catalysis Science and Technology. In: Anderson JR, Boudart, M.,, editor. Berlin: Springer Verlag; 1984.

[14] Adhikari S, Fernando S, Haryanto A. Hydrogen production from glycerol: An update. Energy Conversion and Management. 2009;50:2600-4.

[15] Basagiannis A, Verykios X. Steam reforming of the aqueous fraction of bio-oil over structured Ru/MgO/Al2O3 catalysts. Catalysis Today. 2007;127:256-64.

[16] Shuler M, Kargi F. Bioprocess engineering: Prentice Hall Upper Saddle River, NJ; 2002.

[17] Rennard D, French R, Czernik S, Josephson T, Schmidt L. Production of synthesis gas by partial oxidation and steam reforming of biomass pyrolysis oils. International Journal of Hydrogen Energy. 2010;35:4048-59.

[18] Yan C, Cheng F, Hu R, Fu P. Hydrogen production from catalytic steam reforming of bio-oil aqueous fraction over Ni/CeO2-ZrO2 catalysts. International Journal of Hydrogen Energy. 2010.

[19] Wang Z, Dong T, Yuan L, Kan T, Zhu X, Torimoto Y, et al. Characteristics of Bio-Oil-Syngas and Its Utilization in Fischer- Tropsch Synthesis. Energy Fuels. 2007;21:2421-32.

[20] Marda J, DiBenedetto J, McKibben S, Evans R, Czernik S, French R, et al. Non-catalytic partial oxidation of bio-oil to synthesis gas for distributed hydrogen production. International Journal of Hydrogen Energy. 2009;34:8519-34.

[21] Haryanto A, Fernando S, Murali N, Adhikari S. Current status of hydrogen production techniques by steam reforming of ethanol: a review. Energy Fuels. 2005;19:2098-106.

[22] Rennard D, Dauenhauer P, Tupy S, Schmidt L. Autothermal catalytic partial oxidation of bio-oil functional groups: esters and acids. Energy & Fuels. 2008;22:1318-27.

[23] Byrd A, Pant K, Gupta R. Hydrogen production from glycerol by reforming in supercritical water over Ru/Al2O3 catalyst. Fuel. 2008;87:2956-60.

[24] Wang D, Montane D, Chornet E. Catalytic steam reforming of biomass-derived oxygenates: acetic acid and hydroxyacetaldehyde. Applied Catalysis A: General. 1996;143:245-70.

[25] Wang D, Czernik S, Montane D, Mann M, Chornet E. Biomass to hydrogen via fast pyrolysis and catalytic steam reforming of the pyrolysis oil or its fractions. Ind Eng Chem Res. 1997;36:1507-18.

[26] Marquevich M, Czernik S, Chornet E, Montané D. Hydrogen from biomass: steam reforming of model compounds of fast-pyrolysis oil. Energy Fuels. 1999;13:1160-6.

[27] Garcia L, French R, Czernik S, Chornet E. Catalytic steam reforming of bio-oils for the production of hydrogen: effects of catalyst composition. Applied Catalysis A: General. 2000;201:225-39.

[28] Czernik S, French R, Feik C, Chornet E. Hydrogen by catalytic steam reforming of liquid byproducts from biomass thermoconversion processes. Ind Eng Chem Res. 2002;41:4209-15.

[29] Wang D, Czernik S, Chornet E. Production of hydrogen from biomass by catalytic steam reforming of fast pyrolysis oils. Energy Fuels. 1998;12:19-24.

[30] Galdámez J, García L, Bilbao R. Hydrogen Production by Steam Reforming of Bio-Oil Using Coprecipitated Ni- Al Catalysts. Acetic Acid as a Model Compound. Energy Fuels. 2005;19:1133-42.

[31] Kechagiopoulos P, Voutetakis S, Lemonidou A, Vasalos I. Hydrogen production via steam reforming of the aqueous phase of bio-oil in a fixed bed reactor. Energy Fuels. 2006;20:2155-63.

[32] Pan Y, Wang Z, Kan T, Zhu X, Li Q. Hydrogen production by catalytic steam reforming of bio-oil, naphtha and CH4 over C12A7-Mg catalyst. Chinese Journal of Chemical Physics. 2006;19:190.

[33] Yan C, Hu E, Cai C. Hydrogen production from bio-oil aqueous fraction with in situ carbon dioxide capture. International Journal of Hydrogen Energy. 2010;35:2612-6.

[34] Lin S, Ye T, Yuan L, Hou T, Li Q. Production of Hydrogen from Bio-oil Using Low-temperature Electrochemical Catalytic Reforming Approach over CoZnAl Catalyst. Chinese Journal of Chemical Physics. 2010;23:451.

[35] Vagia E, Lemonidou A. Hydrogen production via steam reforming of bio-oil components over calcium aluminate supported nickel and noble metal catalysts. Applied Catalysis A: General. 2008;351:111-21.

[36] Medrano J, Oliva M, Ruiz J, García L, Arauzo J. Hydrogen from aqueous fraction of biomass pyrolysis liquids by catalytic steam reforming in fluidized bed. Energy. 2010.

[37] Czernik S, Evans R, French R. Hydrogen from biomass-production by steam reforming of biomass pyrolysis oil. Catalysis Today. 2007;129:265-8.

[38] Wang Z, Pan Y, Dong T, Zhu X, Kan T, Yuan L, et al. Production of hydrogen from catalytic steam reforming of bio-oil using C12A7-O--based catalysts. Applied Catalysis A: General. 2007;320:24-34.

[39] Takanabe K, Aika K, Seshan K, Lefferts L. Sustainable hydrogen from bio-oil--Steam reforming of acetic acid as a model oxygenate. Journal of catalysis. 2004;227:101-8.

[40] Adhikari S, Fernando S, Haryanto A. Production of hydrogen by steam reforming of glycerin over alumina-supported metal catalysts. Catalysis Today. 2007;129:355-64.

[41] Gongxuan H. Bio-oil steam reforming, partial oxidation or oxidative steam reforming coupled with bio-oil dry reforming to eliminate CO2 emission. International Journal of Hydrogen Energy. 2010;35:7169-76.

[42] Vagia E, Lemonidou A. Thermodynamic analysis of hydrogen production via autothermal steam reforming of selected components of aqueous bio-oil fraction. International Journal of Hydrogen Energy. 2008;33:2489-500.

[43] Cortright R, Davda R, Dumesic J. Hydrogen from catalytic reforming of biomass-derived hydrocarbons in liquid water. Nature. 2002;418:964-7.

[44] Lehnert K, Claus P. Influence of Pt particle size and support type on the aqueous-phase reforming of glycerol. Catalysis Communications. 2008;9:2543-6.

[45] Iriondo A, Barrio V, Cambra J, Arias P, Güemez M, Navarro R, et al. Hydrogen production from glycerol over nickel catalysts supported on Al 2 O 3 modified by Mg, Zr, Ce or La. Topics in Catalysis. 2008;49:46-58.

[46] Loppinet Serani A, Aymonier C, Cansell F. Current and foreseeable applications of supercritical water for energy and the environment. ChemSusChem. 2008;1:486-503.

[47] Kobe Steel L. Characteristics and uses of supercritical water.

[48] Penninger JML, Rep M. Reforming of aqueous wood pyrolysis condensate in supercritical water. International Journal of Hydrogen Energy. 2006;31:1597-606.

[49] Byrd AJ, Kumar S, Kong L, Ramsurn H, Gupta RB. Hydrogen production from catalytic gasification of switchgrass biocrude in supercritical water. International Journal of Hydrogen Energy. 2011.

[50] Yu D, Aihara M, Antal MJ. Hydrogen production by steam reforming glucose in supercritical water. Energy & Fuels. 1993;7:574-7.

[51] Antal Jr M, Manarungson S, Mok W, Bridgwater A. Hydrogen production by steam reforming glucose in supercritical water. Advances in thermochemical biomass conversion Volume 2. 1994:1367-77.

[52] Davidian T, Guilhaume N, Iojoiu E, Provendier H, Mirodatos C. Hydrogen production from crude pyrolysis oil by a sequential catalytic process. Applied Catalysis B: Environmental. 2007;73:116-27.

[53] Choudhary TV, Goodman DW. CO-free production of hydrogen via stepwise steam reforming of methane. Journal of catalysis. 2000;192:316-21.

[54] Choudhary T, Sivadinarayana C, Chusuei C, Klinghoffer A, Goodman D. Hydrogen production via catalytic decomposition of methane. Journal of catalysis. 2001;199:9-18.

[55] Aiello R, Fiscus J, Zur Loye H, Amiridis M. Hydrogen production via the direct cracking of methane over Ni/SiO2: Catalyst deactivation and regeneration. Applied Catalysis A: General. 2000;192:227-34.

[56] Takenaka S, Kato E, Tomikubo Y, Otsuka K. Structural change of Ni species during the methane decomposition and the subsequent gasification of deposited carbon with CO2 over supported Ni catalysts. Journal of catalysis. 2003;219:176-85.

[57] Villacampa JI, Royo C, Romeo E, Montoya JA, Del Angel P, Monzón A. Catalytic decomposition of methane over Ni-Al2O3 coprecipitated catalysts: Reaction and regeneration studies. Applied Catalysis A: General. 2003;252:363-83.

[58] Odier E, Schuurman Y, Barrai K, Mirodatos C. Hydrogen production from non-stationary catalytic cracking of methane: a mechanistic study using in operando infrared spectroscopy. In: Xinhe B, Yide X, editors. Studies in Surface Science and Catalysis: Elsevier; 2004. p. 79-84.

[59] Iojoiu E, Domine M, Davidian T, Guilhaume N, Mirodatos C. Hydrogen production by sequential cracking of biomass-derived pyrolysis oil over noble metal catalysts supported on ceria-zirconia. Applied Catalysis A: General. 2007;323:147-61.

[60] Vagia E, Lemonidou A. Thermodynamic analysis of hydrogen production via steam reforming of selected components of aqueous bio-oil fraction. International Journal of Hydrogen Energy. 2007;32:212-23.

[61] Aktas S, Karakaya M, AvcI A. Thermodynamic analysis of steam assisted conversions of bio-oil components to synthesis gas. International Journal of Hydrogen Energy. 2009;34:1752-9.

[62] Domine M, Iojoiu E, Davidian T, Guilhaume N, Mirodatos C. Hydrogen production from biomass-derived oil over monolithic Pt-and Rh-based catalysts using steam reforming and sequential cracking processes. Catalysis Today. 2008;133:565-73.

[63] Kechagiopoulos P, Voutetakis S, Lemonidou A, Vasalos I. Hydrogen production via reforming of the aqueous phase of bio-oil over ni/olivine catalysts in a spouted bed reactor. Industrial & Engineering Chemistry Research. 2008;48:1400-8.

[64] van Rossum G, Kersten S, van Swaaij W. Catalytic and noncatalytic gasification of pyrolysis oil. Ind Eng Chem Res. 2007;46:3959-67.

[65] Rioche C, Kulkarni S, Meunier F, Breen J, Burch R. Steam reforming of model compounds and fast pyrolysis bio-oil on supported noble metal catalysts. Applied Catalysis B: Environmental. 2005;61:130-9.

[66] Barrio L, Kubacka A, Zhou G, Estrella M, Martínez-Arias A, Hanson JC, et al. Unusual Physical and Chemical Properties of Ni in Ce1−xNixO2−y Oxides: Structural Characterization and Catalytic Activity for the Water Gas Shift Reaction. The Journal of Physical Chemistry C. 2010;114:12689-97.

[67] Zhou G, Barrio L, Agnoli S, Senanayake S, Evans J, Kubacka A, et al. High Activity of Ce1- xNixO2- y for H2 Production through Ethanol Steam Reforming: Tuning Catalytic Performance through Metal–Oxide Interactions. Angewandte Chemie.

[68] Biomass Resources in the United States. Biomass holds the promise of clean power and fuel — if handled right. Cambridge, MA Union of Concerned Scientist; 2012.

[69] Annual Energy Review 2011. In: Energy Do, editor. Washington, DC2012.

[70] Ayalur Chattanathan S, Adhikari S, Abdoulmoumine N. A review on current status of hydrogen production from bio-oil. Renewable and Sustainable Energy Reviews. 2012;16:2366-72.

[71] Guo Y, Liu X, Azmat MU, Xu W, Ren J, Wang Y, et al. Hydrogen production by aqueous-phase reforming of glycerol over Ni-B catalysts. International Journal of Hydrogen Energy. 2012;37:227-34.

[72] Manfro RL, da Costa AF, Ribeiro NFP, Souza MMVM. Hydrogen production by aqueous-phase reforming of glycerol over nickel catalysts supported on CeO2. Fuel Processing Technology. 2011;92:330-5.

[73] Pan G, Ni Z, Cao F, Li X. Hydrogen production from aqueous-phase reforming of ethylene glycol over Ni/Sn/Al hydrotalcite derived catalysts. Applied Clay Science. 2012;58:108-13.

[74] Huber GW, Shabaker JW, Evans ST, Dumesic JA. Aqueous-phase reforming of ethylene glycol over supported Pt and Pd bimetallic catalysts. Applied Catalysis B: Environmental. 2006;62:226-35.

[75] Davda RR, Shabaker JW, Huber GW, Cortright RD, Dumesic JA. Aqueous-phase reforming of ethylene glycol on silica-supported metal catalysts. Applied Catalysis B: Environmental. 2003;43:13-26.

[76] Xie J, Su D, Yin X, Wu C, Zhu J. Thermodynamic analysis of aqueous phase reforming of three model compounds in bio-oil for hydrogen production. International Journal of Hydrogen Energy. 2011;36:15561-72.

[77] Pan C, Chen A, Liu Z, Chen P, Lou H, Zheng X. Aqueous-phase reforming of the low-boiling fraction of rice husk pyrolyzed bio-oil in the presence of platinum catalyst for hydrogen production. Bioresource Technology. 2012;125:335-9.

[78] Babu B. Biomass pyrolysis: a state of the art review. Biofuels, Bioproducts and Biorefining. 2008;2:393-414.

[79] Bridgwater A, Meier D, Radlein D. An overview of fast pyrolysis of biomass. Organic Geochemistry. 1999;30:1479-93.

[80] Lu Q, Li W, Zhu X. Overview of fuel properties of biomass fast pyrolysis oils. Energy Conversion and Management. 2009;50:1376-83.

[81] Sipilä K, Kuoppala E, Fagernäs L, Oasmaa A. Characterization of biomass-based flash pyrolysis oils. Biomass and Bioenergy. 1998;14:103-13.

[82] Mullen C, Boateng A, Goldberg N, Lima I, Laird D, Hicks K. Bio-oil and bio-char production from corn cobs and stover by fast pyrolysis. Biomass and Bioenergy. 2010;34:67-74.

[83] Tsai WT, Lee MK, Chang YM. Fast pyrolysis of rice husk: Product yields and compositions. Bioresource Technology. 2007;98:22-8.

[84] Torri C, Reinikainen M, Lindfors C, Fabbri D, Oasmaa A, Kuoppala E. Investigation on catalytic pyrolysis of pine sawdust: Catalyst screening by Py-GC-MIP-AED. Journal of Analytical and Applied Pyrolysis. 2010;88:7-13.

[85] Agblevor FA, Mante O, Abdoulmoumine N, McClung R. Production of Stable Biomass Pyrolysis Oils Using Fractional Catalytic Pyrolysis. Energy & Fuels. 2010;24:4087-9.

[86] Mullen C, Boateng A, Hicks K, Goldberg N, Moreau R. Analysis and Comparison of Bio-Oil Produced by Fast Pyrolysis from Three Barley Biomass/Byproduct Streams. Energy & Fuels. 2009;24:699-706.

[87] Mante OD, Agblevor FA. Influence of pine wood shavings on the pyrolysis of poultry litter. Waste Management. 2010;30:2537-47.

[88] Mohan D, Jr. CUP, Steele PH. Pyrolysis of Wood/Biomass for Bio-Oil: A Critical Review. Energy & Fuels. 2006;20: 848-89.

[89] Mohan D, Pittman CU, Steele PH. Pyrolysis of Wood/Biomass for Bio-oil: A Critical Review. Energy & Fuels. 2006;20:848-89.

[90] Chattanathan SA, Adhikari S, Taylor S. Conversion of carbon dioxide and methane in biomass synthesis gas for liquid fuels production. International Journal of Hydrogen Energy. 2012;37:18031-9.

[91] Dave CD, Pant KK. Renewable hydrogen generation by steam reforming of glycerol over zirconia promoted ceria supported catalyst. Renewable energy. 2011;36:3195-202.

[92] Praharso, Adesina AA, Trimm DL, Cant NW. Kinetic study of iso-octane steam reforming over a nickel-based catalyst. Chemical Engineering Journal. 2004;99:131-6.

[93] Davda RR, Shabaker JW, Huber GW, Cortright RD, Dumesic JA. A review of catalytic issues and process conditions for renewable hydrogen and alkanes by aqueous-phase reforming of oxygenated hydrocarbons over supported metal catalysts. Applied Catalysis B: Environmental. 2005;56:171-86.

[94] Fan MS, Abdullah AZ, Bhatia S. Catalytic technology for carbon dioxide reforming of methane to synthesis gas. ChemCatChem. 2009;1:192-208.

[95] Choudhary T, Sivadinarayana C, Goodman D. Production of COx-free hydrogen for fuel cells via step-wise hydrocarbon reforming and catalytic dehydrogenation of ammonia. Chemical Engineering Journal. 2003;93:69-80.

[96] Castro Luna AE, Iriarte ME. Carbon dioxide reforming of methane over a metal modified Ni-Al2O3 catalyst. Applied Catalysis A: General. 2008;343:10-5.

[97] Courson C, Makaga E, Petit C, Kiennemann A. Development of Ni catalysts for gas production from biomass gasification. Reactivity in steam- and dry-reforming. Catalysis Today. 2000;63:427-37.

[98] Brungs AJ, York APE, Claridge JB, Márquez-Alvarez C, Green MLH. Dry reforming of methane to synthesis gas over supported molybdenum carbide catalysts. Catalysis Letters. 2000;70:117-22.

[99] Ferreira-Aparicio P, Rodríguez-Ramos I, Anderson JA, Guerrero-Ruiz A. Mechanistic aspects of the dry reforming of methane over ruthenium catalysts. Applied Catalysis A: General. 2000;202:183-96.

[100] Maestri M, Vlachos DG, Beretta A, Groppi G, Tronconi E. Steam and dry reforming of methane on Rh: Microkinetic analysis and hierarchy of kinetic models. Journal of Catalysis. 2008;259:211-22.

[101] Laosiripojana N, Sutthisripok W, Assabumrungrat S. Synthesis gas production from dry reforming of methane over CeO2 doped Ni/Al2O3: Influence of the doping ceria on the resistance toward carbon formation. Chemical Engineering Journal. 2005;112:13-22.

[102] Courson C, Makaga E, Petit C, Kiennemann A. Development of Ni catalysts for gas production from biomass gasification. Reactivity in steam-and dry-reforming. Catalysis Today. 2000;63:427-37.

[103] Guo J, Lou H, Zhao H, Chai D, Zheng X. Dry reforming of methane over nickel catalysts supported on magnesium aluminate spinels. Applied Catalysis A: General. 2004;273:75-82.

[104] Sahli N, Petit C, Roger A, Kiennemann A, Libs S, Bettahar M. Ni catalysts from NiAl2O4 spinel for CO2 reforming of methane. Catalysis Today. 2006;113:187-93.

[105] Martinez R, Romero E, Guimon C, Bilbao R. CO2 reforming of methane over coprecipitated Ni-Al catalysts modified with lanthanum. Applied Catalysis A: General. 2004;274:139-49.

[106] Tomishige K, Nurunnabi M, Maruyama K, Kunimori K. Effect of oxygen addition to steam and dry reforming of methane on bed temperature profile over Pt and Ni catalysts. Fuel processing technology. 2004;85:1103-20.

[107] Bouarab R, Akdim O, Auroux A, Cherifi O, Mirodatos C. Effect of MgO additive on catalytic properties of Co/SiO2 in the dry reforming of methane. Applied Catalysis A: General. 2004;264:161-8.

[108] Liu B, Au C. Carbon deposition and catalyst stability over La2NiO4/[gamma]-Al2O3 during CO2 reforming of methane to syngas. Applied Catalysis A: General. 2003;244:181-95.

[109] Tsyganok AI, Inaba M, Tsunoda T, Suzuki K, Takehira K, Hayakawa T. Combined partial oxidation and dry reforming of methane to synthesis gas over noble metals supported on Mg-Al mixed oxide. Applied Catalysis A: General. 2004;275:149-55.

[110] Adhikari S, Fernando SD, To SDF, Bricka RM, Steele PH, Haryanto A. Conversion of Glycerol to Hydrogen via a Steam Reforming Process over Nickel Catalysts. Energy & Fuels. 2008;22:1220-6.

[111] Annadurai G, Sheeja R. Use of Box-Behnken design of experiments for the adsorption of verofix red using biopolymer. Bioprocess and Biosystems Engineering. 1998;18:463-6.

[112] Komiyama M, Misonou T, Takeuchi S, Umetsu K, Takahashi J. Biogas as a reproducible energy source: Its steam reforming for electricity generation and for farm machine fuel. International Congress Series. 2006;1293:234-7.

[113] Rasi S, Veijanen A, Rintala J. Trace compounds of biogas from different biogas production plants. Energy. 2007;32:1375-80.

[114] Fan M-S, Abdullah AZ, Bhatia S. Catalytic Technology for Carbon Dioxide Reforming of Methane to Synthesis Gas. ChemCatChem. 2009;1:192-208.

[115] Houghton JT. Climate change 1995: The science of climate change: contribution of working group I to the second assessment report of the Intergovernmental Panel on Climate Change: Cambridge University Press; 1996.

[116] Prather M, Derwent R, Ehhalt D, Fraser P, Sanhueza E, Zhou X. Other trace gases and atmospheric chemistry, Climate Change 1994: Radiative Forcing of Climate Change and an

Evaluation of the IPCC IS92 Emission Scenarios JT Houghton, et al., 73–126. Cambridge Univ. Press, New York; 1995.

[117] Themelis NJ, Ulloa PA. Methane generation in landfills. Renewable Energy. 2007;32:1243-57.

[118] Özdemir H, Öksüzömer MAF, Gürkaynak MA. Effect of the calcination temperature on Ni/MgAl2O4 catalyst structure and catalytic properties for partial oxidation of methane. Fuel. 2014;116:63-70.

[119] Braga LB, Silveira JL, da Silva ME, Tuna CE, Machin EB, Pedroso DT. Hydrogen production by biogas steam reforming: A technical, economic and ecological analysis. Renewable and Sustainable Energy Reviews. 2013;28:166-73.

[120] Yan Q, Yu F, Liu J, Street J, Gao J, Cai Z, et al. Catalytic conversion wood syngas to synthetic aviation turbine fuels over a multifunctional catalyst. Bioresource Technology. 2013;127:281-90.

[121] Lau CS, Tsolakis A, Wyszynski ML. Biogas upgrade to syn-gas (H2–CO) via dry and oxidative reforming. International Journal of Hydrogen Energy. 2011;36:397-404.

[122] Asencios YJO, Bellido JDA, Assaf EM. Synthesis of NiO–MgO–ZrO2 catalysts and their performance in reforming of model biogas. Applied Catalysis A: General. 2011;397:138-44.

[123] Izquierdo U, Barrio VL, Lago N, Requies J, Cambra JF, Güemez MB, et al. Biogas steam and oxidative reforming processes for synthesis gas and hydrogen production in conventional and microreactor reaction systems. International Journal of Hydrogen Energy. 2012;37:13829-42.

[124] Xu J, Zhou W, Li Z, Wang J, Ma J. Biogas reforming for hydrogen production over nickel and cobalt bimetallic catalysts. International Journal of Hydrogen Energy. 2009;34:6646-54.

[125] Lucrédio AF, Assaf JM, Assaf EM. Reforming of a model biogas on Ni and Rh–Ni catalysts: Effect of adding La. Fuel Processing Technology. 2012;102:124-31.

[126] Kohn MP, Castaldi MJ, Farrauto RJ. Biogas reforming for syngas production: The effect of methyl chloride. Applied Catalysis B: Environmental. 2014;144:353-61.

[127] Appari S, Janardhanan VM, Bauri R, Jayanti S, Deutschmann O. A Detailed Kinetic Model for Biogas Steam Reforming on Ni and Catalyst Deactivation Due to Sulfur Poisoning. Applied Catalysis A: General.

[128] Appari S, Janardhanan VM, Bauri R, Jayanti S, Deutschmann O. A detailed kinetic model for biogas steam reforming on Ni and catalyst deactivation due to sulfur poisoning. Applied Catalysis A: General. 2014;471:118-25.

[129] Clark PD, Dowling NI, Huang M. Production of H2 from catalytic partial oxidation of H2S in a short-contact-time reactor. Catalysis Communications. 2004;5:743-7.